A NEW METHOD OF MEASURING SHOCK EXPANSION TUBE TEST FLOW VELOCITIES

Thesis Report

Pat Crombie
[Email address]

Acknowledgements

There are several individuals without whom the completion of this body of work would not have been possible. These people should not go without acknowledgement.

Firstly, thanks must go to Tim Cullen for being one the people who conducted testing in the University of Queensland's X2 shock Expansion Tube facility on my behalf.

Secondly Christopher James, who also conducted experiments and was very generous with his time in helping me to understand the results.

Thirdly, The University of Queensland and the department of hypersonics who made their facilities available for experimentation along with a significant manufacturing budget to produce all the required instruments.

And finally to my supervisor David Gildfind. Without your contributions and behind the scenes organisation none of this work would have amounted to anything. Your advice has been invaluable and you the amount time you have dedicated to answering my questions, running simulations and ensuring all instruments were manufactured and tested in time has not gone unnoticed. I am very thankful for all you have done.

Abstract

Shock expansion tubes are an important tool in the field of hypersonic research. However, these facilities possess a major weakness in the fact there is a great deal of uncertainty associated with the properties of the test flows that they produce.

In an attempt to better characterise these properties, an instrument which was capable of measuring the velocity of the test flows produced by shock expansion tubes was to be designed and tested. This instrument would consist of two pitot probes which would be mounted in a shock tube at different locations to detect the arrival of the test gas. Based on the time difference between the arrival of this gas at each probe, its velocity could be calculated.

Two probes were designed and manufactured for the testing of this concept in the University of Queensland's X2 shock expansion tube. The design, shown in the image to the right, was created with consideration given to the facts that the probe had to; be structurally capable of withstanding the hypersonic flow environment, protect the pressure transducer from this harsh environment, respond rapidly to changes in pitot pressure, be able to take measurements through the thickest boundary layers, create the smallest disturbance to the test flow possible, and record data which was not adversely affected by noise.

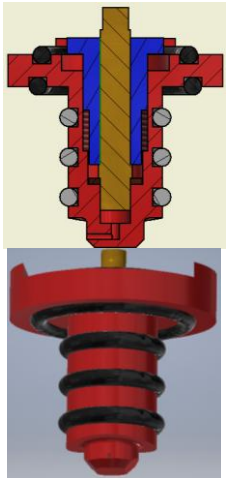

A cross section and isometric view of the pitot probe design. The red component is the probe structure, the yellow is a pressure transducer and the blue component is a threaded screw used to secure the transducer.

This design was tested in the X2, which was configured to produce two high enthalpy test flows with velocities of 9468.1m/s and 9656.5m/s. Over the two experiments, the probes measured the velocity of the two test flows to within 3% of the current best estimates, although determining the arrival time of the test gas at each probe was difficult and there was large potential for error. The data recorded by the two probes was also sufficiently noise free and the instruments responded rapidly to any changes in pitot pressure. There was also no evidence that the probes were significantly disrupting the test flow, however further testing was required to confirm this. In summary, the design was a success and further testing was warranted to confirm these results and develop the concept further.

Contents

1 Introduction

The field of hypersonic research is one in which many advances are expected in the coming years. The rapid expansion of space exploration programs by many countries around the world and the drive to improve scramjet technology means that there is a real push to improve our understanding of fluid flow and flight in this regime. As such, facilities capable of producing hypersonic flows in which testing can be conducted, are a very important part of moving the field forward. Wind tunnels, reflected shock tubes, shock expansion tunnels, and other ground testing infrastructure offer a cheap and cost effective means of gathering experimental data. They allow researchers to do a range of things, such as validate CFD models, test scale models of vehicle designs, and evaluate the effectiveness of hypersonic combustion techniques. Without ground testing equipment, the only other way to gather experimental data is to conduct expensive and complex flight tests in the atmosphere.

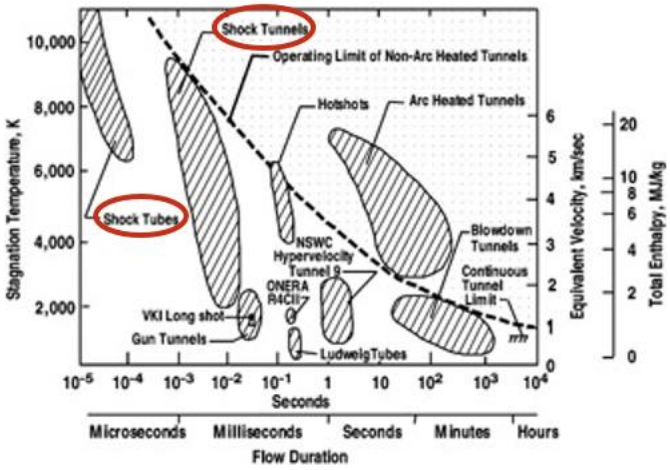

Figure 1.1.1: A graph showing some of the performance properties of hypersonic ground testing facilities. As the plot shows, shock expansion facilities produce the highest enthalpy test flows of all ground testing equipment [2].

One of the most important hypersonic ground testing facilities is the shock expansion tunnel or tube. The reason it is important is that shock expansion tubes produce the highest enthalpy test flows of all the ground testing facilities currently in existence, as Figure 1.1.1 shows. This essentially means that shock expansion tubes represent the upper end of performance for ground testing facilities, in terms of producing high energy hypersonic flows [2]. Therefore, for many investigations or research projects, shock expansion tubes are the only option for gathering experimental data.

To explain them briefly, shock expansion tubes are impulse facilities which generate a high velocity flow of gas in a tube and direct it through a test section in which objects can be placed. Using a range of instruments, the behaviour of this flow as it passes over the object in the test

section can be analysed and its behaviour understood. The mechanics of these facilities will be explained in greater detail in this report, but essentially a driver gas is compressed against a diaphragm until the diaphragm bursts and releases a shock wave in to a tube containing the test gas. The shockwave heats and accelerates the test gas which in turn bursts through another diaphragm and into a low pressure acceleration tube. The low pressure causes a rapid and unsteady expansion of the test gas, further accelerating it down the acceration tube and through the test section. At this stage it is a high velocity, high energy, hypersonic flow which is capable of producing several hundred microseconds of testing time [4].

Given the importance of these shock expansion tubes to hypersonic research there is real impetus to improve these facilities in any way possible. One of the main weaknesses of shock expansion facilities is that there is a high level of uncertainty associated with many of the properties of the test flows that they generate. There are many reasons for this. As alluded to in the previous paragraph and shown in Figure 1.1.1, a test in a shock expansion tube only last for a few hundred microseconds. Therefore making any measurements involves sophisticated instruments and even with these, uncertainties can still be high. In addition, hypersonic flows are particularly harsh environments for instruments to survive in. Even the toughest of probes will eventually be destroyed after a short period of time exposed to the flow. Non-intrusive optical instruments are available for the measurement of certain properties, however they are expensive and complicated. As a result, most facilities have some instrumentation for measuring specific flow properties and use analytical or numerical models to determine the remainder. This is not necessarily a bad way to determine flow properties, however uncertainty associated with the experimental measurements, combined with theory which relies on good but not necessarily perfect assumptions, inevitably lead to a reasonable range of error. The solution to this problem, or at least a way the situation can be improved, is to gather more information about the test flow from instruments. Therein lies the purpose of this investigation.

One of the properties of a hypersonic test flow which is critical to gain a good understanding of, is the velocity. It is typically determined in shock expansion tubes, by calculations based on measurements of other properties, such as the shock speed, and this leads to a high level of uncertainty. The aim of this investigation was to design and test a new prototype instrument capable of measuring the velocity of the test flow directly. Specifically a prototype instrument

for potential use in The University Of Queensland's X2 shock expansion tube. The idea being that the success or failure of this instrument could provide useful information about how it may be possible to measure the velocity of shock expansion test flows in the future, and potentially provide another source from which information about this property can be obtained.

The first step towards achieving this aim was to conduct a literature review. As Section 2 of this report details, this review has two areas of focus. The first of these is shock expansion tubes. In this section of the literature review, the mechanics of these facilities are explored with a particular focus on how test flow velocities are currently estimated, and the reasons behind the uncertainty associated with these estimations. The second area of focus is on four proposed instruments or measurements techniques deemed to have the potential to measure test flow velocities. Specifically:

- Planar Laser Induced Fluorescence
- Rayleigh Scattering Techniques
- Tuned Laser Diode Spectroscopy
- Pitot Probes

These methods or instruments are assessed for their potential to be adapted from a concept into an instrument capable of successfully measuring test flow velocities in the X2 shock expansion tube. Based on this analysis pitot probe technology was selected as the concept with which the investigation would move forward. In short this concept involved using two pitot probes mounted at different locations within the acceleration tube to detect the arrival of the test gas. Based on the difference in arrival time, the velocity of this gas would be determined.

Having selected the pitot probe as the concept upon which to base the remainder of this design project, a brief review of literature pertaining to the past use of pitot probes in hypersonic facilities was conducted, as displayed in Section 3. The idea was to gather information regarding the design challenges facing hypersonic pitot probes and the ways in which these have been overcome in the past to help inform the design of the new probes.

Following this the probe design could begin. Section 4 outlines this process which consists of three key steps. The first is to define the conditions in which the probe must be able to operate. This involved determining the extreme operating conditions for shock expansion tubes and

selecting two proposed test flow conditions to design to. Having defined these, the second step was to outline the operating problems and complications which could potentially prevent the new probe from successfully measuring test flow velocities. For each of these issues, design strategies and considerations were established with the intention of eliminating or minimising the effect of these potential problems on the probe's operation. Finally, having considered all these factors a probe design was then produced which attempted to balance them in the most optimum way possible.

Lastly, Section 5 details the testing of the newly built pitot probes in UQ's X2 shock expansion tube facility. The results of these tests are outlined and analysed to assess whether these instruments are capable of measuring the velocities of test flows produced by shock expansion tubes. The performance of the probes will also be assessed in terms of its ability to respond to pitot pressure changes quickly, take measurements which are not compromised by noise, and its ability to not significantly disturb the test flow. Based on this analysis, a conclusion will be drawn as to whether the probe design was a success and if the concept has any future in hypersonic research. The flaws associate with the new instruments will be outlined along with its strengths.

2 Literature Review

2.1 Shock Expansion Tunnels

Before investigating instruments that have been or could potentially be used to more accurately measure the test flow velocities in shock expansion tunnels, it is first necessary to understand the mechanics of these facilities.

2.1.1 A Brief History

The concept behind shock expansion tubes, or tunnels is relatively simple. In short, a driver gas is compressed behind a diaphragm causing rapid increases in pressure and temperature. This continues until the diaphragm bursts and releases the driver gas into a length of test gas located in a "Shock Tube", causing as shock. As the shock travels through the test gas it compresses and accelerates it until it reaches a secondary diaphragm. This diaphragm offers little resistance and quickly gives way, allowing the test gas to expand into a low pressure "Acceleration Tube". As its name suggests, rapid unsteady expansion and acceleration occurs in this Section of the tunnel, resulting in a high velocity hypersonic flow which can then be used for testing purposes [4]. A basic schematic is shown below in Figure 2.1.1.

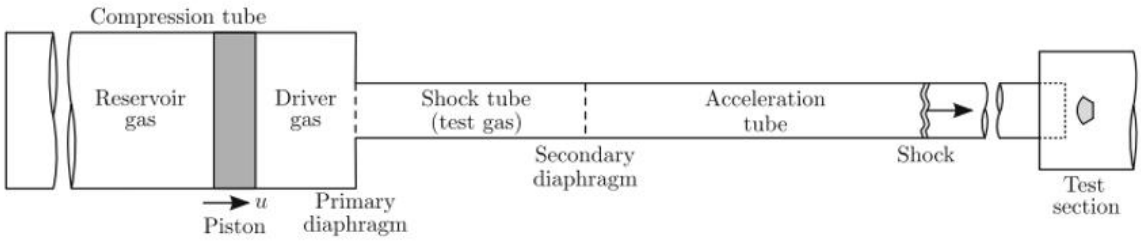

Figure 2.1.1: A Schematic of a simple shock expansion tube. (Adapted from Gildfind, Jacobs, and Morgan [4].)

This sounds reasonably simple, however generating useful test flows is not straight forward. Initial studies into the expansion tube concept by NASA during the 1960s and 1970s, concluded that such facilities were only capable of producing a very limited range of steady test flows. As such, these early studies were discontinued, with the use of reflected shock tunnels dominating ground based hypersonic testing into the 1980s and 1990s. It wasn't until the late 1980s that any serious expansion tunnel testing recommenced at the University of Queensland (UQ). UQ's program aimed to establish why test flows were often noisy and unsteady, and how this

problem could be eliminated. They found that the key to preventing these disturbances was conducting tests in what is known as an over-tailored configuration. This means that the sound speed of the driver gas (after being processed by the initial shockwave) is higher than that of the expanded test gas [1].

2.1.2 The Secondary Driver Concept

The problem with having to run over tailored configurations in expansion tubes, such as the one displayed in Figure 2.1.1, is that the testing is somewhat limited to higher enthalpy flows. Therefore, there was a need to come up with an expansion tube design which could generate lower enthalpy flows yet still operate in an over tailored configuration. This need drove the development of tubes with a secondary driver gas. As indicated by Figure 2.1.2, such expansion tubes have a secondary driver gas (typically helium) located between the driver gas and the test gas and contained by two diagrams. During the operation, a shock originating from the primary driver gas heats and accelerates the secondary driver gas which in turn heats and accelerates the test gas before this gas is expanded and further accelerated towards the test section. The idea behind this concept is that, given an appropriate gas is selected and is initially at a sufficiently low pressure within the tube, the shock processed secondary driver can have a much higher sound speed than the primary driver gas would. Therefore, allowing the expansion process to generate useful test flows at lower enthalpies [4]. Another advantage of using a secondary driver is that for higher enthalpy flows, a stronger shock can be achieved. This can then lead to performance increases in terms of the range of hypersonic flows able to be produce by the expansion tube facility.

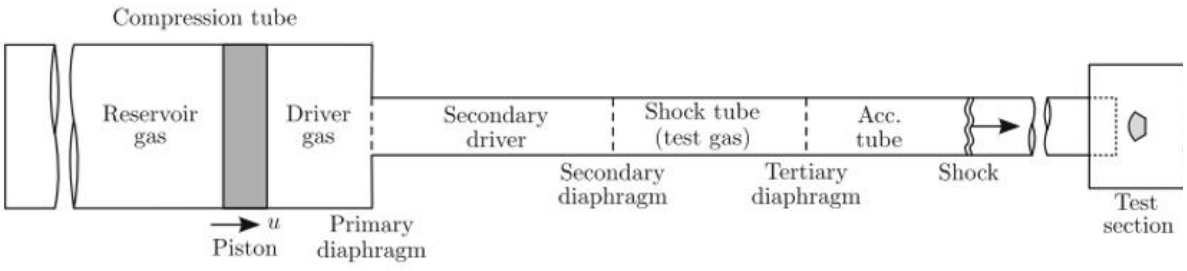

2.1.3 The X2 Shock Expansion Tunnel

The X2 shock expansion tunnel at the University of Queensland is an example of a facility which has the potential to operate in this secondary driver configuration. However it can also be used in the traditional configuration with a single driver gas and this was the case throughout the course of this investigation. Commissioned in 1995, X2 is a 25 meter long expansion tube driven by a free piston, and is depicted by the schematic in Figure 2.1.3.

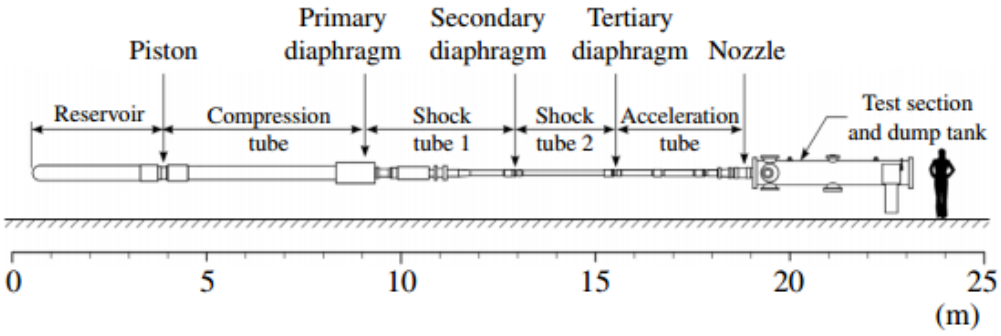

Figure 2.1.3: A schematic depicting the basic mechanics of the X2 expansion tube facility. In this image it is set up to run in the secondary driver configuration [6].

This facility is important as it will be the reference shock tunnel for the remainder of the investigation. It is also the facility available for testing any potential concepts or designs that this investigation may produce.

During operation, a 10.5 kg aluminium alloy piston is fired into the driver gas stored in the compression tube. The primary diaphragm is normally a steel plate with a specific thickness such that when the driver gas has been compressed by the piston to the desired pressure, the plate will give way. What happens after this depends on whether the facility has been setup to run with a secondary driver or not. In the secondary driver case, the primary driver gas will accelerate a secondary driver gas which then breaches a thin secondary diaphragm, typically made from Mylar. The secondary driver gas then accelerates a test gas which in-turn ruptures a tertiary Mylar diaphragm before entering the low pressure acceleration tube (Refer Figure 2.1.3). The process is much the same if the tube is set up without a secondary driver gas, except the test gas is accelerated directly by the primary driver gas and there is no secondary diaphragm [4].

Located between the test section and the acceleration tube is a diverging nozzle which serves the primary purpose of increasing the cross sectional area of the core of the test flow. The acceleration tube of X2 is only 85mm in diameter which limits the cross sectional area of any test flow generated, particularly if thick boundary layers form within the tube. The diverging nozzle increases this flow's cross sectional area and therefore allows for larger items or models to be tested. In addition to this, the nozzle also increases the Mach number of the flow as well as sometimes having the effect of increasing the duration of useful test flows produced by the facility.

2.1.4 Analytical Analysis of Shock Expansion Tunnels

Analytically analysing shock expansion facilities is an important part of characterizing the properties of the test flows produced. Due to the very harsh conditions associated with high velocity Mach number flows, it is difficult to measure the properties of the test flows directly, via instruments or some other technique. Given the instruments shock expansion facilities (such as X2) typically have, analytical methods are still required to determine the velocity of the test flow. Appendix A outlines an example of a basic analysis that can be used to characterize the behaviour of shock expansion tubes with a secondary driver (such as the X2). There are variations of this analysis which are used to characterize flows in many different facilities however, generally the key assumptions are the same or similar.

The most important of these assumptions is that the flow in the tube is inviscid, indicating that there is no friction between the gas and the walls of the tube. In addition, it is also assumed that all shockwaves can be accurately analysed by normal shock theory and that all expansion or compression processes are isentropic. Also where two different gases meet at an interface (for example where the driver gas meets the test gas), it is assumed that the velocity and pressure of both gases are the same. These assumptions allow for a reasonably accurate set of results to be obtained from the analysis however there are some significant shortcomings as the following sections will detail. Highlighting the need for a means of more directly measuring the properties of a test flow.

2.1.5 Current Velocity Measuring Method Used for the X2 Facility

Currently the velocity of the test flow in the X2 is estimated by combining measurements with a theoretical analysis. Typically measurements of the static pressure in the tube are recorded by piezo electric pressure sensors mounted at several locations in the walls along the length of X2, flush with the tube surface. The information these sensors record is very useful, as it allows for the shock speed to be calculated [4]. Directly behind each shock wave there is a large rise in pressure which is recorded by

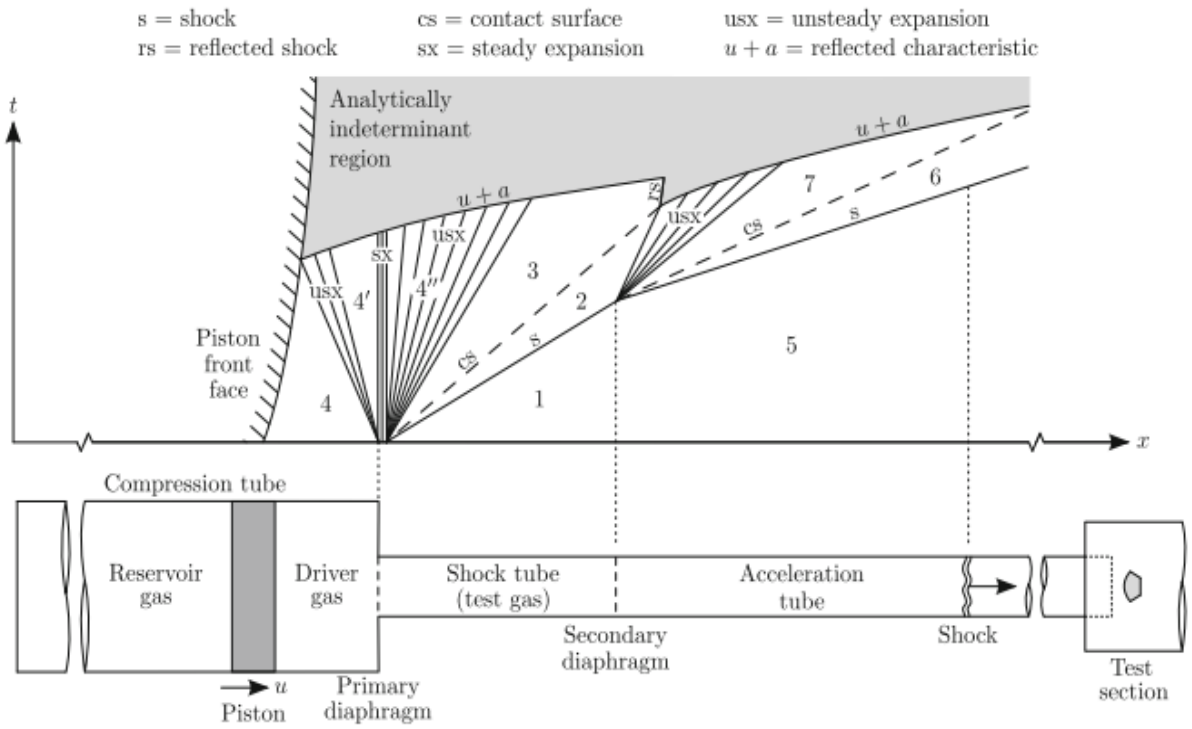

Figure 2.1.4: An X-T diagram showing the basic behaviour of the gas in a shock expansion tube directly after it is fired. Note that the contact surface term refers to interface between two different gases in the tube. (This diagram is directly adapted from "Development of High Total Pressure Scramjet Flow Conditions using the X2 Expansion Tube" by David E Gildfind [1].)

each transducer as an almost instantaneous rise in pressure. Therefore it is possible to determine exactly when the shock passes each transducer and the time it takes to travel between transducers. Given this distance is known, calculating the shock velocity is simple physics. This measured shock speed is then used in conjunction with inviscid flow theory to calculate the velocity of the test flow behind it. Referring to Figure 2.1.4, knowing the shock speed (u_s) separating region 5 from region 6 means that the velocity of the gas in region 6 (u_6), and by extension the test gas in region 7, can be calculated using normal shock theory. These

calculations are conducted using the following equations where γ_a and R_a are the ratio of specific heats and ideal gas constant for the gas in the accelerator tube respectively.

$$M_s = \frac{u_s}{\sqrt{\gamma_a R_a T_a}} \qquad \textit{Eqn 2.1}$$

$$M_6 = \sqrt{\frac{(\gamma_a - 1)M_s^2 + 2}{2\gamma_a M_s^2 - (\gamma_a - 1)}} \quad \textit{Eqn 2.2.}$$

$$T_6 = T_a \frac{[2\gamma_a M_s^2 - (\gamma_a - 1)][(\gamma_a - 1)M_s^2 + 2]}{(\gamma_a + 1)^2 M_s^2} \quad \textit{Eqn 2.3.}$$

$$u_6 = u_s - M_6\sqrt{\gamma_a R_a T_6} \qquad \textit{Eqn 2.4.}$$

Unfortunately this method of determining the test gas velocity does not accurately capture the behaviour of the flow. It is still a quick and effective way of gaining a reasonable estimate of the velocity, however the analytical part of this process relies on several assumptions which are not particularly appropriate. It is sometimes more accurate to assume that the measured shock speed is the same as the test flow and this is something that is regularly done by operators of the X2. There are more sophisticated analysis techniques which can more accurately model the flow in shock expansion tubes, including X2. Computational Fluid Dynamics (CFD) simulations are the most pertinent example of this. These simulations are capable of capturing a wide range of flow behaviours, including viscous effects, which an inviscid flow analysis cannot. They are not limited by simplifying assumptions and are capable of providing more accurate test flow velocity results; although it should be mentioned that these results still carry a level of uncertainty. However, despite the advantages of CFD, the variations of the simplified analytical techniques described earlier in this section, are still more commonly used to characterize test flows in shock expansion tubes (or at least this is the case with the X2 facility). CFD simulations are quite complex and can be difficult and time consuming to set up. In addition, simulations can be very computationally intensive and take a lot of time or resources to run. Therefore, an inviscid flow analysis informed by measurements taken from the facility is still one of the most common methods of determining the test flow velocity in shock expansion tubes. The next two sections of this report outline the short comings of this process and explain why it is sometimes assumed that the test flow velocity is the same as that of the leading shockwave.

2.1.6 Mirels Effect

The assumption of inviscid flow is a somewhat poor assumption to make in the case of a shock expansion tube. This is because significant boundary layers form, which are very much characteristic of viscous flow. These boundary layers are stagnant regions which form along the wall of the expansion tube and absorb gas from the region of the flow behind the leading normal shock. This non ideal effect,

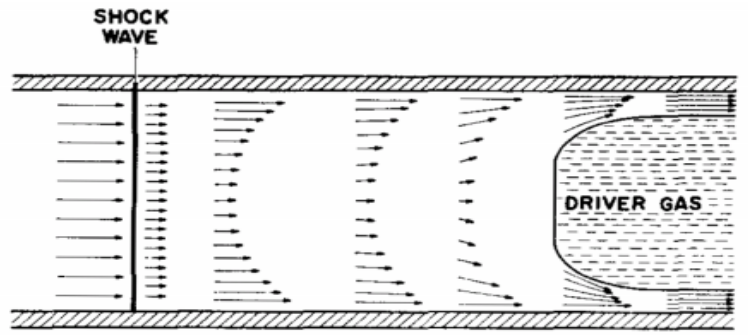

Figure 2.1.5: A Schematic showing how Mirels Effect, impacts flow in shock tubes.[5]

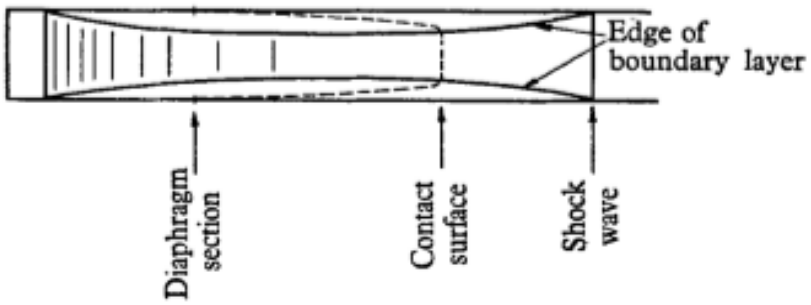

Figure 2.1.6: Another Schematic also showing have boundary layers typically from in shock expansion tubes behind the shock wave. (Directly adapted from "A review of theoretical treatments of shock-tube attenuation" by D. A. Spence and B. A. Woods [8].)

commonly referred to a Mirels Effect after Harold Mirel [14] who devised the first generally accepted mathematical model to describe the phenomenon, causes significant variation from the inviscid flow model discussed in the previous section. Whilst theory predicts that a normal shock travels away from the interface of the driver and test gases (often referred to as the contact surface) at a constant rate, entrainment of gas into the boundary layer between the shock and the interface (Refer to Figure 2.1.5) means that this is not what eventuates in reality. In actual fact, the contact surface accelerates whilst the shock wave decelerates, to a point whether the velocities of both are similar, provided the expansion tube is long enough. Hence the velocity of the test flow produced by the expansion tube facility will obviously be different

to what theory predicts, as will the pressure and temperature. The development of boundary layers also has an impact on the core of the test flow; which must have a smaller cross sectional area due to the space occupied by the boundary layer[14]. This shrinking of the core flow is not accounted for in any way by the theoretical analysis currently used to determine the test gas velocity, as the inviscid flow assumptions prevent this.

It is possible to model Mirels Effect analytically using the theory developed by Harold Mirel, and this is often incorporated into the analysis of shock tubes in an attempt to better characterize the test flow. It should be mentioned however, that whilst Mirels Theory is widely accepted and has been proven to correlate well with experimental results [1], it too is limited by the assumptions it is based on. For example, the original theory incorporates the Blasius model for skin friction, which at the time the theory was devised, was the best model for approximating the effects of skin friction [15]. However, this model of skin friction is also limited in terms of its accuracy, particularly under certain conditions. Different and more modern frictional models exist which can be more effective in certain circumstances. A good example of this is work done by Peterson and Hanson, [16] who adapted Mirels theory to incorporate the Spalding-Chi friction model which was considered to be a superior when simulating high pressure shock tubes. The point being that, even if Mirels theory is incorporated into the analysis used to find the test gas velocity, there is still uncertainty about the result. Therefore, a strong case for experimentally measuring the velocity of test flows within expansion tubes still exists.

2.1.7 Other Short Comings of Current Velocity Estimation Method

Another assumption that the current velocity estimation technique relies on is that the diaphragms in the facility do not impede or disturb the flow in anyway. In reality this is not true, although the disturbances are reasonably small. The rupture of the primary diaphragm is relatively insignificant in terms of the disturbance it causes. This diaphragm is typically steel and through techniques such

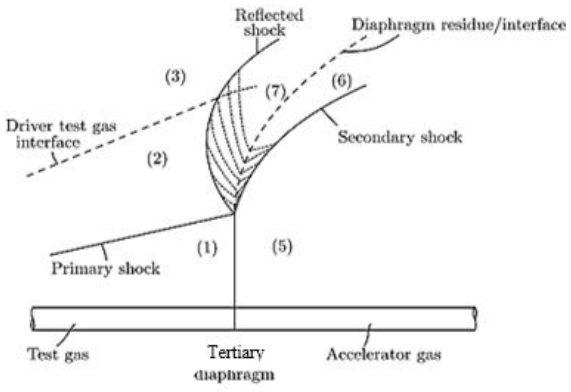

Figure 2.1.7: A modified X-T diagram showing the behaviour of the flow as it impacts and breaches the tertiary diaphragm. (Adapted from "Development of High Total Pressure Scramjet Flow Conditions using the X2 Expansion Tube" by David E, Gildfind) [1].

as scoring, it can be weakened in certain areas such that it fails at a reasonably consistent pressure and in a manner which least obstructs the flow of the driver gas. However, the secondary and tertiary diaphragms can have a more significant effect on the flow in the tube. To simplify the analysis, it is assumed that both these diaphragms are completely eliminated as soon as they are hit by the leading normal shock, absorbing no energy from the flow. This is why these diaphragms are made out of thin, light materials which can be easily ruptured. However, even the minimal weight of these diaphragms has measurable and significant effect. Due to the rapid loading of the diaphragm, as it is impacted by the leading shock, failure tends to occur around the periphery causing the entire mass of the diaphragm to be carried forward by the flow. This diaphragm does eventually break down into small fragments which allows the gas to continue unobstructed through the expansion tube. However, initially accelerating this mass absorbs energy and this is reflected in Figure 2.1.7 by the fact that interface and secondary shock accelerates from zero in a non-instantaneous fashion. This is not accounted for in the theoretical analysis used to determine the test flow velocity and is therefore another reason why a direct measurement technique is needed. Some CFD codes do attempt to capture this behaviour with reasonable success. These codes generally use an inertia model which to takes into account the effects of the diaphragm being accelerated by the flow for a short distance after it ruptures. Such models have been well refined and are effective, however there is still a degree of uncertainty surrounding how and when the diaphragm breaks down which means that these codes are never completely accurate [1, 17].

Finally, there are range of other acoustic disturbances which interfere with the flow in shock expansion tubes. These can originate from a variety of sources such as the bursting of diaphragms and the rough surface of the shock tube walls [4]. These the existence of these disturbances, which again are not accounted for in any of the theoretical modelling, furthers the case for a means of directly measuring the test flow velocity.

2.1.8 Summary

In summary it is clear from the information presented in this section that there is significant uncertainty associated with the determining the velocity of the test flows produced by shock expansion tubes. Even if CFD codes, which have been designed to account for Mirels effect and diaphragm rupture, are used to more correctly determine these properties this element of

uncertainty still exists. Hence justifying the need for an instrument which can be used to better characterize the test flow. In this case, an instrument which can be used to determine the flow velocity.

2.2 Potential Techniques and Instruments for Test Flow Velocity Measurement

This section details four velocimetry techniques (listed below) which have the potential to measure the velocity of the test flows produced by shock expansion facilities, in this case the University of Queensland's X2 facility.

- Planar Laser Induced Fluorescence (PLIF)
- Rayleigh Scattering
- Tuned Laser Diode Absorption Spectroscopy (TDLAS)
- Pitot Probe Measurements

During a review of literature in this area, it was found that the are many different ways to measure the velocity of a hypersonic flow. So many in fact that it was impossible to investigate everyone in an appropriate level of depth. Further investigation in this area may uncover more useful and innovative methods of measuring the velocity in shock expansion tubes not mentioned in this review. However these four techniques were considered the most appropriate to investigate in further depth for several reasons. Firstly because they were the most common velocimetry techniques encountered in the literature. There were several examples of each of these instruments and measurement methods being successfully used in hypersonic test facilities so there was no doubt about their potential in this regard. In addition, many of the other velocimetry techniques encountered were derivations of, or worked in similar ways to, the four methods listed above. For example, there were several different flow tagging techniques encountered in literature however most of these were largely similar to PLIF methods. Finally these four techniques were considered to be the most feasible in terms of actually carrying this project forward into a design stage. They were some of the least complicated velocimetry methods encountered in the review, which would obviously simplify any future design process. In addition, these techniques required instruments and equipment

which could potentially be procured for testing at The University of Queensland. Hence why they the most appropriate for further investigation in the following sections.

2.2.1 Planar Laser Induced Fluorescence Velocimetry

Planar Laser Induced Fluorescence molecular tagging velocimetry (PLIF MTV) describes a range of optical methods used to measure the speeds of fluids. In essence, these techniques involve firing a laser at the moving body of gas to excite specific molecules [18]. When in an excited state these molecules release photons causing them to fluoresce for a short period of time before they return to their ground state. The light emitted by these particles can then be captured by a camera and used to determine the velocity of the particles [19].

This technique has been implemented in many different ways in the past. This is partly because there are several ways in which laser light can be used to excite particles in the flow to a point where they fluoresce [18-21]. Some techniques involve seeding molecules into a flow which have favourable properties for excitation by laser light. A good example of such a molecule is biacetyl, which can be excited with a laser to emit light for a relatively long period of time; a useful property for MTV [20]. However, when it comes to high enthalpy impulse facilities like shock expansion tunnels, seeded particles are often problematic. Among other complications, seeded particles don't always accelerate to the same velocity as the test gas and are difficult to introduce into the flow [22]. Hence PLIF MTV techniques which involve seeding will not be focused on in this section. However, it is possible to use lasers to cause test gas molecules contained naturally within a typical shock expansion tube flow to fluoresce [18, 21].

For example, in 2003 researchers at The Australian National University, in collaboration with Paul M. Danehy [18], used PLIF techniques to measure the velocity of hypersonic flows in the University's T2 and T3 reflected shock tunnels. Reflected shock tunnels don't have the same capabilities as shock expansion facilities in terms of their ability to produce high enthalpy, high Mach number flows. However, the upper performance range of these tunnels still overlaps with the mid-low range performance capabilities of expansion tubes. Therefore, this PLIF velocimetry technology could easily be adapted for use in expansion facilities. Using an excimer-pumped dye laser and a series of lenses, a 3mm wide beam of laser light with a wavelength of 225nm was directed into the test section of the shock tube. This laser beam excited a line of nitric oxide

(NO) molecules which naturally exist in reflected shock tube test flows. An intensified CCD camera and a range of light filters, positioned perpendicular to both the flow and the laser beam, were then used to record the location of the fluorescing NO molecules. From these images, the displacement of the NO molecules and therefore the test flow velocity could be determined. Unfortunately, there were concerns during this investigation that oxygen molecules may have had a quenching effecting on the excited NO molecules, causing them to return to their ground state before their fluorescence could be captured by the cameras. To avoid this being a problem, the investigation was conducted with the test gas containing only 1.1% oxygen. Therefore, this velocimetry technique is most probably not appropriate for measuring the velocity of air test flows, due to the high oxygen content. Since air is a very common test gas in hypersonic facilities globally this method is not particularly appropriate.

A more robust PLIF MTV technique which could possibly be used to measure the test flow velocities produced by shock expansion tubes is the RELIEF method. The Raman excitation laser induced electronic fluorescence (RELIEF) technique involves using two different lasers to excite oxygen molecules to the point of fluorescence. The first laser excites the oxygen molecules into their first vibrationally excited state via a method known as simulated Raman scattering. A short distance downstream, a second laser is used to further excite the molecules to the point where they fluoresce. At this point cameras can be used to record the displacement over time, of the fluorescent molecules and hence directly measure the velocity of the particles [21]. A study conducted by Miles et al [21], used this RELIEF technique to determine the velocity of a turbulent jet of air. In their experiment they used a Nd:YAG laser in conjunction with a Raman Shifter to generate two laser beams with wavelengths of 532nm and 581nm. These were then directed at the air jet in 10ns pulses to tag (excite) a line of oxygen molecules 100μm wide to their first excited state. Further downstream an ArF laser, which produces a 50mJ pulse of light at a wavelength of 193nm, was fired at the tagged molecules to excite them to the Schumann-Runge band at which they emit near ultraviolet light. An ultraviolet camera located 60cm further downstream was used to capture photographs of the fluorescent lines at set times intervals. Through analysis of how far the lines had moved over the time interval between photographs, the velocity of the oxygen molecules and therefore the air jet could be determined [21]. This study only concerned low velocity subsonic flows, however RELIEF

techniques have been used to characterize flows up to Mach 4, and the extension of the technique for use in the hypersonic regime looks very promising [22].

2.2.2 Rayleigh Scattering

Rayleigh Scattering is another laser based velocimetry method capable of determining the velocity of an expansion tube test flow. In short a high powered pulsed laser is used to project a sheet or line of electromagnetic radiation through the cross section of the flow. Provided that the wavelength of the laser is tuned correctly, small molecules contained by the flow, such as the oxygen molecule O, will scatter some of this radiation. Using specialized cameras, often in conjunction with filters to remove any background noise, this radiation can be captured and analysed. If the scattered radiation was caused by a moving particle then its wavelength would have undergone a Doppler shift. The magnitude of this shift will depend on the velocity of the particle as a result of the Doppler effect. Hence by analysing the frequency of scattered radiation, the velocity of the particle which caused the scattering can be determined, therefore revealing the test flow velocity as well [23].

Rayleigh scattering is a highly sensitive velocimetry technique and is capable of producing very accurate results. However, it is also sensitive to background radiation at similar wavelengths to that of the scattered wavelengths. Such radiation can interfere with the velocity calculations and is not always easy to filter out. For example, researchers at the Australian National University made multiple attempts to characterize the velocity of the hypersonic test flows produced by their reflected shock tunnels. However they found it impossible to separate the Raleigh scattered radiation from other radiation present in their facility and therefore could not produce any meaningful results [18, 19]. Ultraviolet lasers have been suggested to reduce this background noise effect as they produce higher frequency beams which increases the intensity of the scattered radiation. Hence the effect of noise is less significant against more intense scattered radiation [24].

2.2.3 Tuned Laser Diode Absorption Spectroscopy

Tuned Laser Diode Absorption Spectroscopy or TDLAS is another process in which laser beams are directed through a gas flow to determine the properties of the flow. In the case of TDLAS, the laser beam is directed through a section of the flow at a detector such as photo diode [25].

As the laser beam passes through the flow it will interact with the particles contained in the gas mixture. Each of these gas particles (or molecules) has an ability to absorb light in particular frequency bands, depending on the species of the particle. These frequency bands are well known for most species hence by tuning a laser correctly, it is possible to get a specific species contained within the flow to absorb some of the light produced by the laser. The amount of light absorbed can be measured by a photo detector as a drop in the intensity of the laser beam. Hence it is possible to determine whether a specific species is present within a gas mixture by tuning a laser to the absorption spectrum of that species and determining if its intensity drops as it passes through the mixture. It is also possible to determine a variety of other properties of the absorbing molecules including their velocity.

As with Rayleigh scattering, the Doppler effect is again used to determine the velocity of the molecules. If the molecules are moving at a different speed to that of the light source (in this case the laser) they will exist in different frames of reference, in which the frequency of the light produced by the laser will be different. Hence if the absorbing molecules are moving at speed, the frequency of light that they will absorb will be different in the laser frame of reference. Therefore, by analysing how much this frequency band changes (shifts), the velocity of the particles and the flow can be determined. This Doppler shift is generally quite small, so by varying the frequency of the laser output around the absorption band of the molecules in question, this shift can be measured allowing for the velocity to be calculated. TDLAS methods have already successfully been used to determine flow properties in shock tubes, one example being the experiments carried out by L. Philippe and R. Houston in 1991 on an oxygen filled shock tube[26].

TDLAS offers an accurate means of determining the velocity of a hypersonic flow in a test tube however it does have one major drawback being that like Rayleigh scattering, TDLAS is sensitive to background noise. The amount of light absorbed by a particular molecule is reasonably small and therefore the change in the intensity of the laser beam, when it is tuned to the absorption spectrum of that species, is typically small. Hence any background radiation of similar frequencies, which can often be present in shock expansion facilities, can interfere with TDLAS measurements [27]. As a result, frequency and wavelength modulation techniques have been developed in an attempt to mitigate the effect of this background noise [25, 26].

2.2.4 Pitot Probes

Pitot probes are an incredibly common instrument, and have all sort applications, including in hypersonic facilities. Pitot probes are already widely used in shock expansion tube facilities to locate the core of test flows and determine the thickness of the boundary layer. Typically, these probes are mounted on a rake in the test section of the tunnel, as Figure 2.2.1 shows [4]. A Pitot probe is a relatively simple instrument which measures the stagnation pressure of the flow directly in front of it. In supersonic and hypersonic flows a normal shock will form in front of the probe meaning that the stagnation pressure measured, is not that of the flow, but rather the stagnation pressure of the flow after it has been processed by a normal shock. From this pressure it is possible to determine the Mach number and velocity of the flow around the probe. However, to do this, it is necessary to know the static temperature (T) and pressure (P). From these two values, the Mach number (M) and subsequently the velocity (V) of the test flow can be found based on the stagnation pressure measured by the probe (P_o). (Where γ is the ratio of specific heats of the test gas)

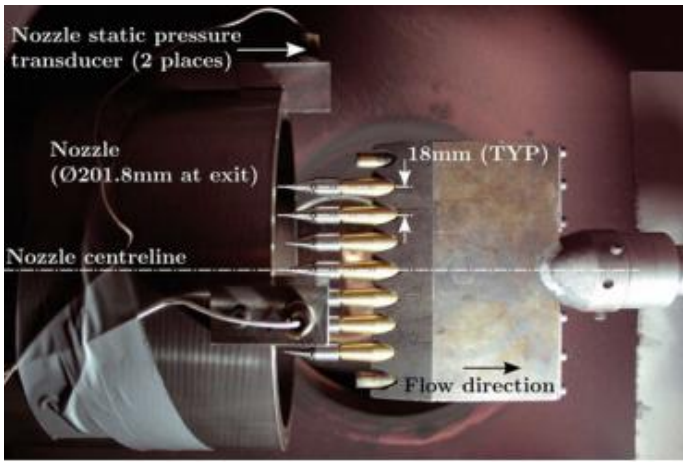

Figure 2.2.1: Pitot probes mounted on rake in the University of Queensland's X2 expansion tunnel [4].

$$\frac{P_0}{P} = \left(\frac{(\gamma+1)^2 M^2}{4\gamma M^2 - 2(\gamma-1)}\right)^{\frac{\gamma}{\gamma-1}} \left(\frac{1-\gamma+2\gamma M^2}{\gamma+1}\right) \quad \textit{Eqn 2.5}$$

$$V = M\sqrt{\gamma R T} \qquad \textit{Eqn 2.6}$$

(Note the equation 2.5 would have to solved by some iterative or numerical method to find M)

The problem with this method, with regard to shock expansion facilities, is that it is very rare that the temperature and static pressure of the test flow are actually known. These properties are as difficult to measure as the velocity and as such this traditional method of using pitot probes to measure velocity is effectively useless.

Despite this, it is not impossible to use pitot probes to measure the velocity of flows within hypersonic facilities. One method which is worth investigating is using two probes to detect the arrival of the test gas at two different locations. The idea being that, by measuring the time it takes for the test gas to travel between these two probes, which are separated by a known distance, the velocity of this gas can be determined. When the test gas arrives at each probe a change in stagnation pressure will be recorded due to the fact that the properties of the test gas will vary from that of the gas used to fill the acceleration tube. Whilst the static pressure and velocity of the two gases are the same at the point at which they interface, the difference in their properties mean that they will behave differently across the normal shock which will form in front of the pitot probe. They will also have different stagnation pressures resulting in a significant stagnation pressure difference between the two gases at the probes.

Figure 2.2.2 displays pitot pressure measurements made by a probe mounted on a rake in the University of Queensland's X2 shock expansion facility. As can clearly be seen from this graph there is a significant reduction in pitot pressure between 0.72ms and 0.78ms which indicates the interface between the test gas and the gas used to fill the acceleration tube passed the pitot probe over this period of time. By measuring the time delay between the arrival of this interface at the two separate pitot probes it would be possible to determine its velocity. Based on the assumption that the test gas is steady, its velocity can be inferred from the interface velocity.

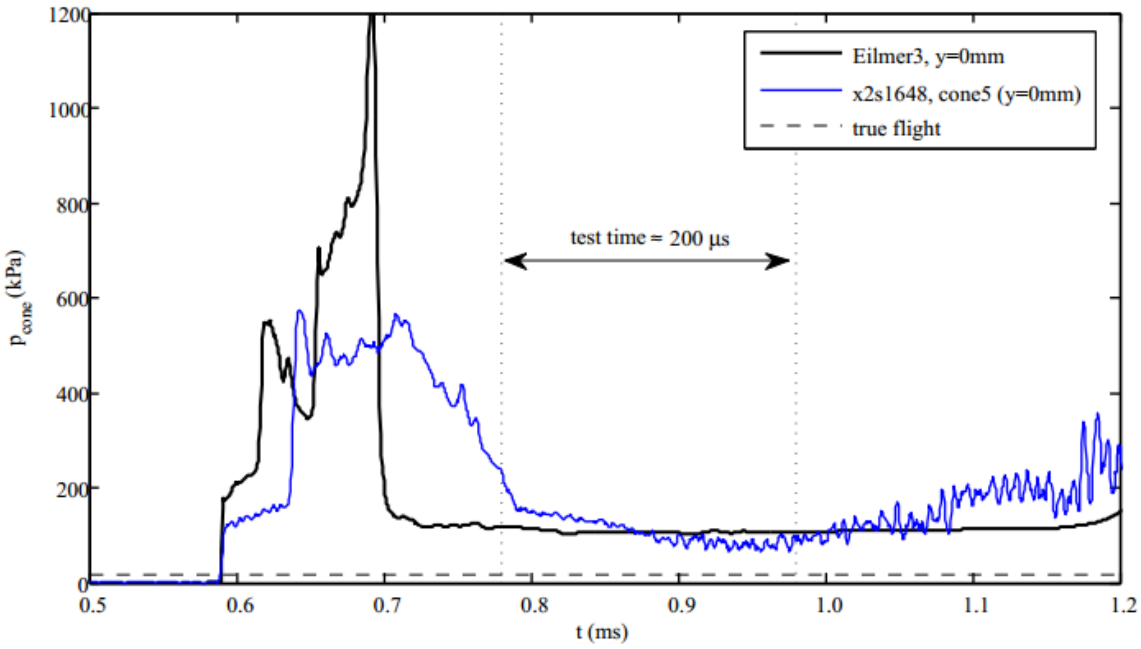

Figure 2.2.2: A plot of the pitot pressure in The University of Queensland's X2 shock expansion tube as measured by a probe mounted on a rake in the test section. The blue line on the graph shows the measurements taken by the probe whilst the black line shows a CFD prediction of the pitot pressure (irrelevant to this investigation). The arrival of the test gas at the probe is indicated by a drop in the measured pitot pressure at around 0.78ms. (Graph sourced from "Development of High Total Pressure Scramjet flow Conditions Using the X2 Expansion Tube" [1, 2].)

There are a few downsides associated with hypersonic pitot probes, the first of which is that they can often disrupt the uniformity of the flow. Since pitot probes often occupy a reasonably large space, compared to the diameter of the shock tubes, they can disrupt an otherwise uniform test flow rendering it useless for actual testing. For this reason, pitot probe measurements currently taken in expansion tubes, are not taken when the facility is actually being used to test a model. In addition, hypersonic flow creates an extremely harsh environment in which to take stagnation pressure measurements. The temperatures and pressures involved mean that transducers normally used to determine this pressure, often cannot withstand direct exposure to the high velocity, high enthalpy flows. As such they need to be protected in some way. A variety shielding caps, such as the ones shown in Figure 2.2.3 been devised to do this exactly this. These caps reduce the pressure and temperature of the flow which contacts the surface of the transducer by blocking the line of sight path between the freestream and the sensor. Unfortunately they all cause an increase in the response time of the pressure sensor which can be problematic for high velocity flows where short response times are essential [4].

Finally a phenomenon known as Helmholtz resonance can also be the source of some difficulty with regards to taking pitot probe measurements in hypersonic flows [10]. Helmholtz resonance is essentially the vibration of air in a small cavity at its resonance frequency. It is relevant to hypersonic pitot probes as the shielding caps and other probe stem designs typically direct the flow through small holes to the surface of the pressure transducer. Helmholtz resonance can occur in the holes and cavities of these protective shrouds causing wild oscillatory responses to be recorded by the pressure transducer. Therefore, this is another factor which needs to be considered in order to make meaningful pitot pressure measurements.

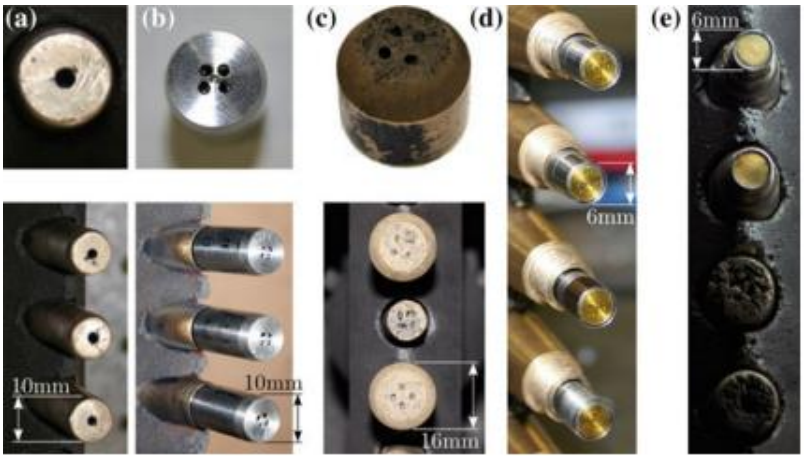

Figure 2.2.3: Different varieties of shielding caps used to protect hypersonic pitot probes [4].

2.3 Evaluating The Best Velocimetry Instrument for Shock Expansion Tubes

Of the velocimetry instruments outlined in Section **Error! Reference source not found.** it was decided that the most appropriate one to move this investigation forward with is the pitot probe. There are several reasons for this decision, the first of which is its simplicity. Compared to PLIF, Rayleigh Scattering and TDLAS techniques, pitot probe velocimetry is relatively simple. The instruments themselves lack complexity and produce an output from which a flow velocity can easily be determined. This compares to the laser based methods, all of which require sophisticated lasers, cameras and other optical equipment to be setup in a very precise manner. In addition, the analysis of the data collected from these lasers based methods can be quite involved and requires a good understanding of the quantum mechanics governing light emission, scattering and absorption. Given the time constraints on this investigation, not having to spend large amounts of time gaining an understanding of the theory behind these velocimetry technique is an obvious advantage.

Another reason why pitot probe technology was chosen over PLIF, TDLAS and Rayleigh Scattering was due to the equipment involved. Lasers, CCD cameras, and other optical equipment are often expensive pieces of equipment to procure. This contrasts with the pressure transducers required for pitot probes which are cheaper and are already widely used in shock tube facilities. The cost of the pitot probe's structural frame, as well as the protective cap will depend on its design but is unlikely to be excessively expensive to produce. In addition, the use of lasers can also be dangerous as they produce powerful concentrated beams of light which could easily cause damage to someone's eyes. This means that precautions have to be taken, such as the removal of any partially reflective surface from the room in which the laser is operating. This may seem trivial but it is a significant task considering today's strict OH&S standards.

Finally, as this investigation is focusing on developing an instrument for testing in the University of Queensland's X2 shock expansion tunnel, the ability to effectively install and operate the instrument in the X2 tunnel must be considered. Critically the facility only has viewing windows in the test section of the tube. This is significant as TDLAS, PLIF and Rayleigh scattering techniques all require optical access to the test flow. However, in order to avoid interfering with any model being tested, the windows in the test system cannot be used for velocimetry. The only other access to the developed test flow is through a series of 18mm holes located on opposite sides along the length of acceleration tube. Since PLIF velocimetry generally requires that a camera and a laser beam have line of sight access to the flow at perpendicular angles to each other it would be very hard to install such equipment in that configuration. Likewise, for Rayleigh Scattering techniques, a camera needs to be mounted such that it can observe light scattered from the laser beam by particles contained in the flow [23]. Again this is difficult to do given the geometry of the acceleration tube. Therefore, to implement either of these two techniques, modifications would have to be made to the facility which is highly undesirable. TDLAS equipment could potentially be installed in the X2 as the laser beam only has to be directed through the flow into a detector [25]. Therefore, it is entirely feasible that the beam could be directed through two of the access holes and into the detector. However, for the reasons stated in the previous two paragraphs, and the fact that background radiation present in the facility could interfere with TDLAS measurements, the pitot probe option was still

preferred. (Perhaps in future, with more time, an investigation into TDLAS velocimetry in shock expansion tubes would be worth conducting, as the technology has the potential to be a very useful tool.) In any-case pitot probes could be designed such that they can be mounted in the access holes of the acceleration tube and as such could be easily installed in the X2 facility.

Obviously pitot probe technology also has its drawbacks. Potential issues such as excessive test flow disturbance, slow response times and noisy data resulting from Helmholtz resonance in the protective cap will all have to be considered. However, these are all issues which should be possible to design a solution to. Firstly, by designing a small streamlined probe it is possible to reduce the disturbance created in the flow. Through examining other hypersonic pitot probe designs and how they managed to minimised flow disturbance, it should be possible to establish what is required in this regard. The challenges surrounding response time can also be addressed by ensuring that the transducer is located as close as possible to the free stream and that the probe stem is appropriately designed to have a minimal response time. Finally Helmholtz resonance is a problem which has been addressed by several researchers, for example, McGilvray et al [10]. By using the solutions these researchers came up with to inform the new probe design it should be possible to ensure the Helmholtz resonance does not interfere with the pressure measurements. In summary, with further research and analysis these issues should be overcome and this design project be successful.

3 Current Hypersonic Pitot Probe Technology

As eluded to in previous sections pitot probes are already in widespread use in the field of hypersonics. Most supersonic and hypersonic pitot probes have a similar configuration. All probes have a stem into which the oncoming air flows. As such there is normally one or more holes in the forward face of the stem to facilitate this. Once the air enters these holes it is stagnated against a pressure sensor from which information about the flow the probe is immersed in can be gathered. The probe also has to be supported in some fashion, although there are many different ways this is done. This section looks at the various ways pitot probes have been designed in the past, with the objective of informing the future design of probes capable of measuring the velocity of test flows in shock expansion tubes [4, 28].

3.1 Probe Stem Design

3.1.1 Shielded Probes

Traditional subsonic pitot probes typically have a largely hollow stem at the bottom of which a pressure sensor can be mounted. However, in the case of hypersonic probes, it is often necessary to shield the pressure sensor in some way due to the high temperatures caused by stagnating the flow. As such there is rarely any direct line of sight from the pressure sensor to the flow itself. Therefore, hypersonic pitot probe stems often have protective caps or shields which block the line of sight to the pressure sensor and protect them from these temperatures [4]. Generally the pressure sensor is located directly behind (or very close to) these caps, as the closer the sensor is to the free stream the faster it will respond to the freestream pressure. This is because the smaller the body of gas between the freestream and the sensor, the more quickly a change in the freestream pressure can be transmitted through this gas to the sensor surface [29].

Figure 3.1.1 shows a range of different caps that have been used in probes at The University of Queensland's hypersonic facilities (including the X2 shock expansion facility). Shield a) is a brass cap with a single hole behind which a diffuser blocks the line of sight to the pressure sensor. Shield b) and c) are stainless steel and brass caps respectively with four vortically aligned holes which spiral into a cavity containing the pressure sensor[4]. This design also addresses the problem of Helmholtz resonance. As eluded to in a previous section, this phenomenon can

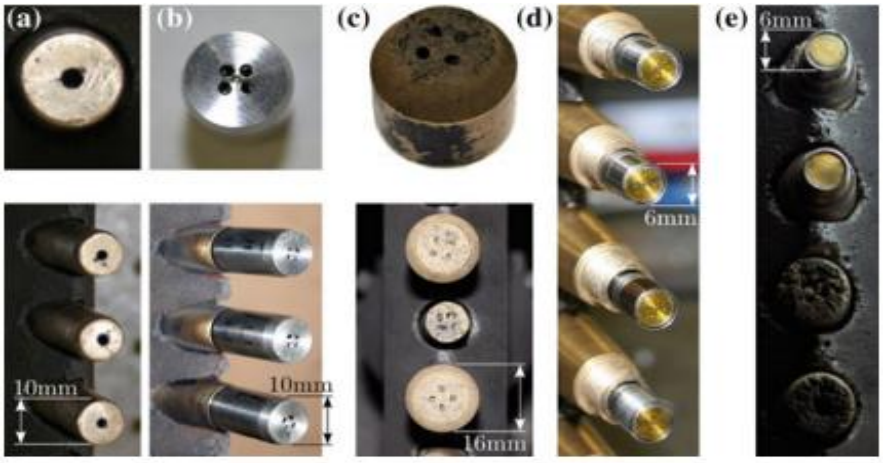

Figure 3.1.1:This figure depicts a range of different pitot probe shields or protective caps and how they are typically mounted in a rake [4].

affect the performance of these protective shields, as there is potential for gas to vibrate at a resonant frequency in the holes and cavities of the shields. This then can result in noisy pressure measurements being recorded by the pressure sensor. The vortically aligned holes of protective caps b) and c) are designed to help damp out the effects of this resonance [10]. Finally shields d) and e) are examples of where brass shims and cellophane are applied directly to the surface of the pressure sensor to protect from the high heat loads [4].

All of these protective caps have been proven to be effective in shock expansion tunnels under certain conditions, however even these methods cannot protect the pressure sensor from the heat associated with high pressure flows at high Mach numbers [4]. One means of solving this problem is to use a protective shield which has an angled surface and a pointed tip, such that an oblique shock forms over the probe as opposed to a bow shock. The temperature of the test gas processed by this shock is far less than that of the gas behind a bow shock, and as such this design significantly reduces the heat loading on the pressure sensor. However the major disadvantage of this design is that, it is not possible to know the angle of the shock that forms around the probe as it is dependent on the Mach number of the flow. Therefore, it is difficult to use the pressure measurement recorded by the flow to determine other properties such as its velocity. Fortunately, at high Mach numbers, shock angles tend to converge to the same value so it is still possible to gather useful information with this probe stem design under these conditions. Gildfind et at developed this protective cap design into a working pitot probe, the

drawings for which are shown in Figure 3.1.2. This shield was angled at 15 degrees to the flow direction with 8 holes directing portions of the gas processed by the oblique shock to a pressure sensor. In the case of the design below that sensor was a PCB transducer [9].

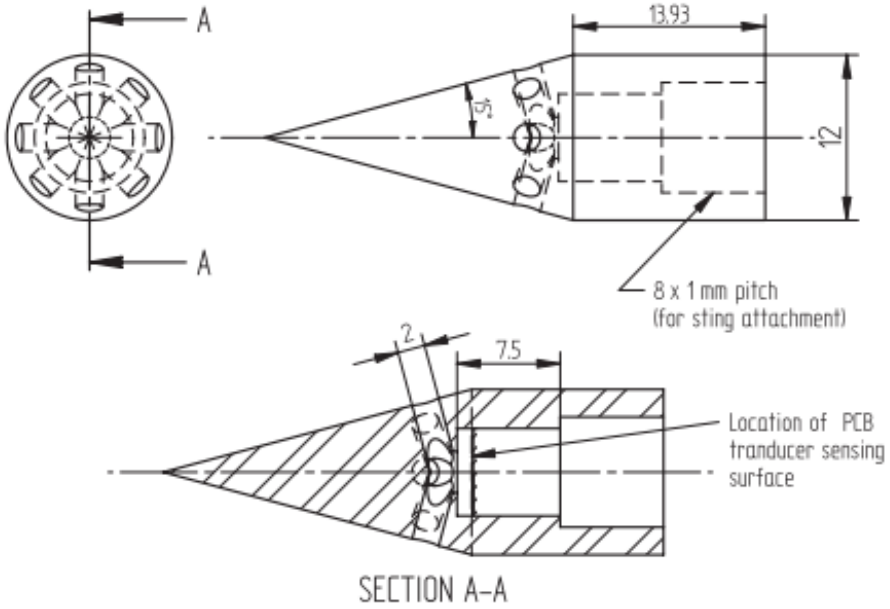

Figure 3.1.2: An detailed schematic of the protective pitot probe cap designed and produced by Gildfind et al.[9]

3.1.2 Unshielded Probes

Most probe stem designs which incorporate a protective shield or cap tend to have a frontal area of around a centimetre. However there are a range of unshielded and generally much smaller probes which have also been used in hypersonic facilitates. These stems can have an outer diameter as little as 0.25mm and as such have no space for protective caps. They are often just a hollow or flattened piece of heat resistant tubing leading to a pressure sensor. Since these probes are much smaller they offer a large advantage in terms of not significantly interfering with the hypersonic flow. Hence better allowing for measurements to be made during a test without disrupting the experiment. However they are also fragile and as such don't see much use in hypersonic facilities where there is a risk of impact with fragments of ruptured diaphragms (common in shock expansion tunnels) or other small objects entrained in the test flow. In addition, these small probes do nothing to address the potential over heating of the pressure sensors and therefore other means of protecting these sensors have to be employed. These means include water and air cooling systems as well as heat shields made from materials

such as graphite. Finally the small diameters of the tips of these probes often mean that the pressure sensor cannot be located in the stem itself. This means that gas from the freestream often has to travel further through tubing to get to the sensor, which is often housed in the structure upon which the probe stem is mounted. The problem with this is that it may significantly delay the response time of the sensor to freestream pressure changes, which can be problematic for impulse facilities in which whole tests occur in a few hundred microseconds[11-13, 29, 30].

An example of a situation where one of these small probe stems has been used is in an investigation conducted by Lafferty and Marren (1996) [11] into the performance of Hypervelocity Wind Tunnel N.o 9 at the White Oak Naval Surface Warfare Centre, in Maryland America. In this investigation, a number of probes, approximately 2.78mm in diameter and 17.78mm long and manufactured from heat resistant tantalum, were mounted on a rake in the wind tunnel and subject to Mach 7 test flows. Figure 3.1.3 shows a cross sectional schematic of how this probe was set up on the rake. Critical to this probe design was the air cooling line located in the cavity containing the pressure sensor (refer to Figure 3.1.3) which pumped cool air into this cavity at 40 psi to keep the sensor at a reasonable operating temperature [11].

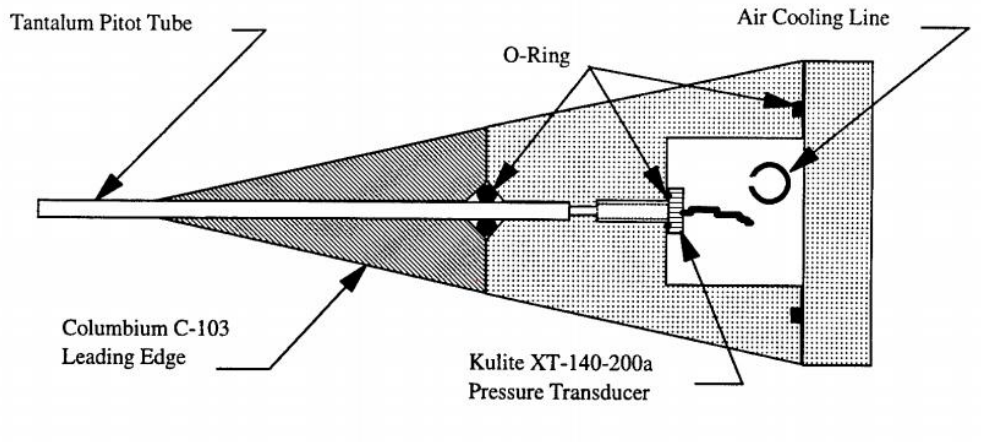

Figure 3.1.3: A cross sectional schematic of the tantalum pitot probe mounted on a rake in Hypervelocity Wind Tunnel N.o 9 [11].

Another example of a small unshielded probe was the design used by Demetriades and Laderman (1973) [13] for hypersonic testing. This simple design (refer to Figure 3.1.4) features a 0.81mm stainless steel tube which is flattened at its exposed end to a height of 0.51mm,

reducing the disturbance it creates in the hypersonic flow. These probes were mounted on a rake in a wind tunnel operating at Mach 9.4, however it is worth mentioning that this probe was used to survey a boundary layer and as such may not have be subjected to the full force of the freestream [13].

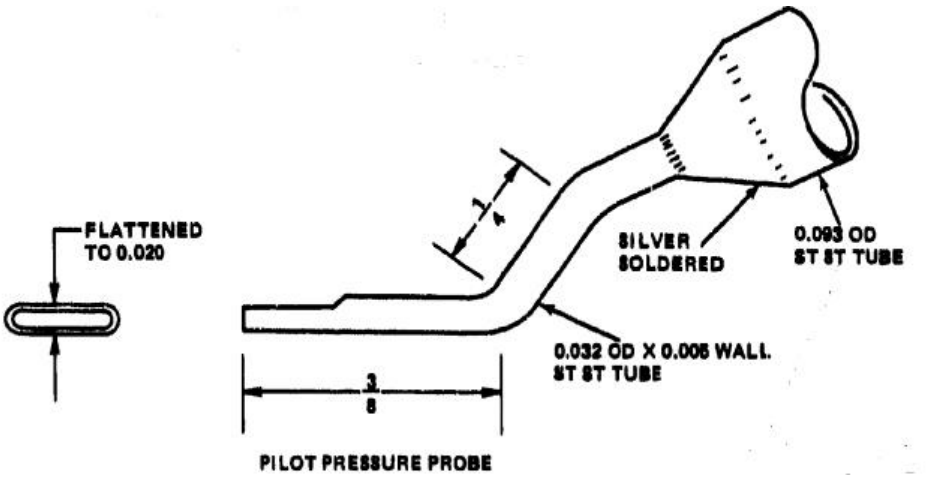

Figure 3.1.4: The pitot probe design used by Demetriades and Laderman, Note all dimensions are in inches. [13]

In addition, in 1988 George Ashby [3] attempted to design a probe which was small enough not to significantly disturb a Mach 6 hypersonic flow. The probe, pictured in Figure 3.1.5, featured a fine 0.33mm tube with a flattened (oval shaped) tip. This tube was successively increased in diameter to 1.016mm at its opposite end to minimize the settling time of the gas which passed through it into the pressure pickup chamber. Inside this chamber was a pressure sensor encased in a water cooled jacket to ensure it did not overheat. Ashby found this probe to be an effective design. Critically, the disturbance it created in the hypersonic flow was very much negligible, whilst it had a response time described as a 'fraction of a second' by Ashby. This was thanks to a design which focused on minimizing the settling time of the gas in the probe. It is worth mentioning however, that the wind tunnel used by Ashby was capable of generating Mach 6 flows for several minutes which is much longer than

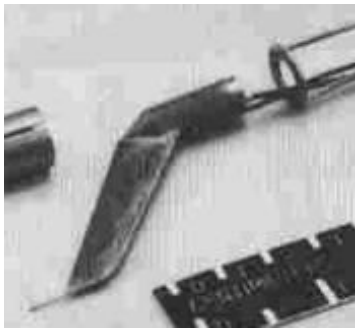

Figure 3.1.5:The miniaturized pitot probe designed by George Ashby to have a minimal disturbance effect on the freestream flow. The sensory end of this probe is the fine tip in the bottom left hand corner whilst the pressure camber is the cylinder at the opposite end [3].

shock expansion tubes. As such the response times of instruments in such facilities do not need to be as small as in expansion tubes.

Finally an unshielded probe was also used in a study conducted by Davis and Carver (1992) [12], aimed at calibrating an arc heated wind tunnel. This probe was significantly different from the previous one in that it was made from copper and water cooled. It was also larger, with a similar diameter to that of the shielded probes in Figure 3.1.1. Gas from the freestream enters the probe through a hole in the very tip and travels through this tube to a pressure sensor housed in the structure supporting the probe itself. To preserve the pressure sensor, a transducer in this case, it was located in a protective chamber behind the probe, where graphite and silica phenolic heat shields protected it from the high stagnation temperatures of the freestream, Copper mounting surfaces were also used to help conduct heat away quickly [12]. Figure 3.1.6 outlines the structure and internal workings of this pitot probe system.

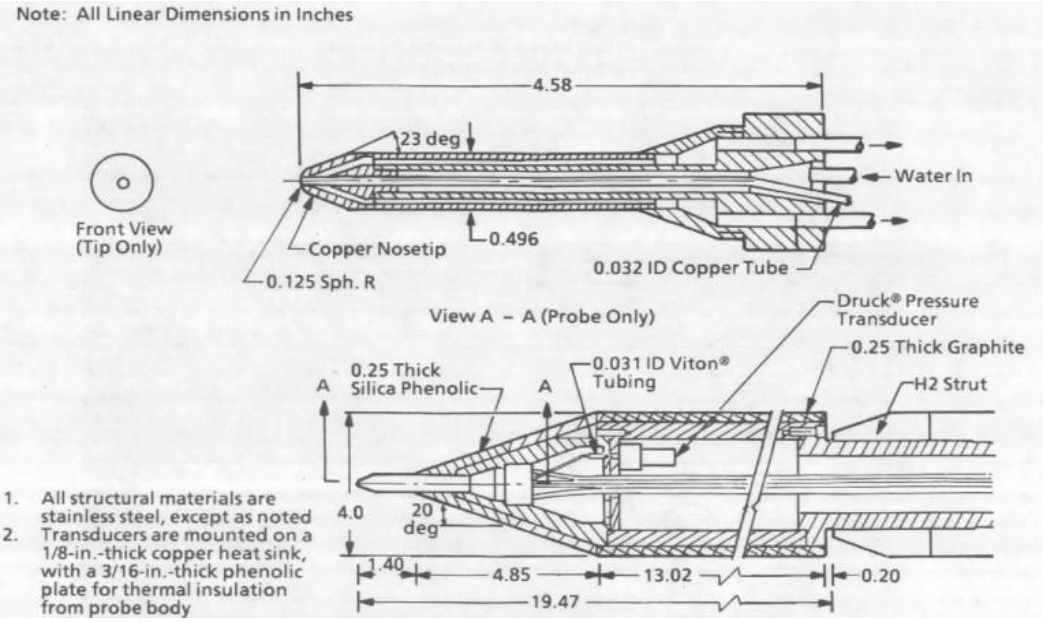

Figure 3.1.6: A cross sectional schematic diagram of the water cooled copper pitot probe used in the arc heated wind tunnel calibration. The top diagram shows the internal workings of the probe itself whilst the bottom diagram depicts how the probe is mounted and connects to the pressure sensor, in this case a Druck ® pressure transducer[12].

3.2 Probe Mounts

The supporting structure upon which pitot probes stems are mounted have three important functions. Specifically, they

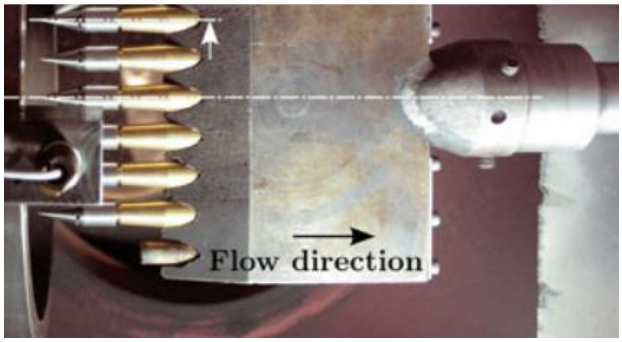

Figure 3.2.1: The rake used in the University of Queensland's X2 shock expansion tunnel. In this image it is supporting a number of probes spaced at 18mm intervals. (Adapted from Gildfind et al.) [4]

have to house and support the probes during tests, be capable of withstanding the drag forces and temperatures that come with being exposed to hypersonic flows, and also accommodate wiring, sensory components and possibly cooling systems associated with specific probe design. The vast majority of pitot probes are mounted on what is known as a rake. These structures are typically much larger than the pitot probe and are designed to carry multiple probes. They are ideal for use in hypersonic facilities as their size allows for them to be well supported structurally, and to protect the delicate parts of instruments they are housing from the harsh flow environment. Generally speaking, rakes resemble a thick flat plate which has had one of its edges chamfered on both sides to create a wedge shape[4, 30]. (Figure 3.2.1 shows an example of the rakes used in the University of Queensland's X2 shock expansion tunnel.) They are typically constructed from a strong heat resistant material. This is particularly important for the leading edge, which is exposed to the most extreme temperatures. As such it is not uncommon for this leading edge to be constructed from a different and more heat resistant material to the rest of the rake. An example of this is the rake used by Lafferty and Marren [11] which has a Niobium (Columbium) leading edge, a metal known to be an excellent conductor with a high melting temperature [11]. Steel is also widely used, especially in shock expansion facilities as its material toughness makes it less vulnerable to damage caused by diaphragm fragments caught up in the flow. Despite rakes being by far the most common structure to which probes are mounted to, they have one major drawback, in that they cause a large amount of interference in the freestream flow. Therefore, it is not possible to have a rake positioned in front of a test piece or model during a hypersonic experiment as it will significantly disrupt the test flow.

Other means of mounting pitot probes in hypersonic facilities vary depending on their application and the design of the probe stem. The most relevant example found in a review of literature was the mount for the miniaturized unshielded probe designed by Ashby (discussed in the previous section). This mount, shown in Figure 3.2.4, is a simple steel structure which supports a hollow cylinder with a pointed tip from which the pitot probe protrudes. The pointed tip of this cylinder houses the pressure sensor and the cooling system for this sensor, and as such was designed to protect these two things from the high stagnation temperatures of the hypersonic flow. Hence its shape, and construction from the Bakelite polymer which is an effective thermal and electrical insulator. This pointed tip also unscrewed from the remainder of

the cylinder which allows for its disassembly as can be seen in Figure 3.2.2. A more detailed schematic of this tip and cylinder is also displayed in Figure 3.2.3 [3].

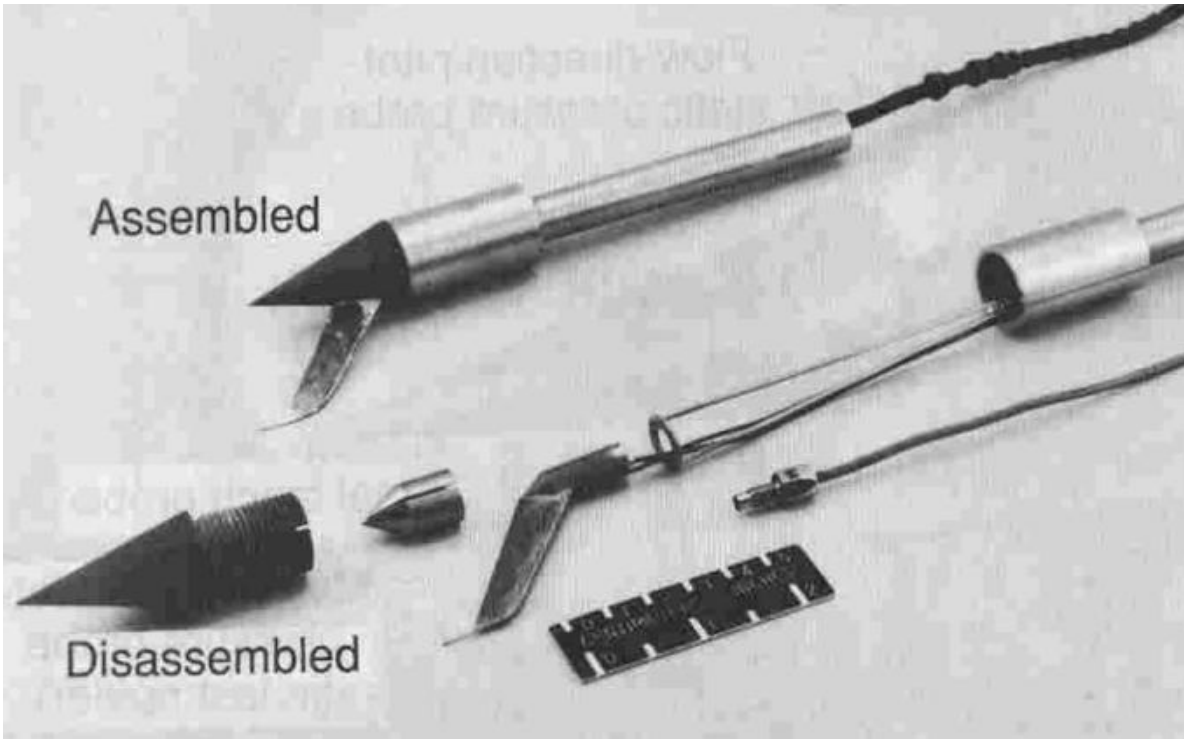

Figure 3.2.2: The pitot probe and the cylindrical part of its mount in assembled and disassembled form [3].

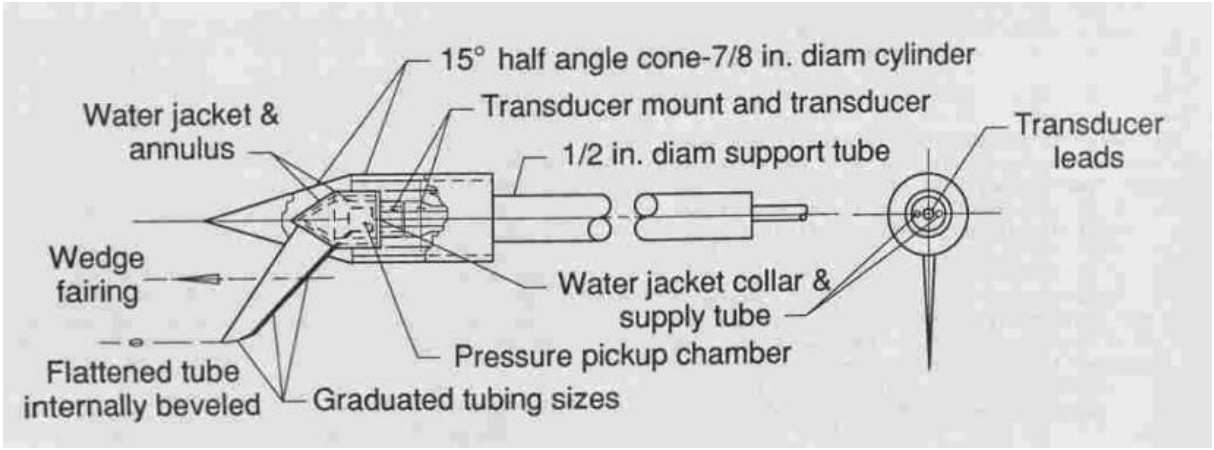

Figure 3.2.3: A schematic of the assembled pitot probe and mount [3].

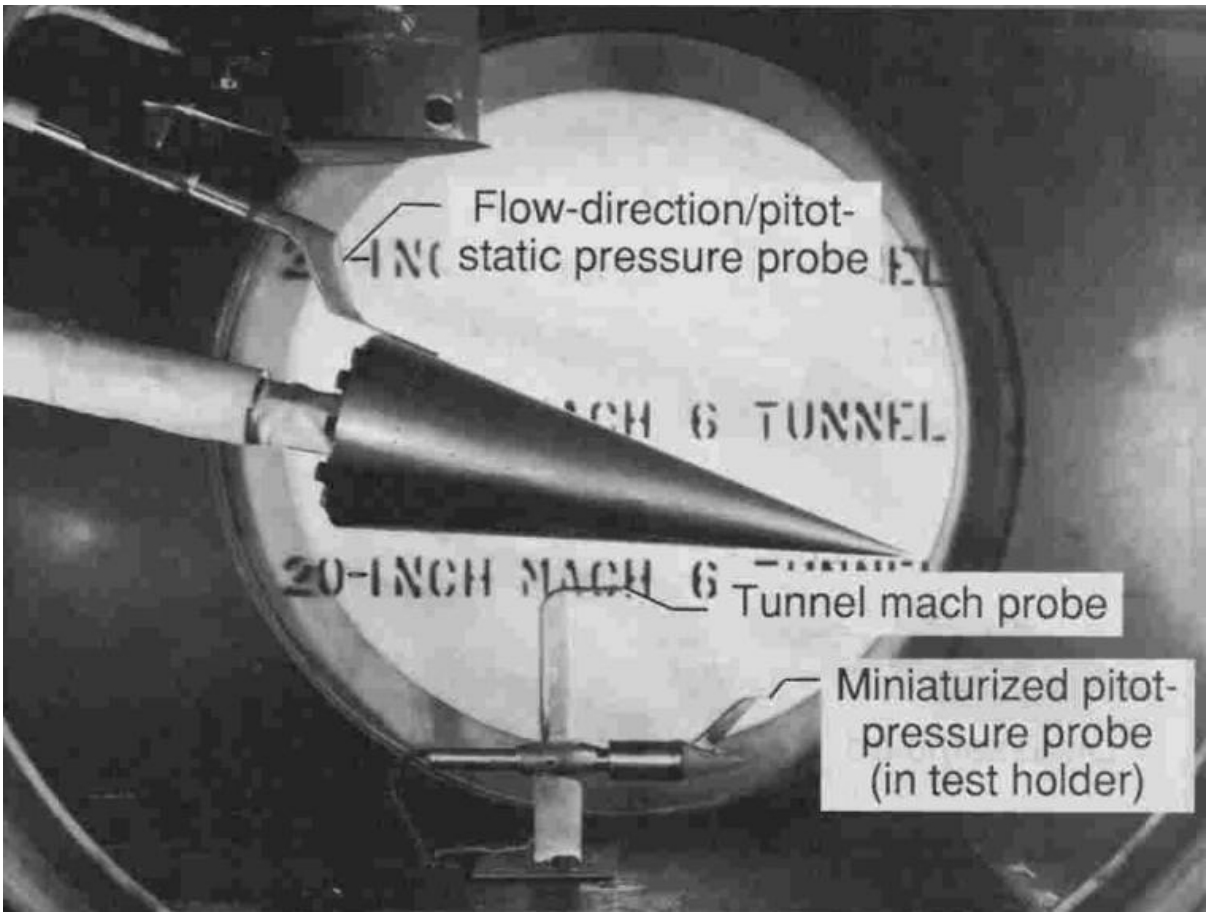

Figure 3.2.4: The miniaturized pitot probe designed by Ashby mounted in a Mach 6 hypersonic wind tunnel [3].

3.3 Pressure Sensors

In almost all the pitot probes encountered in a review of literature, the pressure sensor is a piezoelectric pressure transducer. There are many variations of these devices however the ones suited for use in hypersonic facilities all have several things in common. Firstly, they all have very small response times as this is critical when they are required to make many measurements over a period of a few hundred microseconds. Secondly the size is important as, generally speaking, the smaller the transducers are the more closely they can be positioned to the tip of the pitot probe and the faster they will respond to changes in the free stream pressure. In addition, smaller sensors can also be fitted to smaller probes which in turn cause less of a disturbance to the hypersonic freestream flow. Finally, the ability of these sensors to operate at higher temperatures is also advantageous. As eluded earlier, most pitot probes are

designed to protect their pressure transducers from these temperatures somewhat. However the higher the temperatures the sensor can handle the easier it is to design a probe around. Some examples of transducers that have been used in hypersonic pitot probes before include, the Kulite XT-140-200a, the 1 psid Druck transducer, and PCB transducers like the 112A22 model [4, 11, 12, 29].

Lastly it is also worth mentioning that due to vibrations associated with shock expansion facilities it is necessary to ensure that the transducers are isolated from the rest of the facility. Such vibrations can be picked up by these sensors and lead to erogenous results, therefore some kind of damping technique is required. A good example of this is probe c) (the brass swirl cap probe used at The University of Queensland) in Figure 3.1.1 which isolates its transducers with rubber [4].

4 Instrument Design

This section details the design of a pitot probe system capable of measuring the velocity of the test gas in shock expansion tubes, specifically The University of Queensland's X2 facility. This involved:

- Defining the conditions under which the probe must operate.
- Identifying ways in which probe response times can be reduced.
- Identifying ways in which Helmholtz resonance related noise problems can be minimised.
- Establishing the boundary layers through which the probe will have to take measurements.
- Identifying ways in which test flow disturbances can be minimised.
- Outlining the potential design implications associated with particles entrained within the shock tube gases.

Having done all these things it was possible to make informed design decisions and produce a probe with a strong chance of successfully measuring the velocities of test flows in shock expansion tubes.

4.1 Defining the Operational Environment

Before a design process can be commenced, it is necessary to select a set of conditions or parameters defining the hypersonic environment in which the pitot probe must operate. Since this pitot probe is to be tested and used in the X2 shock expansion tunnel, it would ideally be able to survive the most extreme flow conditions this facility can produce. In addition to surviving these extreme conditions, the probe should be able to take accurate pitot pressure measurements over the entire operating range of the X2, whilst not causing any significant test flow interference. Shock expansion facilities are used for a range of experiments, however scramjet flight and planetary re-entry simulations are two of the most common. Critically these simulations, represent two of the most extreme hypersonic test flows that expansion tubes are used to produce. Planetary re-entry testing involves high speed, high temperature test flows, typically referred to as high enthalpy flows. On the other hand, low enthalpy flow conditions are required for scramjet simulations. These tests occur at much lower velocities and temperatures

than the planetary re-entry ones, however they also involve much higher total pressures and heat transfer rates. Therefore, ideally the pitot probe design should be able to handle the high temperatures and velocities of re-entry simulations whilst also being able to withstand the pressure forces and high heat transfer rates of scramjet flight. In addition, the probes must create little or no disturbance in the core flow under both of these test conditions [6].

4.1.1 Scramjet Test Flows

Scramjet flight simulations in shock expansion tubes are typical of most of the low enthalpy testing conducted in these facilities. Hence why it is important for this design process, that a full understanding of the hypersonic environment created during these tests is gained. In a paper entitled "*Performance Considerations for Expansion Tube with Secondary Driver"* Gildfind et al outlines a range of flow conditions which are described as "predominately representative of the low-enthalpy flow conditions for which expansion tubes will be used in the coming years" *[6].* These conditions are displayed in Table 4.1-1 and will be used as design parameters throughout the remainder of this project. Obviously any pitot probe produced should be able to function in these conditions in order to be viable. Hence the data below will be useful for running simulations later in the design process.

Table 4.1-1:Typical Scramjet test flow conditions [6].

Mach Number	**Temperature (K)**	**Velocity (m/s)**	**Static Pressure (kPa)**	**Stagnation Pressure (MPa)**
10	226	3011	1.368	128
12	228	3633	0.950	457
14	233	4282	0.698	1469

Whilst these tabulated conditions provide a good indication of the low enthalpy test flows normally produced in shock expansion tunnels, they are not the most extreme low enthalpy flows possible. To date, the highest total (stagnation) pressure recorded in the X2 expansion tube (and any other facility) was 10.4GPa at Mach 15 [1]. This provides an insight in to the absolute maximum pressure hypersonic flow the probe would ever be exposed to and will help inform the design procedure in that regard.

4.1.2 Planetary Re-entry Simulations

The high enthalpy test flows associated with planetary re-entry define the maximum flow temperatures and velocities that the pitot probes must be designed to. In addition to outlining a range of typical scramjet flow conditions, Gildfind et al also outlines a range of planetary re-entry simulations which are typical of shock expansion tube testing (Refer to Table 4.1-2) [6].

Table 4.1-2: Typical Mach 10 planetary re-entry simulations in shock expansion tubes [6].

Mach Number	Temperature (K)	Velocity (m/s)	Static Pressure (kPa)
10	3287	11000	9.00
10	3925	12000	9.21
10	4621	13000	2.38
10	5370	14000	5.37
10	6185	15000	5.32
10	7070	16000	1.82

It can be seen that all the simulations listed in this table are conducted at Mach 10. This is because planetary re-entry occurs at very high Mach numbers which are too difficult to replicate in shock expansion tunnels. However at high Mach numbers it is commonly accepted that aerodynamic characteristics become independent of the Mach number. Hence equivalent re-entry simulations can be run at Mach numbers which are lower, but still high enough that they are independent of aerodynamics.

Table 4.1-2 shows that the new probe design will need to be able to withstand freestream temperatures in excess of 7070K, and velocities of 16000m/s to be able to handle typical planetary re-entry simulations. The actual temperatures the probe would experience if the freestream temperature was 7070K in a Mach 10 flow would actually be much higher, due to the fact that a shockwave would form upstream. Normal shock theory indicates that the actual temperature at the probe could be more than 20 times the free stream temperature (144140K). In reality there is no chance that such a temperature would be reached as real gas effects mean that normal shock theory massively over estimates the post shock temperature. However it is a fact that the temperature will increase across a shockwave and any probe design will be potentially exposed to very high temperatures (greater than 7070K).

4.1.3 Test Conditions

The previous two sections have described some of the more extreme flows that can be run in shock expansion tubes. These are important to keep in mind during the design process, and where possible, the pitot probe should be designed with the goal of being able to operate in all of these conditions. However it is impossible and beyond the scope of this project to conduct tests at all of the flow conditions described. Instead testing was intended to be conducted at the parameters described in Table 4.1-3. These conditions were chosen for two reasons. Firstly and primarily, it was easy to configure the X2 to these conditions based on its current setup. The University of Queensland regularly use these facilities at Mach 7.5 and therefore it is not possible or necessary to have the whole system re-configured for this investigation. Secondly, the conditions in the table below are very representative of the operating envelope of the X2 and other expansion tube facilities, with one set being a high enthalpy flow and the other a low enthalpy flow. Due to the fact that these will be the test conditions, they are also worth keeping in mind during the design process. For the success of this investigation it is important that there is a focus on making sure the probe is able to operate successfully under these conditions.

Table 4.1-3: The conditions under which the probe design will be tested.

Mach Number	Temperature (K)	Velocity (m/s)	Static Pressure (kPa)
7.5	700	3500	13
7.5	2000	10000	5

It is worth mentioning however that time constraints, and access to the test facility may limit the ability of the probe to be tested at both of these conditions. In which case only one of the conditions would be tested, and this would be selected based on whichever of the above two test conditions best suited the experimental schedule of the operators of the X2 facility. (I.e. whichever of the two conditions the shock tunnel could be most easily configured to produce. Access to the X2 was limited and as such there was a need to be flexible.) In addition, the conditions in the above table will not be the exact same as those at which testing is eventually conducted. However they are still very representative of the likely test conditions and as such the design process will be conducted based on the assumption that testing will be able to be conducted at both conditions listed in Table 4.1-3.

4.2 Transducer Response Considerations

One of the critical aspects of this design process is ensuring the pressure transducer's response to the changing pitot pressure of the freestream is appropriate. This means designing the probe such that the pressure transducer responds quickly to changes in the free stream pressure as well as making sure that that Helmholtz resonance is not an issue.

4.2.1 Response Time

Minimizing the response time of the probe is important, as tests in shock expansion tubes are typically conducted over several hundred microseconds. Achieving an appropriate time of around 100μs or less depends mostly on a few critical parameters. Firstly, generally speaking the shorter the distance of the pressure transducer from the point in the free stream where the pressure is being measured, the faster the response time. This is purely because it means there is less medium through which a change in pressure has to be transmitted, therefore this happens more quickly. For this reason, the design of the new probe should aim to minimize the distance of the pressure transducer from the freestream.

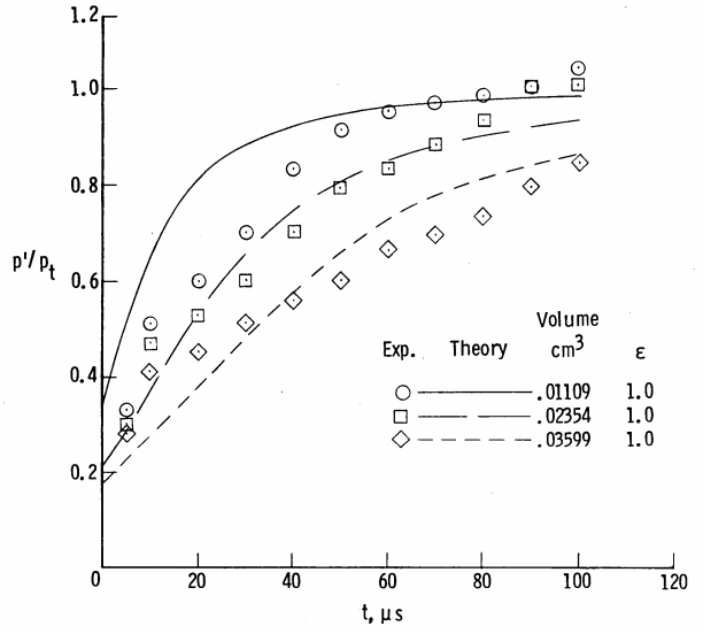

Figure 4.2.1: A graph of the ratio of the measured pitot pressure to total freestream pressure vs time, for a simple probe. It can be clearly seen from this graph that the measured pitot pressure approaches the freestream stagnation pressure more quickly when the internal volume of the probe is less. This is true of both the theoretical and experimental results in this study which was conducted by J. A. Moore [7].

In addition, multiple studies have identified the volume of gas between the pressure transducer and the tip of the pitot probe as having a significant effect on the response time [7, 31, 32]. Experimentation and theoretical analysis has shown that probes with larger internal volumes tend to have slower response times. This is evident in Figure 4.2.1 which shows the that the pressure measured by a transducer in a pitot probe (p') approaches the stagnation pressure of the freestream (p_t) more quickly if the internal volume of the probe is less. This graph is sourced from a study conducted by J. A. Moore [7] who used a simple theoretical model to estimate the response times of different pitot probe configurations and then compared these estimates to experimental results gathered from testing in an expansion tube. It shows that both experimental and theoretical results for a simple probe design indicate that minimizing the pitot probe volume has benefits for the instruments response time. The response times achieved in this study by Moore range from 20μs to 100μs and, as can be seen from the volume values displayed in Figure 4.2.1, involve probes designs where very little gas separates the pressure transducers from the freestream [7]. Therefore, it is obvious that if a short response time is to be achieved by this probe design, then internal volume minimization will be an important factor.

Moore also found that using baffles or some form of transducer shielding has a detrimental effect on pitot probe response time, although this effect was not so significant as to prevent an adequately quick response time. Depending on the configuration of the baffle it can have the effect of reducing the response time by around 60μs [7].

Finally, if a change in the inner diameter of the probe is required, then it is better that the tube diameter increases from the tip to the pressure transducer. This generally offers a benefit in terms of the response of the probe. The main reason this is the case is that when a smaller tube becomes wider it is easier for a pressure disturbance to propagate through, due to the decreased wall friction in the wider tube. However it is also important to ensure that the volume of these tubes is minimized so this must be taken into consideration it the proposed probe design is to have a change in internal diameter [31].

In summation, by designing a probe such that the transducer is as close to the freestream as possible and has as little internal volume as possible whilst also giving consideration to the effect of including a baffle and a diameter change in the design, the probe response time will be roughly optimized.

4.2.2 Helmholtz Resonance

Due to fact that a typical pitot probe design incorporates a forward facing cavity into which a gas flows, resonance in this cavity is something which needs to be considered. This Helmholtz resonance creates pressure oscillations which can interfere with the measurements that are made by the pressure transducer. The nature of the resonance is defined mostly by the geometry of the cavity or cavities. Modelling this phenomenon has been conducted using a number of methods. A large amount of research has been conducted into the resonance of simple cylindrical forward facing cavities in supersonic missiles. It was found that for shallow cavities, where the length to diameter ratio (L/D) was small (less than 1), resonance effects were not significant, however fluctuations and perturbations in the freestream flow were amplified. This amplification effect is consequential as it is capable of magnifying disturbances in the flow which would not normally be measurable, to a point where they can be easily detected by modern sensors. Ladoon et al [33], found that the significance of the amplification appeared to increase with the cavity length [10, 33, 34].

For cavities with larger L/D ratios (>1) resonance becomes more of a consideration. In this case, the gas in the cavity has a tendency to self-excite and resonate at the primary mode of vibration for that cavity. Not all resonance occurs at this

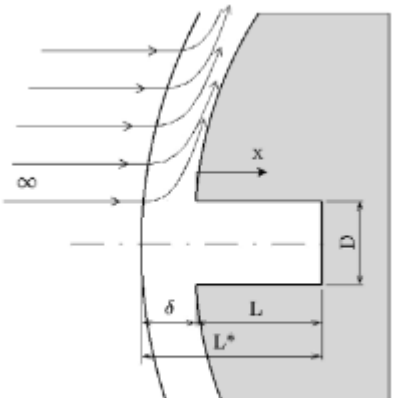

Figure 4.2.2: A typical cylindrical cavity in a supersonic flow.[10]

primary mode however it certainly contains a majority of the vibrational energy, particularly for shorter cavities. Research has found that it can be modelled, to a reasonable extent, with simple harmonic relations. The equation below gives a good estimate of the resonant frequency of a simple cylindrical cavity with a depth L, diameter D behind a shock with a standoff distance of δ. (Refer to Figure 4.2.2)

$$f = \frac{\sqrt{\gamma RT}}{4(\delta + L)}$$

(Where, δ, R and T are the ratio of specific heats, the ideal gas constant and the temperature of the gas in the cavity.) [10] The amplitude of this resonance is also a function of cavity depth (L) with the amplitude increasing as the cavity depth increases [10, 33, 34].

What the information in the previous two paragraphs indicates, is that it would be advantageous to minimize the depth of any cavities in this pitot probe design. The lower the amplitude of noise amplification and resonance is, the lower the amplitude of the pressure variation will be, leading to a reduced noise content in the measurements made by the probe's pressure transducer. Whilst this information pertains specifically to cylindrical cavities, the mechanics of resonance and noise amplification are similar for other simple geometries. Even if the geometries are completely different, cavity depth minimization is still a good principal to design by as vibration mechanics dictate that the longer a column of air is, the lower its resonant frequency will be resulting in a higher amplitude of pressure oscillation.

Even with cavity depth minimization as a design principal, it may still be necessary to take further steps to ensure Helmholtz resonance does not inhibit the effectiveness of this probe. Another method of reducing the effect of this phenomenon is to introduce swirl into the flow of gas entering the probe tube or cavity. This has the effect of breaking down the wave structures which cause resonance, helping to prevent self-sustaining pressure oscillations from occurring. In 2009 McGilvray et al [10], designed a pitot probe with vortically aligned inlet holes leading to a cavity containing the pressure transducer. These holes induced swirl into the flow and were found to reduce the pressure oscillation amplitude by an order of magnitude compared to a more conventional baffled probe. Therefore, introducing swirl into the flow is a concept which

may be worth looking at for this pitot probe design, to lower the risks of problems with Helmholtz resonance.

4.3 Other Design Considerations

4.3.1 Boundary Layers

Boundary layers form along the walls of all shock expansion tubes creating a region of flow in which the conditions vary significantly from the free stream. This phenomenon is important to acknowledge as any pitot measurements taken from within this region would not be representative of the free stream behaviour. Therefore, any probe design must have the ability to protrude through the boundary layer or be close enough to the core flow to take meaningful measurements. In this case, the pitot probe only has to clear the boundary layer formed in the accelerator gas. This is because the only purpose of these probes it to detect the stagnation pressure change associated with the arrival of the test gas. It does not matter whether the probes detect the boundary layer of the test gas or the core flow, so long as they detect a pressure change. What is important however, is that the probe takes measurements from above (or just below) the boundary layer of the gas in the acceleration tube. Inside this layer the velocity is significantly less than in the core flow therefore any probe which takes measurements from this region will detect the pressure change associated with the test gas arrival much later than it actually arrives.

In order to get an idea of what the thickness of the boundary layer in the accelerator gas would be for this probe design, some basic CFD modelling was conducted. Using a CFD code produced by the University Of Queensland known as Eilmer, basic simulations of the acceleration tube were conducted. The first was a designed to simulate the scramjet test flow outlined in Section 4.1.3 where the test gas travels at 3500m/s and has a static pressure of 13kPa. In this case the boundary layer was assumed to be laminar as it simplified the computational power required to run the simulation significantly. The simulation in Figure 4.3.2 took several days to run and it was anticipated that assuming a turbulent boundary layer would cause the simulation take significantly longer. Therefore due to time pressures on this investigation, it was not possible to also conduct a turbulent boundary layer simulation. To run such a simulation would have been ideal in terms of gathering design information, however at least with the laminar simulation it

would be possible to gain some indication of the boundary layer thickness of the gases in the acceleration tube.

To briefly describe how the simulation was set up, as the acceleration tube is circular, the flow was assumed to be axisymmetric and hence an axis-symmetric simulation was conducted. The Eilmer CFD code operates by solving the Naiver Stokes equation over finite elements and as such it was necessary to define these finite elements. A simple rectangular mesh grid was developed to represent the axis-symmetric geometry of the acceleration tube of the testing facility. Figure 4.3.1 shows a small part of this mesh near the wall, and as the graphic shows, the cells were more heavily clustered towards this wall. This was done as it was expected that a boundary layer would form along this surface. In order to be able to capture the behaviour of the flow in this region it was necessary to have a higher density of cells.

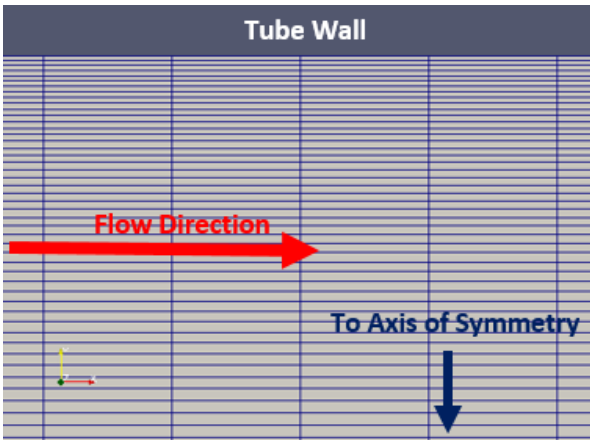

Figure 4.3.1: A part of the mesh of finite cells used to generate the CFD simulations.

The simulation also needed to have defined boundary conditions and initial conditions. The top edge of the simulation grid was assigned a fixed temperature wall boundary condition defining the shock tube wall as a constant temperature surface at 298.15K. Conversely the bottom edge represented the axis of symmetry and as such was defined as a frictionless wall or “slip wall”. In addition, the left and right hand boundaries of the simulation had to represent the inlets and outlets of the acceleration tube. Assuming the flow entering the acceleration tube was the fully developed test flow, the inlet boundary condition was a supersonic inflow defined by the parameters in the table below.

Table 4.3-1: The properties defining the inlet boundary condition

Temperature (K)	Velocity (m/s)	Static Pressure (kPa)
700	3500	13

On the other hand, the outlet boundary condition was based on the pressure of the dump tank into which the test gas will flow. In this case this dump tank pressure was 120Pa. Finally the initial conditions of the flow within the tube, (before the test gas enters it) were set to the acceleration tube fill conditions required for a 3500m/s, 13kPa test flow. These are outlined in Table 4.3-2.

Table 4.3-2: The acceleration tube fill conditions for a 3500m/s 13kPa scramjet flow test.

Temperature (K)	**Static Pressure (kPa)**
298.15	120Pa

Having defined these things it was then possible to begin running simulations. Initially this was done on a mesh grid which only represented the first 0.5m of the acceleration tube. The idea was that these would produce solutions quickly, which would allow different mesh sizes to be tested. For all CFD simulations, it is important to ensure that the mesh grid contains enough small cells to represent the behaviour of the flow accurately. If the number of cells in the simulation is increased and this causes a change in the solution, then the results are not independent of the mesh grid and a further increase in the number of cells is required. Therefore finer and finer mesh grids were used to generate a solution for the flow through the first 0.5m of the acceleration tube at a certain point in time, until the solution generated stopped changing. Having proven the simulation results were now independent of the mesh grid it was then expanded to represent the full length of the X2's acceleration tube and a range of solutions for different points in time were generated. The relevant results of these CFD simulations for the 3500m/s, 13kPa test flow conditions are shown in Figure 4.3.2, Figure 4.3.3, Figure 4.3.4 and Figure 4.3.5. With the exception of Figure 4.3.2, all the results in the graphics below represent the solution pertaining to the time at which the test flow is right at the end of the test tube. This gives the boundary layer as much time to develop as possible, which in turn results in the thickest boundary layer possible. It is important for this design project that the pitot probe be able to protrude through the thickest of boundary layers, in order to be able to take measurements at any point in the acceleration tube. It also means the probe design will be conservative, in terms of being able to detect pressure changes in the presence of thick

boundary layers, which could be useful if the boundary layer turns out to be turbulent and hence slightly thicker.

.

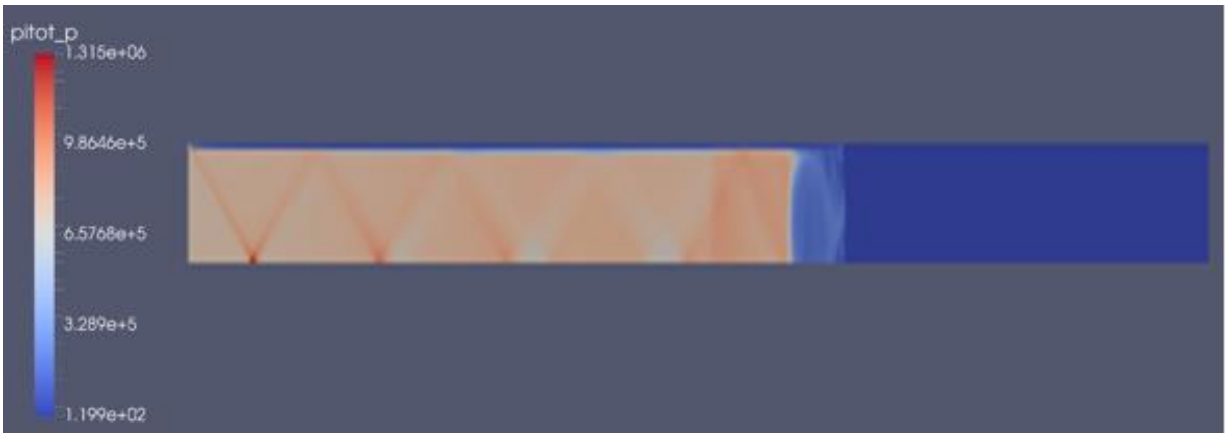

Figure 4.3.2: An example of the CFD simulations conducted to determine the boundary layer thickness in the acceleration tube of the X2 shock expansion facility. The image above shows the pitot pressure (Pa) in the top half of the acceleration tube. The model is axis-symmetric and in this case is simulating the a typical 3500m/s scramjet flow along the approximately 4m long acceleration tube. The dark blue area is undisturbed gas, the light blue area is this same gas but directly after it has been shock processed, and the orange-yellow region is the test gas. On the top edge of the simulation the boundary layer can be as thin low pressure blue region. (Please the note the aspect ratio of the image above has been changes to make it appropriate for viewing in this document.

Figure 4.3.3: The test gas at the end of the acceleration tube where the boundary layer is the thickest. As can be seen from the measurement displayed in image, the high pitot pressure associated with the arrival of the test flow interface occurs at approximately 3.42mm from the tube wall.

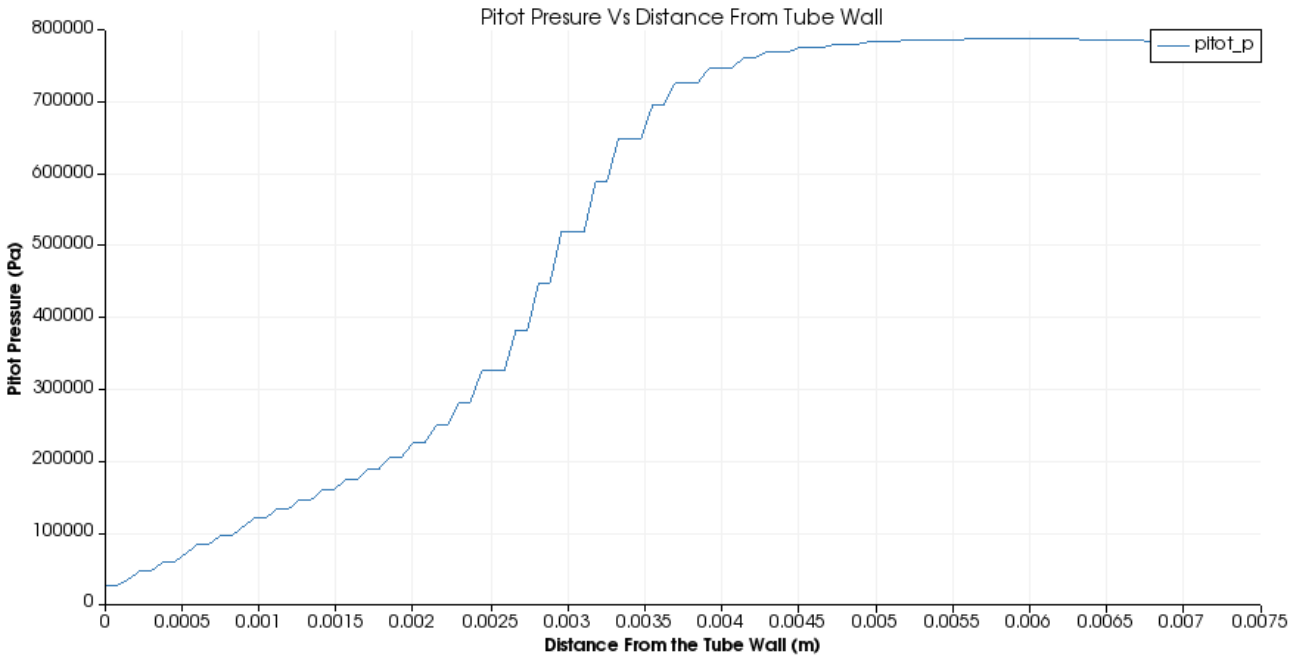

Figure 4.3.4: A plot showing pitot pressure vs distance from the acceleration tube wall, at the interface between the test gas and the accelerator gas. At between approximately 2.5mm to 3.5mm from the tube wall there is a significant increase in the pitot pressure which indicates the location of the edge of the test flow and hence the boundary layer thickness.

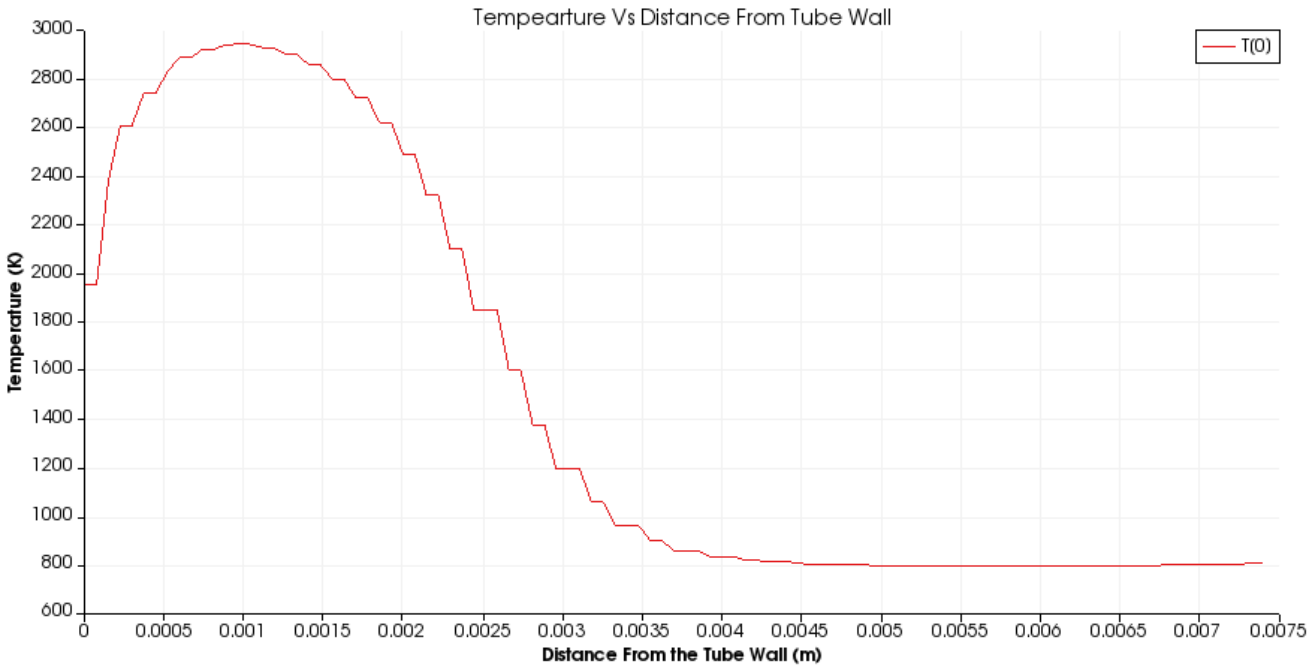

Figure 4.3.5: A plot showing temperature vs distance from the acceleration tube wall at the interface between the test gas and the accelerator gas. Again between approximately 2.5mm to 3.5mm from the tube wall there is a significant change in temperature which gives an indication of the boundary layer thickness.

From these simulation results it was found that the pitot probe would have to protrude at least 2.5mm into the flow to be able to detect any of the pitot pressure change associated with the arrival of the test gas. Figure 4.3.3 shows the boundary layer in the shock processed acceleration gas is effectively non-existent, however there is a thick boundary layer between the test gas and the tube wall. To be effective, the pitot probe must be able to detect the test gas and as such, must protrude through a large portion of this boundary layer. Based on the two graphs in Figure 4.3.4 and Figure 4.3.5 the boundary layer is approximately 4mm - 4.5mm thick. However it appears that the pitot pressure increase associated with the arrival of the test gas can begin to be detected as close as 2.5mm from the tube wall. This is evident in the gradient change in the pitot pressure graph at this distance from the wall. Therefore if the probe is to be effective in 3500m/s, 13kPa test flows, it must be able to detect pitot pressure changes at least 2.5mm from the acceleration tube wall. Preferably the probe will protrude further into the flow as the pressure changes will be more significant and hence will result in better measurements less susceptible to background noise. Based on the pitot pressure graph, it was decided that 3.5mm would be a good distance for the probe to protrude into this specific test flow, as the pressure change is significant at this distance and should result in good pitot measurements.

In an ideal world, another CFD investigation would have been conducted into the thickness of the boundary layer in the second of the designated test flow conditions (10000m/s, 5kPa and 2000K, refer to Table 4.1-3). However when this was attempted it was found that, due to the high enthalpy nature of this flow, there was significant particle dissociation occurring within the flow. The Eilmer CFD code had not been properly configured to be able to deal with these effects and even if it had been, generating a CFD solution would have been very computationally intensive. As such it was not possible to conduct a CFD analysis for this flow condition. However, given that this high enthalpy test flow has a much lower pressure and density than the lower enthalpy, 3500m/s, 13 kPa simulation, it was anticipated that it would have a thinner boundary layer than this low enthalpy condition. Therefore if the probe is design based on the results of the previous simulation, it should be capable of taking measurements in higher enthalpy 10000m/s, 5kPa test flows. In essence, the low enthalpy test flow condition is the worst case scenario in terms of the boundary layer thickness.

4.3.2 Flow Disturbance Considerations

As previously mentioned, it is important to consider how the probe will interact with the flow through the tube and in particular, the test flow. Creating a uniform test flow in expansion tubes is quite difficult and there is every chance that placing a pitot probe in the path of the flow will have a significant disruptive effect and compromise the results of any testing. Therefore, in the design of the probe for this investigation, it was important to take steps to try and reduce the possibility of this happening. One thing that can be done is to reduce the size of the probe as much as possible. In the review of Current Hypersonic Pitot Probe Technology (Section 3 of this report) it was found that probes with small, streamlined geometries created the least disturbance within the flow in which they were immersed. The most pertinent example of this was the probe designed by George Ashby [3], which was specifically made as small and streamlined as possible so that it could be placed directly in front of a model being tested and not affect the results. According to his report this design was highly effective in this regard [3]. Therefore, by applying these size minimization and streamlined geometry concepts to the current project it should be possible to reduce any disturbance the probe creates in the flow.

Reducing the distance the probe protrudes into the shock expansion tube will also help reduce the disturbance it creates. The key to doing this is to ensure the tip is submerged far enough into the flow to be able to detect the arrival of the interface between the accelerator gas and the test gas, when it first arrives, but no further. This means it has to have a length slightly longer than the maximum boundary layer thickness of the test gas or very close to it. As the simulations of the previous subsections have indicated, this distance is around 3.5mm. Hence if the maximum protrusion distance of the new probe could be as close to this length as possible, it should ensure the disturbance created in the flow is minimised as much as possible.

4.3.3 Particles Entrained Within the Flow

Due to the nature of how shock expansion tubes operate, there are often particles of reasonable size entrained within the high velocity flows generated by these facilities. Typically these particles originate from the Mylar diaphragms which rupture during each test. Most of the diaphragm breaks down soon after

Figure 4.3.6: Two pitot probes mounted on a rake in a hypersonic test facility. Damage caused by flying particles can clearly be seen on the faces of these instruments [4].

rupture due to the harshness of the flow, however some small particles survive and travel all the way through to the test section. Cases of particles originating from the steel primary diaphragm becoming entrained in the flow are much rarer, thanks to the fact that this diaphragm is scored to rupture in a predetermined manor. However there are still occurrences where small portions of the steel plate rapidly travel down the facility. The significance of these particles, with respect to this probe design, is that if one of these were to impact the probe it could potentially cause damage or a failure. The impact loads which would result from such an event would be very high as even though the particles are small, they possess a lot of kinetic energy thanks to their high velocity. The damage to the simple forward facing probes shown in Figure 4.3.6 is a testament to this fact. There is no real precedent to estimate the magnitude of these loads as the particle sizes and velocities vary significantly. Therefore when designing the new probe, attention should be paid to previous probe designs used in shock expansion tubes, to gauge the kind of structural integrity required to resist the impact of particles entrained in the hypersonic flows. This is the only real indication available, upon which some sort of estimate of the required resilience of the structure can be based.

4.4 The Design Specifications and Calculations

Based on the considerations discussed in Sections 4.1, 0 and 4.3 the following probe design was produced . Figure 4.4.1 shows some images of a 3D model of the design, including two exploded views showing how the various components go together.

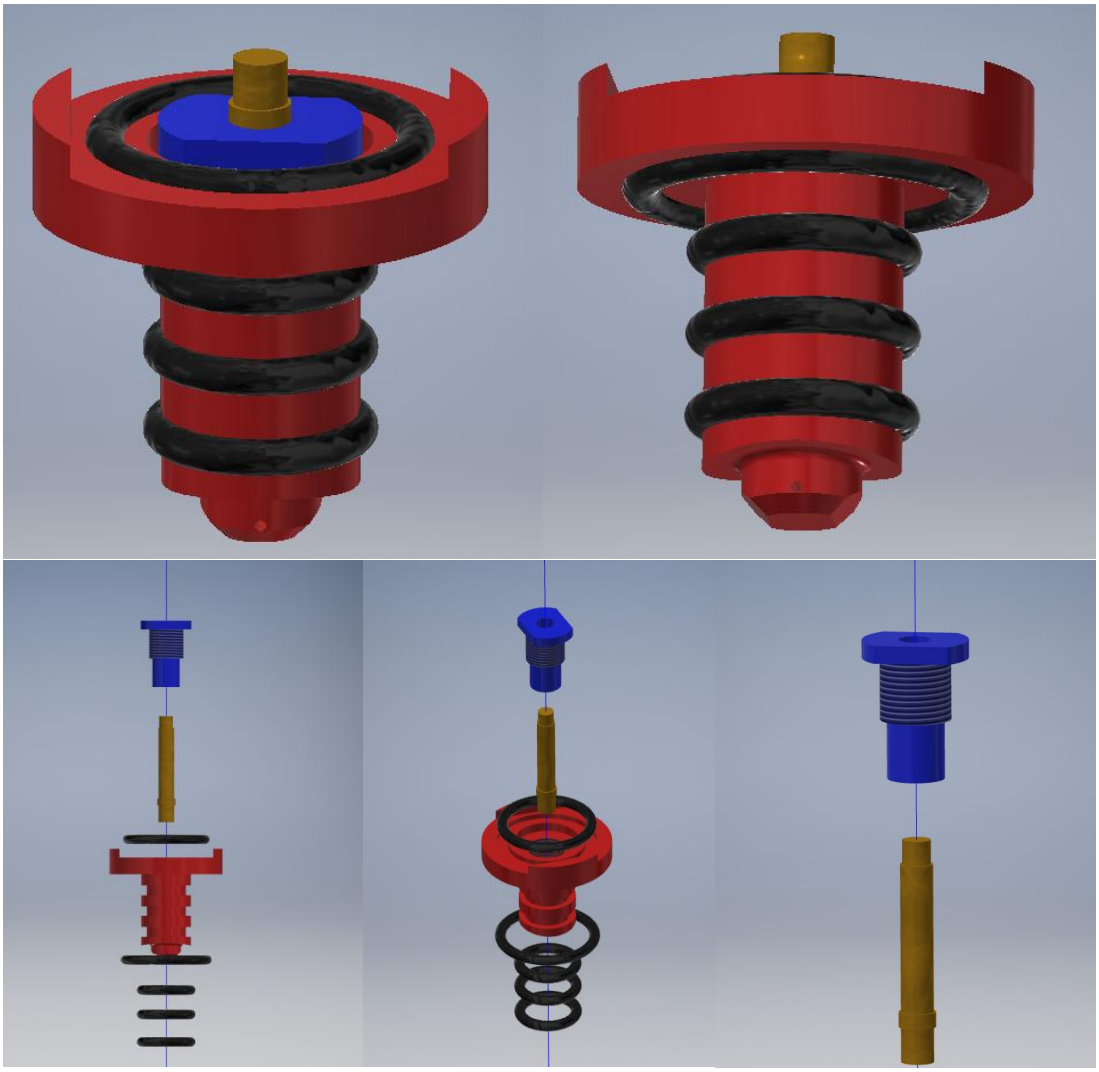

Figure 4.4.1: A 3D model of the pitot probe design produced based on the considerations discussed earlier in this section. In these images the red component is the main pitot probe body which houses the pressure transducer (gold) which in turn is held in place by a threaded sleeve (blue). The black rings are O-rings used to seal the expansion tube around the pitot probe. The whole structure is clamped to the X2 expansion tube using a metal block, the drawings of which are included in Appendix – B

To describe it briefly, the red structure is the main component of the probe. It has been specifically shaped for mounting in the 24.32mm deep, 18mm diameter holes, which have been bored into the acceleration tube of the X2. As can be seen from Figure 4.4.1 there are three groves along its length and one on both sides of its head to accommodate O-rings. The centre

has been bored out and partially tapped such that it can accommodate the sensory end of the PCB model 112A22 pressure transducer, (gold) and the threaded sleave (blue). Finally, the very tip of this component has a much smaller diameter than the rest of the structure. This is the part which protrudes into the expansion tube itself. It is essentially a small lump of metal through which intersecting holes are drilled to allow gas from the expansion tube to enter a small cavity containing the pressure transducer. Therefore, when it is installed in the expansion tube, a small volume of the gas from the test flow will enter the cavity and stagnate, allowing for a reading of the pitot pressure to be recorded by the transducer. The whole probe was to be made entirely from stainless steel (with the obvious exception of the O-rings and the pressure transducer) and full technical drawings are included in Appendix – B if a more detailed understanding of the design is required.

4.4.1 Material Selection

The first step in designing this pitot probe was to select a material from which to manufacture the instrument. As eluded to earlier the chosen metal in this instance was stainless steel. Stainless steel was selected for several reasons. Firstly, steel is one of the toughest and most versatile materials available. The environment in which the probe will operate is one where it will be exposed to high temperatures (in excess of 7070K), drag, and impact loads, and as such has to be made from a material which can withstand all of these. Steel is recognised as one of the strongest and most affordable materials available, and also has good structural integrity at high temperatures. In shock expansion tubes, flying particles and objects are quite common due to the breakup of diaphragms. Therefore, it is important that the pitot probe be made from a tough material which can resist high impact loads. Again steel has very good toughness properties and as such was ideal for the role. In summary the versatility of steel is the main reason why it was the material selected for this probe design. A review of literature (refer to Section 3) also shows that stainless steel is a commonly used material in hypersonic pitot probes, including probes used in the X2 expansion tunnel. Therefore, it makes sense to continue using a material that has been proven to be successful in the past.

4.4.2 Main Body Design

After selecting a material, the design of the probe geometry could begin. A large part of this design was adopted from the static pressure sensors currently used in the X2 expansion tunnel. In fact the geometry of the thickest part of the stem and the head of the probe was almost identical to that of the static sensors. The advantage of this was that the new probe could be mounted in the expansion tube in the exact same way as the old sensors. As Figure 4.4.2 shows, the static pressure sensors were clamped to the outside of the expansion tube using a metal block and two bolts. Therefore the same bolted clamp arrangement could be used to mount the pitot probe. Another way in which the probe design was the same as the static sensors, was in its use of O-rings to seal the tube. Obviously this O-ring arrangement has been successfully used to ensure no gas escaped the expansion tube in the past therefore there no need to move away from this successful formula now.

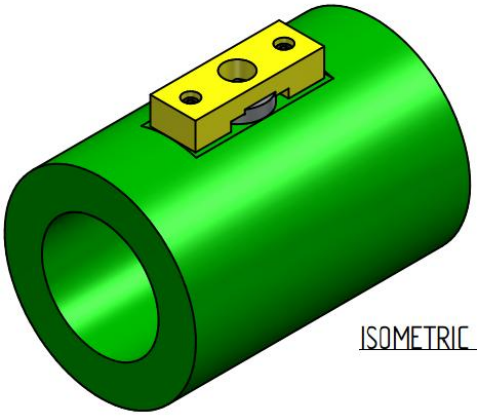

Figure 4.4.2: A model of the clamping system used to mount the X2's static pressure sensors. Due to intentional design similarities, the new pitot probe will be mounted in the exact same way.

The way in which the pressure transducer was mounted in the new probe was also inspired by the static pressure sensor. Figure 4.4.3 displays a cross section of the design, showing how the threaded sleave is used to securely hold the pressure transducer within the probe itself. As can be seen, the blue sleeve screws into the red probe body, clamping the transducer against a copper washer and hence holding it firmly in position. As was eluded to earlier, a very similar mounting technique has been successfully used to mount pressure transducers in the static sensor hence there no reason to doubt that it would work for this application.

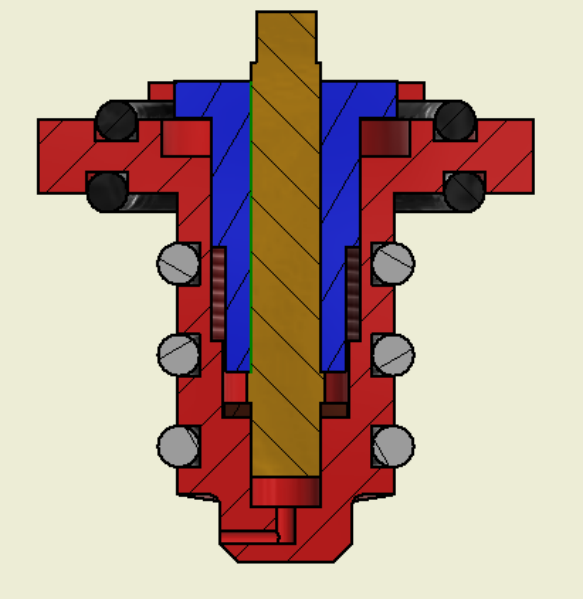

Figure 4.4.3: A cross section of the pitot probe design showing how the threaded sleave secures the pressure transducer within the probe.

4.4.3 Pressure Sensor

The pressure sensor that was selected for this probe was the PCB model 112A22 transducer. There are several reasons for this. Firstly it is reasonably small and compact, and therefore easy to integrate into a small pitot probe. Secondly it also had a very fast response time (less than $2\mu s$) as well as a high resistance to temperature and pressure. This is important for pitot probes in shock expansion tubes where high pressures, high temperatures, and very short test times (approximately $100\mu s$) are a reality of every experiment (refer to Section 4.1). According to the data sheet for the model 112A22 sensor, it was a capable of withstanding pressures and temperatures of up to 3.45MPa and 1650K respectively [35]. Both these values were actually less than what the sensor was likely to experience in the shock expansion tunnel however, previous use of this sensor at the University of Queensland in the X2 expansion tunnel has shown, that it is capable of operating in much harsher conditions than its datasheet states. This pre-empts the third and most significant reason why the sensor was chosen. PCB model 112A22 pressure transducers have been widely used in hypersonic test facilities at the University of Queensland, including extensive use in pitot probes in the X2 expansion tube. The capabilities of these instruments are therefore well known and understood. The general consensus is that if the model 112A22 sensors are not in the direct line of sight of the flow, (which is the case with this design) then they are generally capable of withstanding the heating and pressure loads associated with expansion tube testing. If overheating of the transducer is a problem, there are several steps which can be taken to help prevent this. For example, the sensory surface can be covered with grease, cellophane or even a brass shim. The point is that experience has shown the 112A22 model pressure transducer can be versatile and effective in shock expansion tubes, and that one can have confidence in being able to take useful measurements with this instrument. Hence why it has been selected for use in this pitot probe. In addition, due to its regular use at The University of Queensland, procuring these instruments was straight forward and cost effective compared to alternatives.

4.4.4 Probe Tip Design

The most complex part of the probe design process was the tip, which

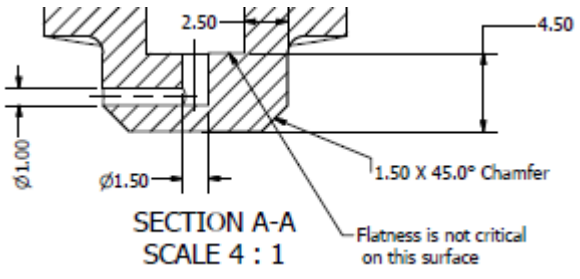

Figure 4.4.4: A drawing of the tip of the pitot probe. From this view the hole through which the freestream gas can access the cavity can be seen. Other important features include the chamfer where the probe tip joins the main body and the fact that this main body has a concave shape to conform to the profile of the shock expansion tube wall.

protruded into the tube itself and is shown in more detail in Figure 4.4.4. This tip was inspired by the shielded probe designs discussed in Section 3.1.1, and a variation of this transducer shielding concept has been adopted here. To describe it briefly, two intersecting holes, one horizontal and one vertical, are drilled in the tip to connect a small cavity containing the pressure transducer the freestream flow. This provides the line of sight protection that the transducer requires to prevent heat damage, and as will now be discussed, has been optimised to best suit its design purpose.

Firstly, in order to make the response time of the probe as fast as possible, the volume of the cavity containing the pressure transducer and the distance of this transducer from the freestream had to be minimised. This basically meant making the tip as small as possible, particularly the internal cavity. Hence why the diameter of this cavity is only as large as required to accommodate the sensory tip of the pressure transducer. It is also only approximately 2mm deep depending on the thickness of the copper washer upon which the transducer was mounted.

Secondly, in an attempt to prevent Helmholtz resonance becoming a problem, the length (or depth) of the two intersecting holes linking the freestream to the pressure transducer was made as short as the design configuration would allow. Therefore, any resonance which may occur in this hole, will have a high frequency and low amplitude, hence contributing a little as possible to any noise picked up by the pressure sensor. Applying this design concept to the instrument meant that the horizontal and vertical holes shown in Figure 4.4.4 had a depth of 3.52mm and 3mm respectively. A single curved hole would have been preferable for Helmholtz purposes however this was impossible to manufacture. An angled hole directly connecting the cavity to the outside environment was a possibility, however there were concerns that this would effectively create line of sight access to pressure transducer and potentially overheat it. Hence why the two intersecting holes configuration was chosen. The concept of trying to induce swirl into the flow in the cavity, in order to disrupt any resonance, was also considered However it was difficult to incorporate into this particular probe and as such it was decided that enough of an effort had already be made to prevent resonance problems. If, at the end of this investigation was is clear that Helmholtz resonance is an issue for this pitot probe design, then

introducing swirl into the flow is a concept that can looked at with a view to improving the instrument.

Thirdly, the height (protrusion distance) of the probe tip, and the location of the freestream access hole, was directly influenced by the thickness of the boundary layers through which the probe would have to protrude. Based on the analysis conducted in Section 4.3.1 it was decided that the probe should be able to detect pitot pressure changes at 3.5mm from the tube wall, to effectively determine the arrival of the test gas. Despite the fact that this analysis did not account for turbulent boundary layers it was thought that enough conservative assumptions had been made, and that the results were appropriate to use for this design. As such, the freestream access hole leading to the pressure transducer was located at exactly 3.5mm from the wall of the acceleration tube (in its installed configuration). This meant that the transducer would be able to detect the test gas arrival, whilst the total height of the probe tip was kept to a minimum. To accommodate this access hole, the total height of the probe had to be 5.5mm.

The design of the tip of this probe was also limited by manufacturing capabilities. For example, the 1mm chamfer, which exists at the point where the probe tip joins the main body (refer to Figure 4.4.4), was only included because a finer chamfer was not possible at this location. Shaping the external surface of this pitot probe tip was most likely to be done in a CNC milling machine. Given the fact that the main body of the probe will be curved to match the shape of the expansion tube wall (Refer to Figure 4.4.4), there are limits to how small the aforementioned chamfer can be. Ideally this would be as small as possible, as this curved surface may cause any flow which impacts it to travel up the wall of the probe tip and potentially interfere with the flow entering the hole. With regards to the diameters of the holes allowing access to the freestream, both of these were minimised in-order to minimise the volume between the freestream and the pressure transducer. In turn, it was hoped this would maximise the response time of this instrument. As such, 1mm was the diameter of the horizontal hole, one the smallest sizes possible using conventional manufacturing practices. Likewise, the vertical hole had a diameter of 1.5mm, which was only larger than the horizontal hole as it was easier to drill the smaller horizontal hole into a larger vertical one, in terms of making them intersect neatly.

It was also necessary to ensure the probe was capable of withstanding the drag loads that it would have to undergo in the expansion tube. To gain an approximation of how high these loads would be a Newtonian flow analysis was applied. Newtonian fluid mechanics are known to give a good estimation of the pressure drag on blunt bodies in hypersonic flows. According to the most accurate version of the theory, (known as Modified Newtonian Theory) the pressure coefficient (c_p) pertaining to the drag force on the forward facing surface of a blunt body above Mach 5 is: (Where θ is the angle of the surface the flow is impacting measured for the normal to the flow direction.)

$$c_p = 1.839 \sin^2(\theta)$$

Based on this relationship the drag coefficient C_d, assuming the probe tip is an approximately cylindrical body, can be found using the following integral.

$$C_d = \frac{1.839}{2} \int_{\pi}^{0} \sin^3(\theta)\, d\theta$$

This approximates to $C_d = 1.226$, which means that the drag pressure (P_d) acting on the frontal area of a cylinder can be approximated using the following equation, given the velocity (u_∞) and density (ρ_∞) of the freestream flow.

$$P_d = \frac{1}{2} C_d \rho_\infty u_\infty^2$$

Since the pitot probe tip was cylindrical in shape, these relations could provide a good enough estimate of the pressure (in Pascals) which would act on the pitot probe tip during operation. This relies on the assumption that there is no viscous drag, however this is not a bad assumption to make, and is common in preliminary hypersonic design calculations. Table 4.4-1, Table 4.4-2 and

Table 4.4-3 display a summary of the calculations used to determine the drag pressure under the scramjet, planetary re-entry and test conditions outlined in Section 4.1 of this report.

Table 4.4-1: A table summarising the pressure drag calculations for the three scramjet conditions mentioned in Section 4.1.1

Condition	**Scramjet at Mach 10**	**Scramjet at Mach 12**	**Scramjet at Mach 14**
Free Stream Pressure (Pa)	1368	950	698
Free Stream Temperature (K)	226	228	233

Free Stream Density (K)	0.021090932	0.014518002	0.010438008
Free Stream Velocity (m/s)	3011	3633	4282
Drag Pressure (kPa)	117.213	117.462	117.319

Table 4.4-2: A table summarising the pressure drag calculations for the test conditions mentioned in Section 4.1.3

Condition	**Test 1-Low Enthalpy Flow**	**Test 2-High Enthalpy Flow**
Free Stream Pressure (Pa)	13000	5000
Free Stream Temperature (K)	700	2000
Free Stream Density (K)	0.06470881	0.008710801
Free Stream Velocity (m/s)	3500	10000
Drag Pressure (kPa)	485.914	533.972

Table 4.4-3: A table summarising the pressure drag calculations for the planetary re-entry conditions mentioned in Section 4.1.2

Condition	**Re-Entry at 11km/s**	**Re-Entry at 12km/s**	**Re-Entry at 13km/s**
Free Stream Pressure (Pa)	9000	9210	2380
Free Stream Temperature (K)	3287	3925	4621
Free Stream Density (K)	0.009540275	0.008175947	0.001794565
Free Stream Velocity (m/s)	11000	12000	13000
Drag Pressure (kPa)	707.630	721.707	185.911
Condition	**Re-Entry at 14km/s**	**Re-Entry at 15km/s**	**Re-Entry at 16km/s**
Free Stream Pressure (Pa)	5370	5320	1820
Free Stream Temperature (K)	5370	6185	7070
Free Stream Density (K)	0.003484321	0.002997023	0.000896954
Free Stream Velocity (m/s)	14000	15000	16000
Drag Pressure (kPa)	418.634	413.364	140.757

As can be observed from the tables, of the values calculated, the most significant drag pressure will act on the probe during re-entry simulations conducted at 12km/s and is 721.7kPa. There is of course, the chance that other simulations may produce conditions which lead to a higher pressure drag than the 12km/s re-entry simulation, or that the pressure drag associated with the driver gases which flow down the expansion tube after the test flow also lead to a higher pressure drag. However, for this initial prototype this is a good worst case to design to. Critically this pressure drag is also significantly higher than the pressure drag that will be experienced by the probe under its outlined test conditions (refer to Table 4.4-2). Therefore, selecting the drag value for re-entry at 12 km/s as the worst case scenario is a conservative design decision considering the testing conditions for the instrument.

Using this maximum drag pressure value of 721.7 kPa a finite element simulation was conducted on the probe tip using Ansys Workbench to determine the maximum static stress the probe tip would experience. A pressure load with a magnitude of 721.7 kPa was applied to forward facing surfaces of a model of the instrument and the Von-Mises (or equivalent) stresses were determined. As Figure 4.3.3 shows the maximum stress in the probe structure occurs were the tip joins to the main body. Critically this stress is very low at 2.91MPa which is orders of magnitude less than the yield strength of stainless steel, which is typically well in excess of 300MPa. Therefore, one could conclude that there is no risk of the probe failing and that it has

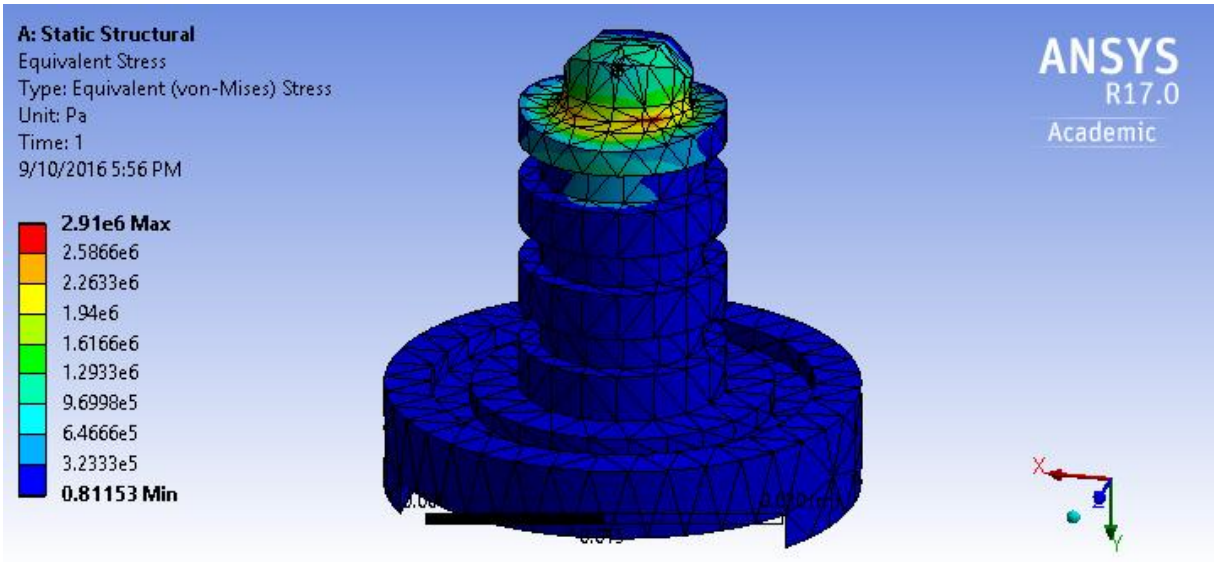

Figure 4.4.5: A finite element simulation of the pitot probe under a pressure loading designed to represent the highest possible pressure drag which could potential act on the tip. From the above graphic showing the Von-Mises (or equivalent) stress acting on the probe under this loading, it can be seen that the maximum stress at any location in the structure is 2.91MPa

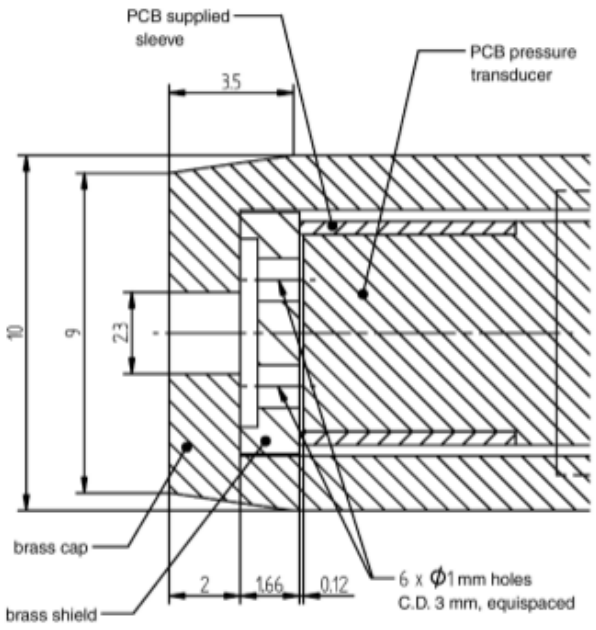

Figure 4.4.6: An technical drawing of a pitot probe currently used in the X2 shock expansion tube. As can be seen, the thickness of the probe walls is 2mm [10].

in fact been overdesigned. However, there is a very good reason for this overdesign. Whilst drag forces within shock expansion facilities are high, there is a far more significant risk to probe's structural integrity. As eluded to in Section 4.3.3, the hypersonic flows produced by shock expansion tubes often contained particles traveling at high speeds which have the potential to impact the probe tip with significant force. Therefore the appropriate structural integrity has to be built into the probe tip to be able to withstand these impact loads. The only real indication of what this might require is previous probe design. Figure 4.4.6 displays a technical drawing of a pitot probe currently use in the X2 Shock Expansion Tube Facility. As can be seen from this drawing, the thickness of the probe walls is 2mm. This was a typical thickness for all the pitot probes used in the X2 and similar shock expansion facilities. (Refer to Section 3.1.1, Figure 3.1.1 for more examples of such instruments.) As such the minimum thickness of the walls of the new probe directly facing the oncoming flow were a minimum of 2.5mm which was slightly thicker than the probes currently used. This would hopefully introduce some contingency into the design an ensure that this preliminary design would not fail structurally. The only place where the thickness of walls of the probe tip was not at least 2.5mm was on the top surface where distance between the horizontal hole and the top surface of the probe was 1.5mm. However, this surface was parallel to the flow direction hence it was unlikely to be impacted by any particles and as such can afford to be

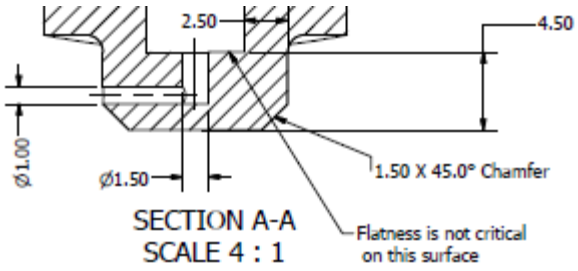

Figure 4.4.7: A drawing of the tip of the new pitot probe.

slightly thinner.

5 Instrument Testing

Based on the design discussed in Section 4 and displayed in Appendix – B two pitot probes were manufactured by a workshop at the University of Queensland. Therefore, it was possible to begin the testing of the new instruments. Unfortunately it was not possible to conduct a test at both of the conditions outlined in Section 4.1.3 due to the availability of the X2 facility. However is was possible to test the probes in a high enthalpy test flow comparable to the one listed in Table 4.1-3. This section details the instrument testing process and the results obtained from it.

5.1 Experimental Set Up and Procedure

The pitot probes were installed in the walls of the acceleration tube of the X2 shock expansion tube facility. Specifically, with reference to Figure 5.1.1, the two probes were installed at at3 and at5 respectively.

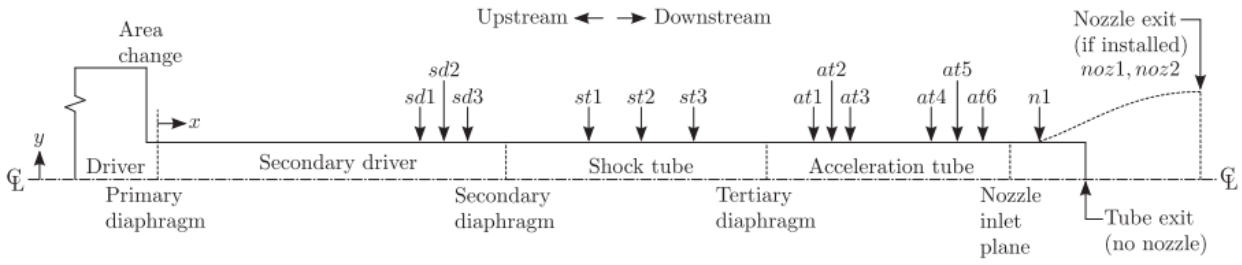

Description	x, mm	y, mm
Driver area change	-110	-
Primary diaphragm downstream face	0	-
Transducer $sd1$	2,577	42.5
Transducer $sd2$	2,810	42.5
Transducer $sd3$	3,043	42.5
Secondary diaphragm downstream face	3,418	-
Transducer $st1$	4,231	42.5
Transducer $st2$	4,746	42.5
Transducer $st3$	5,260	42.5
Tertiary diaphragm downstream face	5,976	-

Description	x, mm	y, mm
Transducer $at1$	6,437	42.5
Transducer $at2$	6,615	42.5
Transducer $at3$	6,796	42.5
Transducer $at4$	7,590	42.5
Transducer $at5$	7,846	42.5
Transducer $at6$	8,096	42.5
Nozzle inlet plane	8,343	-
Transducer $n1$	8,652	42.5
Tube exit (no nozzle)	9,105	42.5
Nozzle exit (if installed), $noz1, noz2$	10,731	100.8

Figure 5.1.1: A schematic of the X2 shock expansion tube facility show the exact location of the instrument mounting points within the facility. (This diagram is directly sourced from "Production of High-Mach-Number Scramjet Flow Conditions in an Expansion Tube" by Gildfind et al [9].)

These two locations were chosen for specific reasons. Firstly, these two instrument mounting points were separated by a significant distance, in this case 1.05m. The further the distance between the probes the longer it will take for the test gas to travel between them and therefore the less significant the effect of any delay in the response of the probes. In addition, due to the nature of the X2 facility it is only possible to mount the probes in line with each other in the direction of flow. Therefore it is advantageous to have them separated by as much distance as

possible, as a disturbance will be created by the first probe which could potentially affect the measurement recorded by the second. A larger distance between the instruments gives the flow more time to return to its initial state, and damp out the effect of this disturbance. Hence why it is important to have a reasonable separation distance. Another reason why at3 and at5 were chosen as the best location for the two probes, was that they were also a reasonable distance from each end of the acceleration tube. It was important that the leading probe was not too close to the tertiary diaphragm as the test flow undergoes rapid and unsteady expansion in this first part of the tube. Therefore it does not develop into a test flow with a reasonably constant velocity until further down the acceration tube, and hence it is obviously important that the leading probe only detect the flow once this has occurred. By the same token the trailing probe must also not be too close the end of the acceration tube. The disturbance this probe will create has the potential to interfere with the flow traveling through the test section. Hence, the further between this probe and the test section, the higher the chance that the disturbance will have been damped out of the test flow by the time it reaches this section. Therefore considering all the factors discussed in this paragraph it is obvious why at3 and at5 were sensible locations to mount the two probes.

Having installed the probes, the facility was prepared to produce a high enthalpy test flow, similar to that outlined in Section 4.1.3. Diaphragms were installed in each of the appropriate locations and facility was pressurized with air and a driver gas (consisting of 90% helium and 10% argon) as per Table 5.1-1. The piston is then fired and the test is run. This process was conducted twice in order to gather two set of data.

Table 5.1-1: The shock tube initial fill conditions.

Section	Driver Gas Initial Conditions	Shock Tube Fill Conditions	Acceleration Tube Fill Conditions
Pressure (Pa)	2.79×10^{7}	3000	10
Temperature (K)	2700	298.15	298.15

The resultant test flows produced by the expansion tube are detailed in Table 5.1-2 and Table 5.1-3. The shock processed accelerator gas flow properties have also been included. The data presented in these two tables was determined by combining measurements taken during the experiments with an adaption of inviscid flow theory which has been slightly refined

characterize the behaviour of the flow within the X2 specifically. To elaborate, static pressure sensors mounted in the acceration tube measure the velocity of the leading shock and the assumption is made that the test flow is also traveling at this speed. An assumption which, from experience, is known to be a good one due the prevalence of boundary layer effects (see Section 2.1.6 Mirels Effect). The other properties can then be determined using an adaption of the theory discussed in the Literature Review and outlined in

Appendix – A. The values in the tables below represent the best understanding of the of the flow conditions produced during the two tests.

Table 5.1-2: The test flow produced by the first experiment

Flow	Velocity (m/s)	Pressure (Pa)	Temperature (K)	Mach Number	Stagnation Pressure (MPa)	Pitot Pressure (Pa)
Test Flow	9468.1	5490.187	2965.9	9.24	4949.78	520300
Shock Processed Accelerator Gas	8897.2	9851.805	8741.4	3.59	1.596	151000

Table 5.1-3: The test flow produced by the second experiment

Flow	Velocity (m/s)	Pressure (Pa)	Temperature (K)	Mach Number	Stagnation Pressure (MPa)	Pitot Pressure (Pa)
Test Flow	9656.5	4229.07	2884.3	9.6	6099.3	423300
Shock Processed Accelerator Gas	9067.6	10240	9094.8	3.59	1.656	157700

For each test there were two sets of experimental data, collected from instruments installed in the facility, which were relevant to this investigation. The first and most obvious of these was the response produced by the new pitot probes. The second, was the measurements made by static pressure sensors which were also installed in walls of the X2. As the name suggests, these sensors measured the static pressure of the flow passing through the facility and were installed in all sensor mounting points not containing a pitot probe (sd1, sd2, sd3, st1, st2, st3, at1, at2, at4, at6 as per Figure 5.1.1). It was the data collected from these static sensors located in the acceration tube and from the two pitot probes which would from the basis for experimental analysis outlined in the next subsection of this report.

5.2 Results and Analysis

The primary purpose of this investigation was to evaluate the performance of the pitot probe design using the experimental results gathered from testing in the X2. At a basic level this involved, determining the velocity of the test flow as measured by the two pitot probes and contrasting it against the expected test flow velocity. Based on how the two compare a judgement could then be made as to whether the probes were capable of successfully

measuring the test flow velocity, and therefore the overall effectiveness of the instruments. However it was also possible to draw other conclusions about the performance of the probes, and therefore gain a better understanding of the strengths and weaknesses of their design. In addition to evaluating ability of the instruments to measure the velocity of the test flows generated by the shock expansion facility, this results and analysis subsection will also touch on:

- The response time of the instruments.
- The disturbance to flow through the facility, caused by the presence of the two probes.
- Noise present in the probe responses.

5.2.1 Test Flow Velocity Measurements

Determining the test flow velocity from the measurements made by the two probes involved examining the responses of both instruments during each test, and determining the point at which the test flow first arrives. The following graphs detail the response of both probes over the time period in which the contact surface between the test flow and accelerator gas was expected to arrive. (Refer to Appendix – C for more extensive plots of the probe responses.)

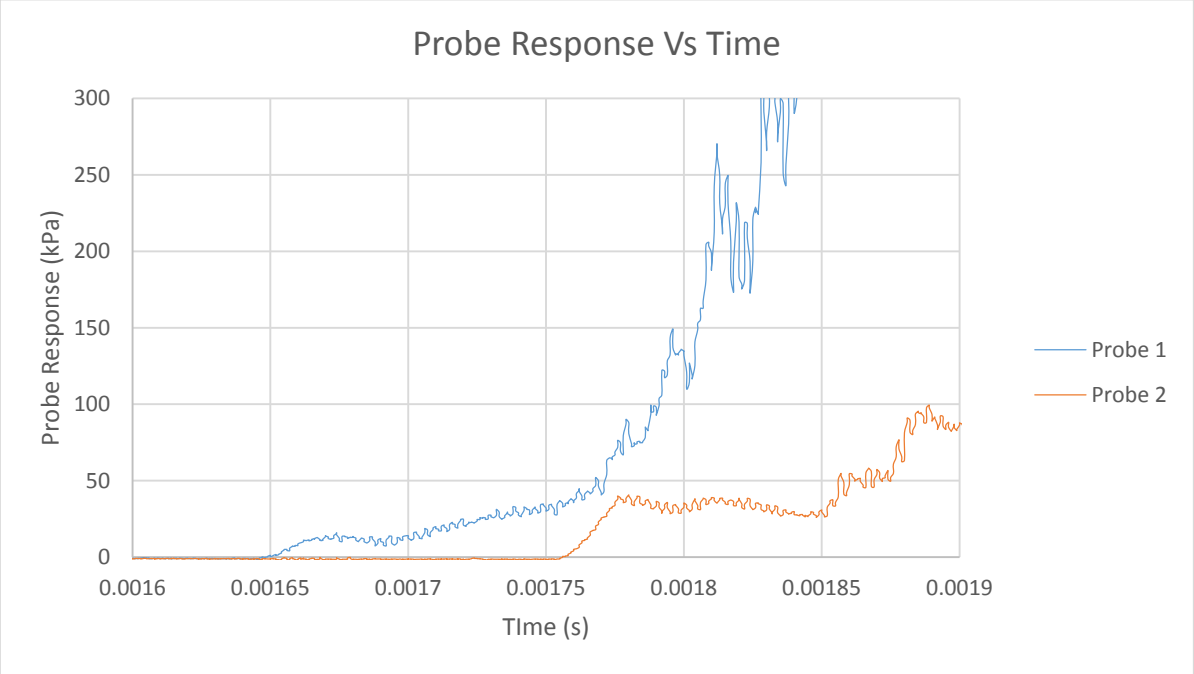

Figure 5.2.1: The pitot probe response over the time period of interest for the first test run in the X2.

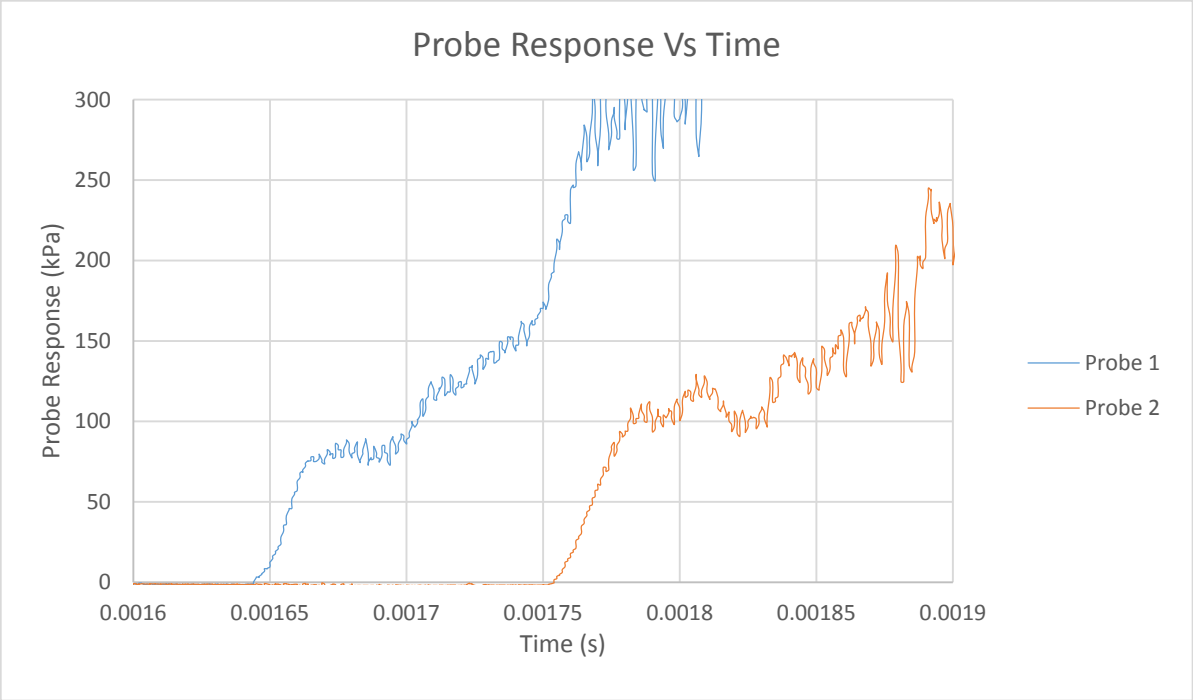

Figure 5.2.2: The pitot probe response over the time period of interest for the second test run in the X2.

It was clear from the plots when the leading shock arrives, as this is signified by the initial spike in the probe response. However the time of the arrival of the test gas is more difficult to determine. It was expected that the arrival of this gas would coincide with some change in pitot pressure, followed by a region of relatively constant pitot pressure. However this is not exactly what the results show.

Based on the data measured from the static pressure sensors it was determined that the average speed of the leading shock was approximately 9717.7m/s and 9586.4m/s for the first and second tests respectively. (The process via which this was obtained will be explained in Section 5.2.2.) Using inviscid flow assumptions and not accounting for any reaction effects, it was possible to estimate the velocity of the test flow based on the leading shock speed. (Refer to equations 2.1 -2.4 in Section 2.1.4.) This inviscid flow assumption ignores boundary layer effects and as such will underestimate the actual test flow velocity. From this it was possible to get a ball park estimate of the expected time difference between the arrival of the leading shock

wave and the test flow at each of the probes (refer to Table 5.2-1). Because of the inviscid assumptions made, the times displayed in Table 5.2-1 will be an overestimate of the difference in arrival time between the shock and the contact surface. (In reality the test flow eventually travels at a speed similar to that of the leading shock, however it initially is significantly slower and making inviscid flow assumptions is one way to model this behaviour.) Therefore it can be concluded that the arrival of the test flow at each probe must occur within the time periods outlined in Table 5.2-1, after the leading shock has arrived.

Table 5.2-1: The calculations leading to an estimate of the difference between the arrival time of the shockwave and the arrival time of the test flow at each of the pitot probes.

	Test 1		**Test 2**	
	Leading Probe (Probe 1)	**Trailing Probe (Probe 2)**	**Leading Probe (Probe 1)**	**Trailing Probe (Probe 2)**
Distance From Start of Acceleration Tube (m)	0.82	1.87	0.82	1.87
Average Leading Shock Velocity (m/s)	9717.7	9717.7	9586.4	9586.4
Estimated Test Flow Velocity based on Inviscid Flow Assumptions(m/s)	9099.63	9099.63	8976.5	8976.5
Expected Time Difference Between Shock Arrival and Test Flow Arrival (s)	5.7312×10^{6}	1.31×10^{5}	5.81×10^{6}	1.33×10^{5}

Looking at the data presented in the plots, there is no sudden change in pitot pressure within the time period in which the arrival of the test flow was expected. This was because the probes weren't designed to have a response time quick enough to be able to detect this. However it was still possible to determine when the test gas was passing over the probe as the nature of test flows is such that they have relatively constant properties. Therefore the sections of Figure 5.2.3 and Figure 5.2.4, directly after the initial spike (caused by the arrival of the leading shock), where there is no major fluctuation in pressure, represent the test flow. These regions have been identified with as much accuracy as possible in Figure 5.2.3 and Figure 5.2.4. By measuring the difference in time between the start of the two regions of steady pressure, it was possible to determine the velocity of the test flow they correspond to. In an attempt to do this with some level of accuracy, one of the sets of data was shifted in time such that it overlaid the other set of data. The time shift corresponding to this (Δt), was adjusted until the points on the two probe response graphs representing the beginning of the test flow, were aligned. Plots showing these two probe responses overlaid are displayed in Figure 5.2.5 and Figure 5.2.6.

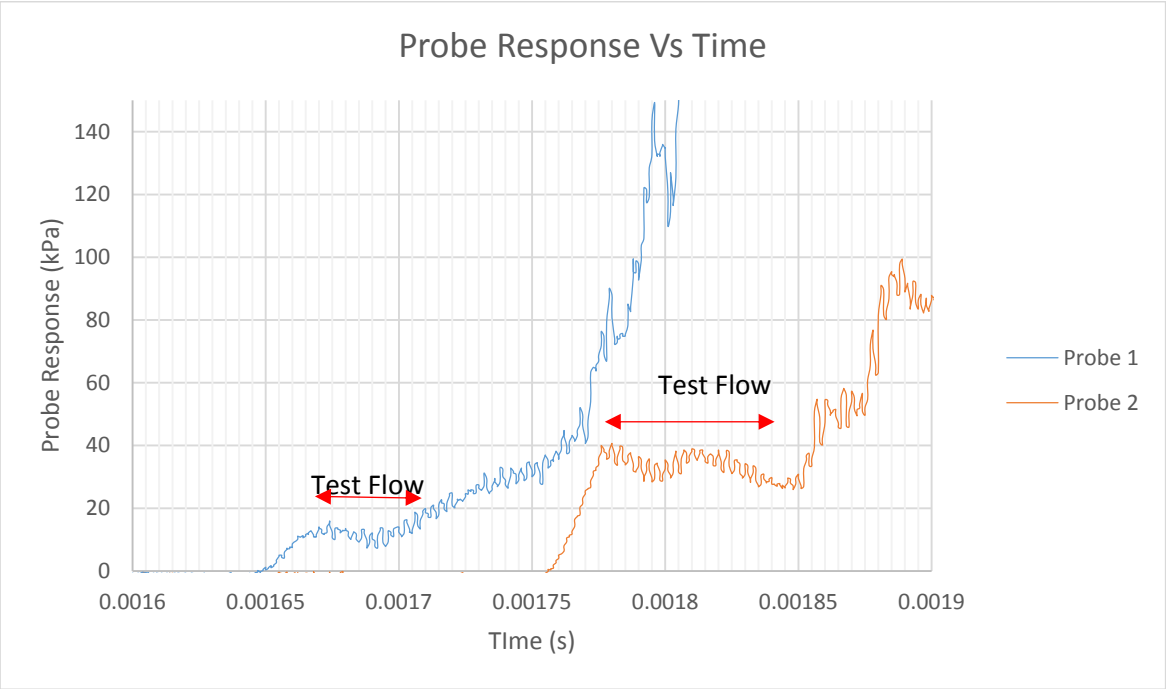

Figure 5.2.3: A plot showing the pitot probe response for the first test run in the X2. The sections of the pitot pressure-time curve suspected to correspond to the test flow have also been marked as has the time difference between. (Note the increase in the length of the test flow is part of its development as it passes through the acceleration tube.)

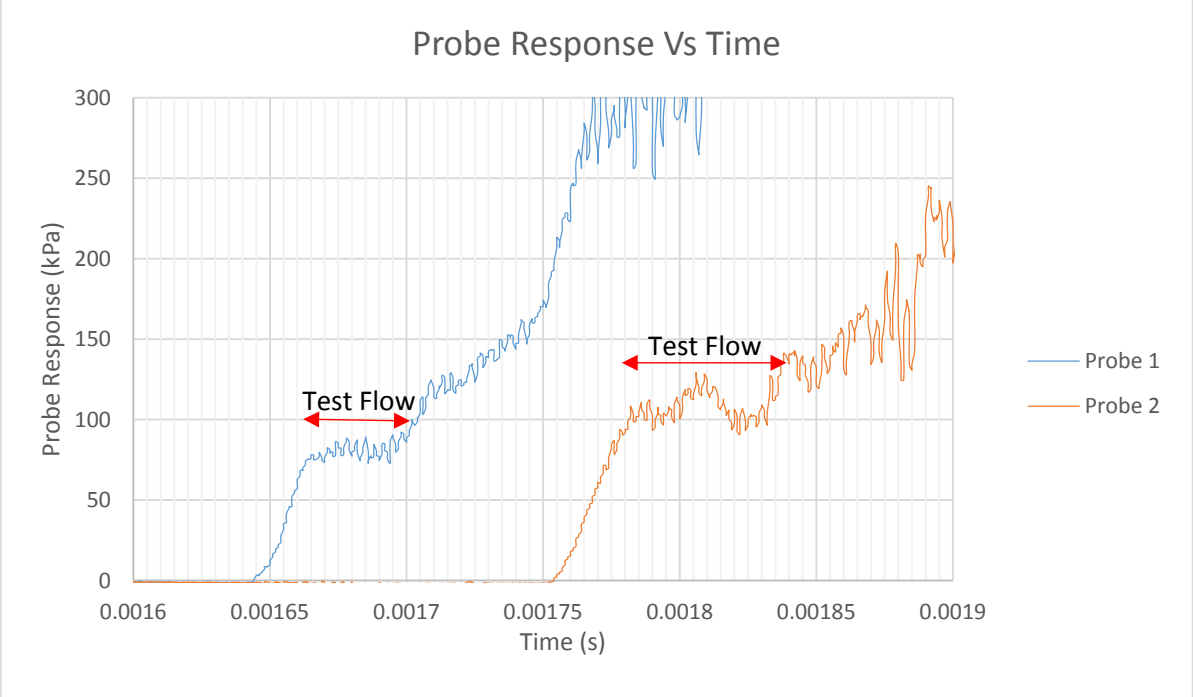

Figure 5.2.4: The pitot probe response over the time period of interest for the second test run in the X2. The sections of the pitot pressure-time curve suspected to correspond to the test flow have also been outlined. (Note the increase in the length of the test flow is part of its development as it passes through the acceleration tube.)

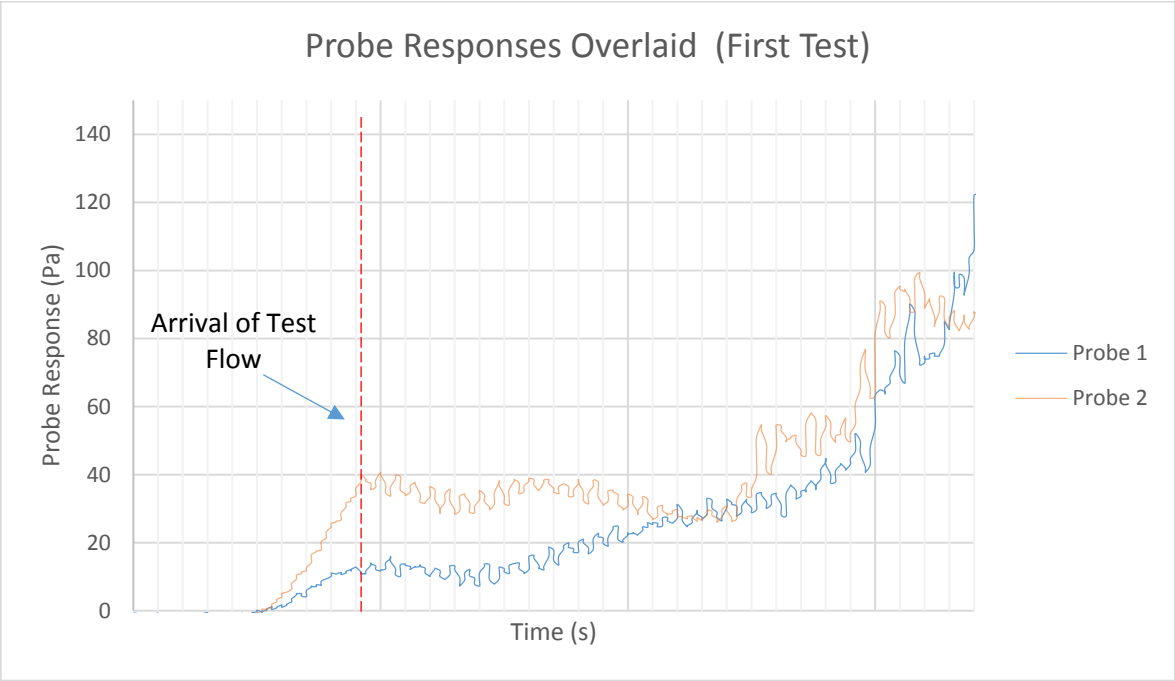

Figure 5.2.5: A plot showing the two pitot probe responses from the first test overlaid such that the points in the responses representing the beginning of the test flow are aligned. The time shift which needed to be applied to the pitot pressure data to achieve this was 108μs.

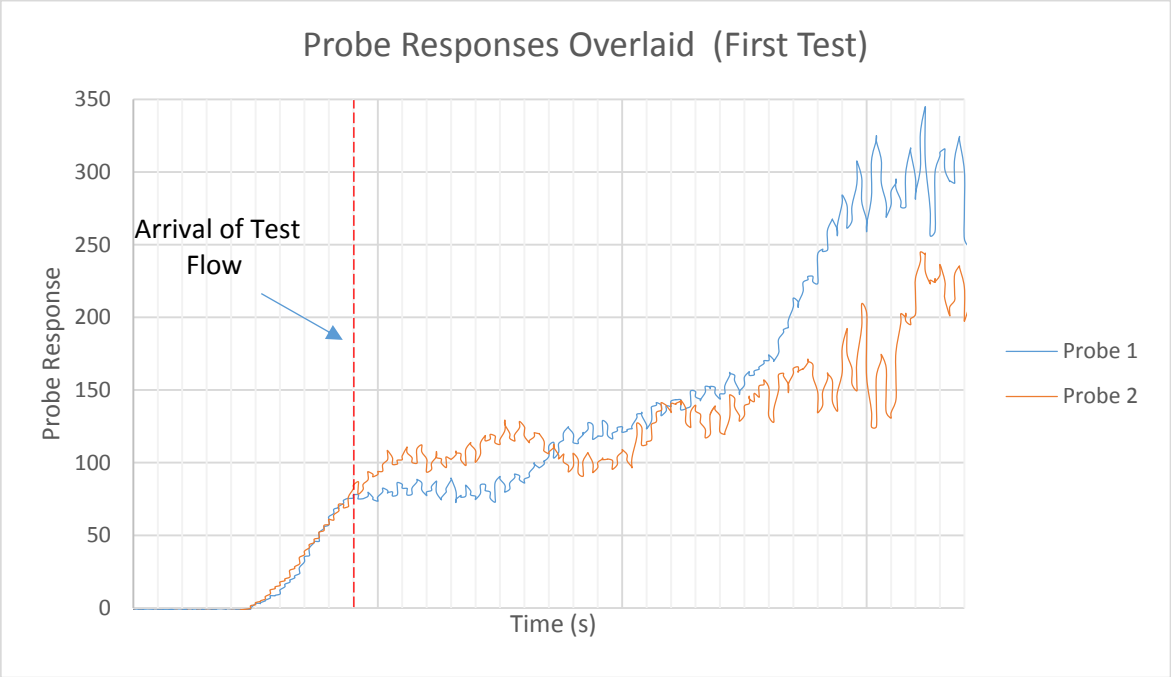

Figure 5.2.6: A plot showing the two pitot probe responses from the second test overlaid such that the points in the responses representing the beginning of the test flow are aligned. The time shift which needed to be applied to the pitot pressure data to achieve this was 110μs.

The time shifts required to produce the probe response overlays in Figure 5.2.5 and Figure 5.2.6 are displayed in Table 5.2-2. From these time shifts, the velocities of the test flows could be calculated and these are also displayed in the table for both of the tests conducted.

Table 5.2-2: A table showing the difference between the time at which the test flow is detected at each probe and the velocity subsequently calculated from this measurement. The current best estimates of the test flow velocity are also included for comparison to the values calculated using the probes.

	Test 1	**Test 2**
Time Difference Δt (µs)	108	110
Distance Between Probes (m)	1.05	1.05
Velocity As Measured by the New Probes (m/s)	9722.22	9545.45
Reference Velocity (m/s)	9468.1	9656.5
Percentage Error (%)	2.68%	1.15%

The results shown in Table 5.2-2 were incredibly promising. Using these two new pitot probe instruments, test flow velocity measurements have been made and were also very reasonable. For these probes to predict test flow velocities to within 2.68% of the current best estimates, strongly indicates that these instruments have real potential to take accurate measurements. It should also be mentioned however, that whilst these initial tests have largely been successful, there were some obvious flaws with this velocimetry technique. The most significant of these was the fact that any measurement made is going to be very sensitive to the way in which the probe response graphs are interpreted. Specifically, defining the points on these graphs where the test flow arrives is quite difficult and somewhat subjective. The response of the pitot probes to the test flow's arrival is far from instantaneous, and there is no sharp change in the resulting graph. Rather there is a more gentle transition from the steep increase in pitot pressure associated with the initial shockwave, to the more constant region representing the test flow. Defining a test flow arrival point on this transition part of the response graph is quite difficult. If the response plots are interpreted even slightly incorrectly this could cause a huge error in the resulting velocity measurement. For example, if the time difference, for the first test in this experimental investigation, was interpreted as being 107µs (as opposed to 108µs), then the measured velocity changes by 90.9m/s. Due to how difficult it can be to define the arrival of the test flow at each probe it is entirely foreseeable that the time difference could be wrongly interpreted by several microseconds, resulting in a velocity uncertainty of several hundred

meters per second. Therefore it is important to keep the success of this initial test in perspective. None the less the results were very positive in terms of the potential of these instruments to take accurate measurements.

5.2.2 Instrument Response Time

As outlined earlier, it was also worth assessing the effectiveness of the pitot probes in terms of their response time to any change in pitot pressure. Hence allowing a conclusion to be drawn as to whether there was need to alter the design of the instrument to improve its sensitivity. It was decided that the best way to establish how quickly the probes responded to a change in pitot pressure was to compare them to the static pressure sensors. These static sensors operated using the same pressure transducers as the pitot probes however there was no structure obstructing their access to the flow. Hence their response to changes in pressure was only limited by the response time of the pressure transducer. Therefore, comparing the response of these sensors to the pitot probes would provide an idea of how much the probe's response was compromised by the flow having to travel through the probe tip to reach the pressure transducer. From this a judgement can be made as to whether the design of this tip facilitates a fast response time.

Both the probe and the static pressure sensors were capable of detecting the arrival of the leading shockwave. This shock wave could be assumed to be moving at a relatively constant velocity and as such its movement could be displayed on a linear position vs time plot. Such a plot could be generated using the pressure data obtained from the four static sensors located in the acceleration tube. (Refer to Appendix – C for plots of the responses of these pressure sensors.) Given the location of each of these sensors was known, and the leading shock could be considered to have arrived when an increase in pressure was detected, Figure 5.2.7 and Figure 5.2.8 were produced. Also marked on these plots is the time and location at which each of the two pitot probes detect the arrival of the leading shock. Based on the variance of the pitot probe detection points from the shock location vs time curve, the response time of the probes could be evaluated. (It is also worth mentioning that it was the gradients of these curves which were used to determine the leading shock velocities for the calculations in Section 5.2.1) If the probe tip design was 100% efficient then these points would lie directly on the position vs time curve. If there was a delay in the response, the probe detection points would lie below the

curve. Based on Figure 5.2.7 and Figure 5.2.8 there appears to be some delay in the detection the leading shockwave, however this delay seems quite small. In fact, during the second test it appears that the trailing pitot probe has responded faster than the static pressure transducers. Although this could easily have been caused by background noise interfering with the detection of the leading shock at one of the static pressure sensors. Regardless of this, comparative to the static sensors, the response times of the pitot probes are quite good.

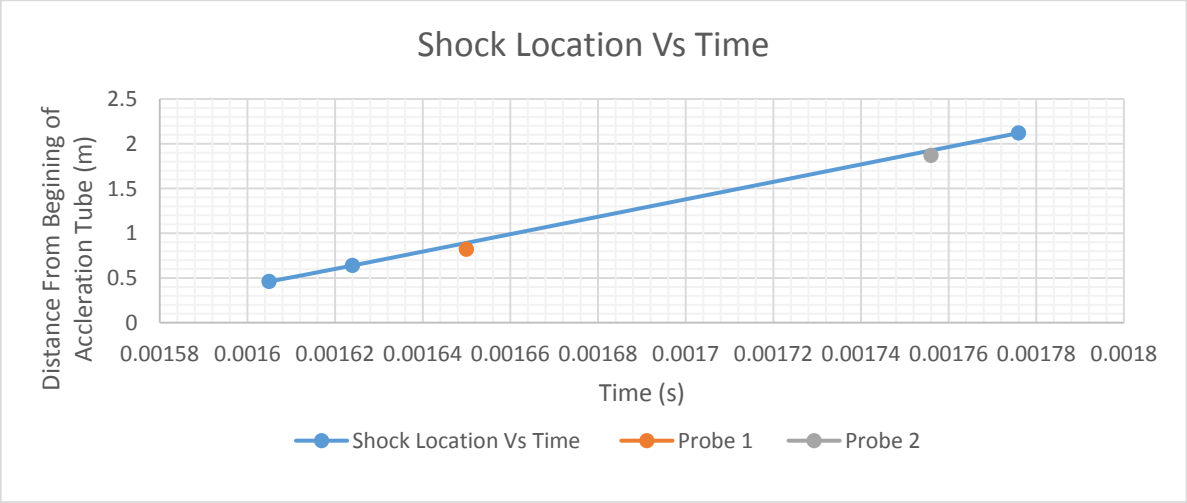

Figure 5.2.7: The shock location vs time plot produced from the static pressure sensor data obtained from the first test. (Note data from the pressure sensor located at at4 has not been used as it was deemed to be erroneous.) Also marked is the position and time at which the two pitot probes detect this leading shock.

Table 5.2-3:A table showing how the response times of the pitot probes vary from those of the static pressure sensors.

	Test 1		Test 2	
	Probe 1	**Probe 2**	**Probe 1**	**Probe 2**

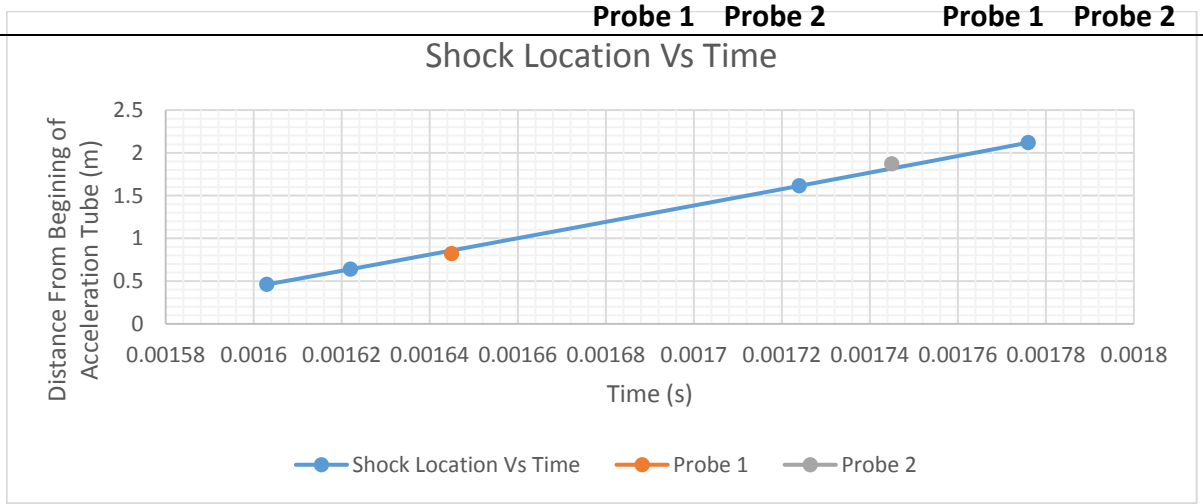

Figure 5.2.8: The shock location vs time plot produced from the static pressure sensor data obtained from the second test. Also marked is the position and time at which the two pitot probes detect this leading shock.

Time Shockwave Detected by Probe (µs)	1650	1756	1645	1745
Expected Detection Time (µs)	1642.26	1750	1640.76	1750
Response Time Delay (µs)	7.74	5.69	4.24	-5.3

Table 5.2-3 outlines the difference between the expected arrival of the shockwave and the time at which it is detected by the pitot probes. What this table shows is that the maximum response delay of the probes is 7.74 microseconds which is of the same order of magnitude as the response time of the pressure transducers used to take the measurements. Such a small delay in the response time can be considered negligible and this is supported by the fact that one of the appears to respond even faster than the static sensors during the second test. Therefore, based on the information available, it has to be concluded that the probe tip doesn't cause any significant delay in the response time of the instrument compared to the static pressure sensors. These static sensors are known to have very good response time, hence this preliminary probe design can be considered successful in terms of its ability to react quickly to changes in pitot pressure. The response time of this instrument has met, if not exceeded its design expectations.

5.2.3 Interference with The Test Flow

It is difficult to draw any concrete conclusions from the experimental data about the disturbance effect of the probes on the test flow. Ideally a pitot rake would have been used to survey the test flow as it passed through the test section of the X2. However this did not eventuate. The other data was not really collected with the intention of using it to analyse the probe interference in the flow. None the less it was possible to make some assertions as to the disturbance created by the two instruments. Based on the pitot pressure readings made by the trailing probe, it does not appear that the leading probe has created a disturbance which affects the flow further downstream. Referring to Figure 5.2.3 and Figure 5.2.4, for both tests it appears that the region of the rear probe response graph, corresponding to the test flow, maintains largely constant properties. To be more specific, the pitot pressure corresponding to this test flow is reasonably steady (compared to other parts of the response graphs) which is what would be expected for an undisturbed test flow. If this test flow had been significantly disrupted by the leading pitot probe, to the point where it was no longer useful for testing, it was thought that the pitot pressure measured by the trailing pitot probe would be chaotic and unsteady.

Generally this was not the case, indicating that either the leading probe creates very little disturbance in the test flow, or that this disturbance had been largely damped by the time it reached the trailing probe. There were some fluctuations in the response of the rear probe corresponding to the test flow, particularly in the first test. However these fluctuations were not too much larger than the fluctuations in the test flow pitot pressure measured by the leading probe. Hence they did not indicate that the test flow was unsteady or had been significantly disturbed. This did not necessarily mean that the test flow was actually steady and useful for testing, however it was a positive indication that this was the case.

It was also expected that if the leading pitot probe caused a significant disturbance in the flow through the shock tube, then a drop in pitot pressure would be measured at the trailing probe. This is because there would be a stagnation region directly behind the leading probe, and flow from this region would travel some distance down the shock tube before it would return to the same conditions as the rest of the test flow. Therefore it was expected that the velocity and hence the pitot pressure detected at the second probe would be less than the first. However this was not the case, rather the pitot pressure at the second probe is higher than the first. The most likely reason for this is that the test flow is still developing as it travels down the tube from the first probe to the second probe. This is a positive sign as it indicates the disturbances caused by each of the probes are not propagating downstream with the test flow, rather they are being damped out. Again it is not possible to make this conclusion with any certainty however the signs from the data are positive.

Realistically, to truly determine the effect of the probes on the test flow, further testing is required. As mentioned earlier, surveying the test flow with a pitot rake would be a good place to start. However based on the experimental data gathered there is no reason to assume that these probes cause significant disruption to the test flows produced by the shock tube facility.

5.2.4 Noise Effects

Based on Figure 5.2.1 and Figure 5.2.2, the noise present in the data recorded by both probes was reasonably low. There are clearly oscillations present in the data recorded, however the magnitude of these oscillations are not significant. The oscillations which are present, all seem to be of the same frequency. Figure 5.2.9 shows, using a simple approximation technique, that

this oscillating frequency is very similar for all of the probes at approximately 312.5kHz to 337.5khz. These approximations have be made based on a sample of each probe response corresponding to the pitot pressure of the test flow, and it seems clear that the oscillating frequency is constant throughout the response of every probe. 312.5kHz to 337.5khz is a very high noise frequency, which is one of the reasons why the magnitude of the noise (particularly in the test flow region of the response) is so low. There are a variety of potential sources for a

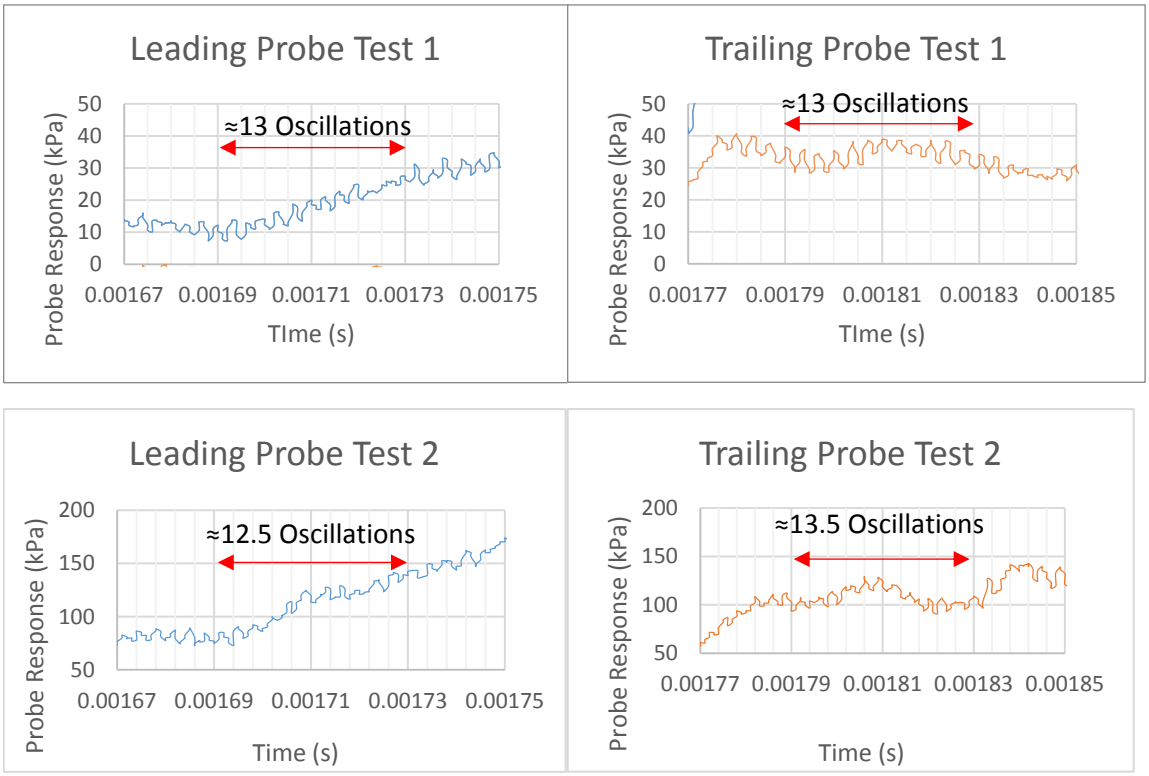

Figure 5.2.9: Samples of the pitot probe responses representing the test flow region of the data. In this important region of the graphs, all the responses seem to oscillate approximately 12.5-13.5 times over a 40μs period. This corresponds to an oscillating frequency of approximately 312.5kHz to 337.5kHz.

noise frequency like this, including the structure of the expansion tube facility, and oscillation within the pressure transducer itself. The PCB model 112A22 transducer was known to have a resonant frequency greater than 250kHz (according to product specifications [35]) so it was entirely possible that this was excited. Regardless, by virtue of the fact that the amplitude of the noise was very low in all the important parts of the response graphs, it had to be concluded that the probe design was a success, in terms of its ability to produce responses relatively free of noise. The concerns during the design phase of this investigation about Helmholtz resonance issues appear not to have materialized.

5.3 Summary and Discussion of Instrument Performance

The overall conclusion of this preliminary testing of these pitot probe instruments is that, for a preliminary design they were largely a success. Firstly and most importantly, the two probes managed to predict the velocity of the test flow to within 3% of the current best estimates. This was a major achievement for this investigation however there are some important things to recognise about the success of the two probes. The most important of these things was that it was difficult to determine, from the probe's responses exactly when the test flow arrived at each probe. As eluded to earlier, the test flow was identified as the region of the response graph where the pitot pressure is essentially constant. However these regions were hard to identify on some of the response graphs as the pitot pressure was never truly constant. The same problem applies to identifying the point at which the test flow arrives at the probe. There is no sharp change in pitot pressure visible in the response graphs at the point at which this happens, rather the initial pitot pressure increase associated with the arrival of the leading shockwave morphs into the region of steady pressure suspected to be associated with the test flow. The lack of a clear point of transition means there is scope for significant error to be made here. As has already been discussed, wrongly identifying the time at which the test flow arrives at each probe by even 1μs can result in a change in the measured velocity by nearly 100m/s for these high enthalpy shock tests. Based on how difficult it was to estimate the test flow arrival times during this analysis it is foreseeable that these values could be easily wrongly estimated by several microseconds resulting in velocity measurements with large uncertainties. However despite this significant issue, the fact that reasonably accurate measurements were made means that this design investigation can still be classified as a success. Even if the velocity measurements hadn't been accurate, the data collected by the two probes still provided a useful insight into the behaviour of the flow through the shock expansion tubes. Clearly these instruments have enough potential to collect useful information.

The probes were also deemed to be a success in terms of their ability to respond quickly to a change in pressure. As Section 5.2.2 outlined, the response times of the new probes were found to be comparable to that of the static pressure transducers installed in the X2 shock expansion facility. Whilst this was a very good result, there was still some uncertainty as to just how rapid the response of the probes really were. To elaborate, the instruments obviously detected the

arrival of the leading shock wave very quickly however, there was some doubt about their sensitivity to pressure changes after this shockwave. Ideally more testing should be conducted, perhaps with optical instruments or conventional hypersonic pitot probes, to verify that this new design still responds rapidly to pressure changes behind the leading shock. However, based on the data available, the sensitivity of the pitot probes was excellent.

The performance of the new probe design in-terms of the noise present in the pressure data recorded by the instruments was also found to be favourable. Somewhat surprisingly there were no significant Helmholtz related complications, and the noise that was present had a relatively low magnitude. In addition, there was no evidence that the pitot probes were compromising the ability of the expansion tube to produce steady test flows. Though it must be acknowledged that part of the reason for this was the fact that there was very little data which could be used to establish the effect of the probes on the test flow. Therefore the conclusion with regards to this, was that more testing is required, however there were no obvious signs of significant flow disruptions.

In summary, the testing of this preliminary pitot probe design aimed at measuring the test flow velocities in shock expansion facilities has to be considered a success. Although there are some questions about the how accurately these instruments will be able to take measurements, every other aspect of the experimental data was positive. As has been alluded to, some of these results should be verified by further testing, however further testing is probably appropriate given the promise that this velocimetry concept has shown. Seeing as testing would have also been conducted for low velocity and low enthalpy test flows had it been possible, this would be an intelligent inclusion in any future test program. In any case, in light of the success of this pitot probe based velocimetry technique in these preliminary experiments, further research, development and testing is highly recommended.

6 Conclusion

Shock Expansion tubes are a vitally important tool for hypersonic research. They have capabilities unmatched by any other ground testing facility in terms of generating high enthalpy hypersonic test flows. Without them, many of the advancements in the fields of scramjet flight, planetary re-entry and supersonic combustion would not have been possible. However, one of the major weaknesses of shock expansion tubes is that there is a great deal of uncertainty surrounding the properties of the test flows they generate. This investigation aimed to reduce this uncertainty by designing and testing a new instrument capable of measuring the velocity of these test flows. The idea being that information gathered from this instrument will give researchers more data with which to better understand the properties of the test flows produced by expansion tubes.

Shock expansion tubes generate high velocity test flows by firstly compressing a driver gas behind a primary diaphragm. At a specific pressure this diaphragm bursts and releases a shockwave into a shock tube containing the test gas. This shockwave compresses, heats and accelerates the test gas which then ruptures a secondary diaphragm and expands into an acceleration tube. The unsteady expansion causes the gas to further accelerate up to the final velocity at which it passes through the test section. Some facilities also employ a secondary driver stage where the driver gas accelerates a secondary driver gas which in turn accelerates the test gas. This arrangement offers some specific performance benefits however the basic configuration would be the focus of this investigation. The primary reason for this was that all testing was to be conducted in the University of Queensland's X2 shock expansion facility which would not be incorporating a secondary driver stage.

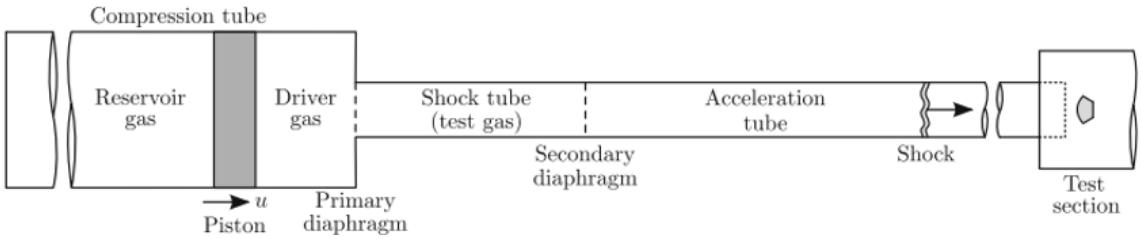

Figure 6.1.1: A Schematic of a simple shock expansion tube [4].

Currently, test flow velocities are determined using a combination of instrument measurements and theoretical analysis. Typically static pressure sensors mounted in the acceleration tube

measure the leading shockwave velocity and then employ an inviscid flow analysis to determine the test flow velocity. (Although in some cases the test flow velocity is just considered to be the same as the shockwave velocity.) However, there are inherent inaccuracies involved in using inviscid flow theory. Most significant of these is the fact that it fails to account for boundary layer behaviour, otherwise known as Mirels effect. Other inaccuracies stem from energy absorbed by diaphragm rupture and acoustic disturbances. Hence there is a clear need for an instrument to better characterise test flow velocities.

After reviewing literature, four velocimetry techniques or methods were found which were considered to have strong potential to be able to measure the velocity of the test flows produced by hypersonic facilities. These were:

- Planar Laser Induced Fluorescence (PLIF)
- Rayleigh Scattering
- Tuned Laser Diode Absorption Spectroscopy (TDLAS)
- Pitot Probe Measurements

After considering the strengths and weaknesses of each technique it was decided that the pitot probe method was the most appropriate to continue forward with. In brief, this concept involved using two pitot probes mounted in the acceleration tube of a shock expansion facility to detect the arrival of the test gas. Based on the difference in detection time and the distance between the two probes the velocity of this gas could be determined. There were many reasons why the pitot probe concept was chosen over the other three however the main ones were these. Firstly the simplicity of the technology involved, comparative to the other velocimetry methods, offered multiple benefits. These included, lower costs, smaller chances of problems and shorter design, production and analysis times. Secondly the pitot probe concept was also the only method which did not involve the use of lasers. Lasers are expensive, complicated and often dangerous so given the time and budget constraints on this investigation a laser based velocimetry technique might have posed a risk to the successful completion of this investigation. Finally the new instruments had to be installed in the X2 shock expansion facility for testing. However optical access to the test flow in the X2 was very limited. In fact, to implement the PLIF or Rayleigh Scattering velocimetry techniques would have most likely

required structural changes to the X2 and TDLAS instruments would also have been difficult to install. The pitot probes on the other hand could easily be designed to be mounted in pre-existing 18mm access holes in the acceleration tube. Hence why it was the chosen concept upon which to base the instrument design.

Having selected the pitot probe concept it was then possible to move towards designing an instrument. A brief review of literature was conducted into hypersonic pitot probe design to gauge how other designers had created these instruments. Some of the important findings from this review were that; all probes used piezoelectric pressure transducers which needed to be protected from the flow in some way, steel was a popular material although brass and copper were not uncommon, and small streamlined probes were used in cases where minimum flow disturbance was required. The variety of ways designers dealt with different design issues was very useful in terms of informing the new probe design.

Based on the literature reviews of shock expansion tunnels and previous hypersonic pitot probe design it was perceived that the most pertinent design challenges for the new probe would be:

- Ensuring the probe was structurally capable of surviving the harsh hypersonic flow.
- Ensuring the pressure sensor was adequately protected from the hypersonic flow.
- Ensuring the response time of the probe to pitot pressure changes was adequate to detect the arrival of the test flow.
- Ensuring the measurements made by the probe were not affected by Helmholtz resonance.
- Ensuring the disturbance to the test flow caused by the presence of the probe is minimised.
- Ensuring the probe is not submerged in any boundary layers such that it can't detect the arrival of the test flow.
- Ensuring the probe could be mounted in the X2 shock expansion facility.

These were effectively the criteria to which the probe was designed. The final result is pictured

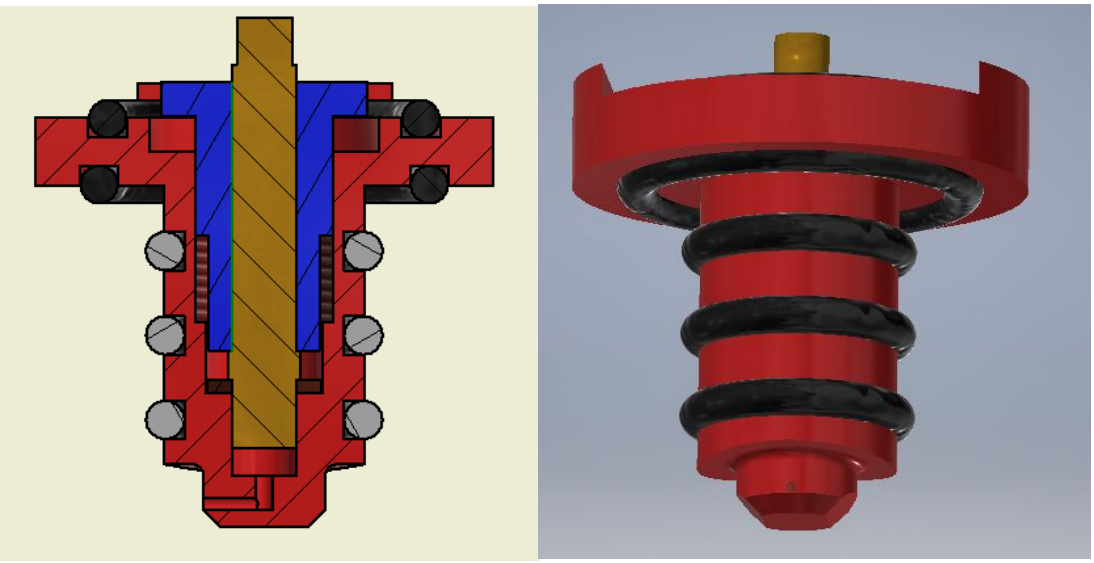

Figure 6.1.2: A cross section and isometric view of the pitot probe design. The red component is the probe structure, the yellow component is a pressure transducer and the blue component is a threaded screw used to secure the transducer.

in Figure 6.1.2.

To summarize how each one of these was addressed, firstly to ensure the probe was structurally sound enough, it was first necessary to define the hypersonic flow environments in which the probe would be expected to survive. This involved defining the most extreme high and low enthalpy flows the expansion tubes could be expected to produce as well as the conditions in which testing was expected. Estimations of the drag force that would act on the probe could then be made using Newtonian flow mechanics. From this point finite a element analysis was conducted to ensure the probe could withstand the applied drag forces for the worst case scenario. In addition it was known that particles entrained within the flow, (most likely originating from ruptured diaphragms), were likely to impact the probes and create large impulse loads on the structure. As such the probe was designed to have thicker walls than comparable instruments identified in the literature review of previous designs. The thinking being that if the other probe survived the impact of particles entrained within the flow, then the new design should also survive this particle impact. Secondly, to protect the pressure transducer (shown in yellow in the above Figure), line of sight access to the freestream was obstructed, with the flow directed around a 90^{o} bend to access the sensing surface. Literature had suggested this was an effective way to prevent damage to this component. Thirdly to minimize

the response time of the probe, it was ensured that the volume of the holes linking the sensor to the freestream were as small as possible, as studies had shown this was directly linked to the instruments response time. This same concept the was also applied to the cavity containing the transducer itself.

In terms of addressing potential Helmholtz resonance problems, the design principal was to make the holes linking the freestream and the pressure sensor as short as possible. This would increase the resonant frequency (in the longitudinal direction) of these cylindrical cavities which in-turn would lower the amplitude of noise that would be picked up by the pressure sensor. In addition, with regards to the minimising the disturbance cause by the probe, the primary method of addressing this was to minimise the size of the probe. As the literature review revealed, the smaller and more streamlined the probe, the smaller the disturbance to the test flow. However this contrasted somewhat with the need of the probe to avoid submersion in the boundary layer of the test flow. As some preliminary computational fluid dynamics analysis showed, the probe would be required to be able to take measurements 3.5mm from the tube wall in order not to be compromised by the boundary layer. This meant that the minimum height of the probe tip had to be 5.5 mm such that the sensing hole could be 3.5mm from the tube. Finally the requirement that the probe must be able to be mounted in the X2 was met by basing large parts of the design on static pressure sensors which were already mounted in the 18mm access holes in the X2. Essentially all parts of the device excluding the probe tip were copied directly from this static sensor as there was no need to redesign a new way to mount the probe. In summary it was the combined consideration of all these factors which lead to the pitot probe design shown in Figure 6.1.2.

The final step of this investigation was to test the new pitot probe velocimetry concept in the X2 shock expansion tube. After manufacturing two probes, they were installed in the X2 and two experiments were conducted producing two high enthalpy test flows with velocities of approximately 9468.1m/s and 9656.5m/s. During each of these experiments data was collected from static pressure sensors mounted in the acceleration tube and each of the two pitot probes. After analysing the responses of both probes and identifying, as accurately as possible, the time at which the test flow arrived at each probe, the velocities of the test flows were calculated. What these calculations showed was that the pitot probes had reasonably accurately measured

the velocities of the test flow. For both experiments the measured test flow velocity was within 3% of the current best estimates. These were highly promising results and strongly indicated that this velocimetry technique had the potential to effectively measure test flow velocities in shock expansion tubes. It was noted however that it was quite difficult to identify the location of the test flow on the pitot probe response graphs and therefore the time of arrival of this flow at each probe was difficult to determine with any accuracy. This meant there were significant levels of uncertainty associated with the velocities measured by the probes. It is foreseeable that, measurements made by these probes could easily possess large levels of error based on the smallest of errors made in interpreting the response graphs. In any case the results of this particular investigation were still very positive.

Further analysis of the experimental data also allow several more conclusions to be made. Firstly, by comparing the times at which the leading shock was detected by the pitot probes and the static pressure sensors it was found that essentially the probes detected this shock just as quickly as the static sensors. This indicated that the response times of the probes were excellent, though in an ideal situation more testing would be done to further validate this conclusion. The data also showed that relatively little noise was present in the pressure measurements recorded by the probe, or at least in the parts of the probe response that were of interest. Finally there was no evidence in the experimental results that the probes caused significant disruption to the test flow. However, there was really no way to know if this was actually the case based on the information that was obtained. Further testing was required to make any solid conclusion regarding whether the two probes created a disturbance capable of compromising the integrity of the test flow, however there were not any obvious indications that this was the case in these results.

In conclusion, in broad terms, the initial aims of this investigation have been largely achieved. An instrument has been designed which was shown to have the potential to measure the velocity of the test flow in a shock expansion tube with reasonable success. There were legitimate concerns surrounding the uncertainty of the velocity measurements and difficulties interpreting the response graphs produced by the two probes. In addition, it is still largely unknown as to whether the use of the pitot probes in an expansion tunnel causes significant disruption to the test flow. It is also unknown how these probes perform under different

expansion tube operating conditions to the ones at which testing was conducted. However what is important is that the results of the investigation have shown that this velocimetry technique has potential. All indications are that the pitot probes, have to a certain extent, performed as intended, and could be the key the better characterizing test flows in shock expansion tubes. Certainly further testing is warranted to further explore the potential of this concept, and either validate or disprove the findings of this study.

Appendix – A

Theoretical Analysis of Shock Expansion Tubes

It is possible to conduct a basic analytical analysis of shock expansion tubes. The following procedure, directly adapted from *"Performance considerations for expansion tube operation with a shock heated secondary driver"* by David E Gildfind et al, outlines one way this can be done and gives an idea of the assumptions that underpin the common understanding of these tubes. [6]

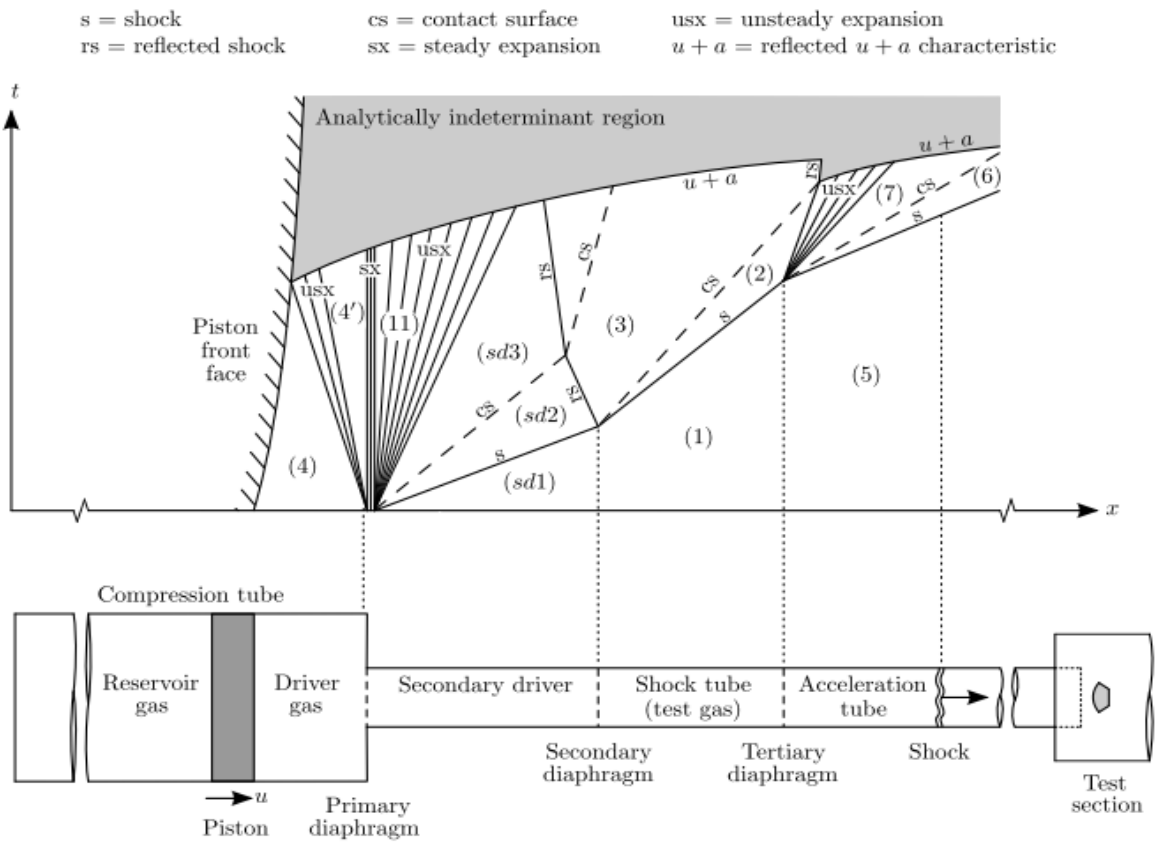

Figure.1: An X-T diagram showing the basic behaviour of the gas in a shock expansion tube directly after it is fired. (This diagram is directly adapted from "Development of High Total Pressure Scramjet Flow Conditions using the X2 Expansion Tube" *by David E Gildfind [1].)*

Table 0-1: The definition each variable used in the following analysis.

Variable	Property
T	Temperature (K)
P	Pressure (Pa)
M	Mach Number
a	Sound Speed (m/s)
u	Velocity (m/s)
γ	Ratio of Specific Heats
R	Ideal Gas Constant (J/kg/K)

Note: Throughout this analysis the first subscript of each variable indicates the region, (outlined in Figure.1) the property refers to. If a second subscript is a naught (0), this indicates the property refers to the stagnated state of the gas.

As the series of expansion lines displayed in Figure.1 indicate, the first thing that occurs after the diaphragm bursts is an expansion in both directions. Assuming there is a reasonably large area change across the diaphragm (between the driver and shock tubes), the unsteady expansion of the approximately stagnant driver gas has only a small effect on its stagnation properties. Therefore, for the sake of the analysis the following was assumed [1].

$$T_4 \approx T_{4'} \approx T_{4',0} \qquad \textit{Eqn 1.1}$$

Where the temperature of the compressed, heated driver gas (T_4) was found assuming isentropic compression with a density ratio of λ from an initial known fill temperature of $T_{4,i}$

$$T_4 = T_{4,i}\lambda^{\gamma_4 - 1} \textit{ Eqn 1.2}$$

Considering there was a reasonable area change across the diaphragm it was safe to assume the flow exiting the driver tube was 'choked'. This is a term which indicates the flow is at Mach 1, the maximum Mach number a subsonic flow can achieve without being expanded. Therefore:

$$M_{11} = 1 \qquad \textit{Eqn 1.3}$$

$$T_{11,0} = 1 + \frac{\gamma_{11}-1}{2} M_{11}^2 \textit{ Eqn 1.4}$$

Combining equation 1.2 and 1.4, assuming $\gamma_4 = \gamma_{11}$.

$$T_{11} = \frac{2T_4}{\gamma_4 + 1} \qquad \textit{Eqn 1.5}$$

Also assuming ideal gas relations are valid and $R_4 = R_{11}$ the sound speed (and subsequently the velocity) across the primary diaphragm is:

$$a_{11} = u_{11} = \sqrt{\gamma_4 R_4 T_{11}} \qquad \textit{Eqn 1.6}$$

The pressure immediately downstream of the diaphragm can also be found based on the result of Equation 1.5, assuming the diaphragm bursting pressure (P_4)is known.

$$\frac{P_{11}}{P_4} = \left(\frac{T_{11}}{T_4}\right)^{\frac{\gamma_4}{\gamma_4 - 1}} = \left(\frac{2}{\gamma_4 + 1}\right)^{\frac{\gamma_4}{\gamma_4 - 1}} \quad \textit{Eqn 1.7}$$

Upon exiting the driver tube, the gas is processed by an unsteady expansion, which increases its velocity to u_3. The following relationship applies across this unsteady expansion, assuming isentropic flow, $\gamma_{sd3} = \gamma_{11} = \gamma_4$and making use of the fact that $a_{11} = u_{11}$.

$$u_{sd3} + \frac{2a_{sd3}}{\gamma_{sd3} - 1} = u_{11} + \frac{2a_{11}}{\gamma_{11} - 1} \rightarrow u_{sd3} = \frac{a_{11}(\gamma_4 + 1) - 2a_{sd3}}{\gamma_4 - 1} \qquad \textit{Eqn 1.8}$$

Just as in Equation 1.6 it is also true that:

$$a_{sd3} = \sqrt{\gamma_{sd3} R_{sd3} T_{sd3}} \qquad \textit{Eqn 1.9}$$

Therefore substituting Equation 1.6 and 1.9 into 1.8 and given $R_{sd3} = R_4$ rearranging yields:

$$u_{sd3} = \frac{\sqrt{\gamma_4 R_4}}{\gamma_4 - 1}\left(\sqrt{T_{11}}(\gamma_4 + 1) - 2\sqrt{T_{sd3}}\right) \qquad \textit{Eqn 1.10}$$

This expanded driver gas meets the secondary driver gas at location known as the contact surface, also referred to as the interface. At this interface the pressures are equal, therefore the pressure of the secondary driver gas P_{sd2} equals of the pressure of the expanded driver gas P_{sd3}. Therefore the following the isentropic relations apply where P_{sd1} is the initial fill pressure of the gas in the secondary driver tube.

$$\frac{P_{sd3}}{P_{11}} = \frac{P_{sd2}}{P_{11}} = \frac{P_{sd2}}{P_4}\frac{P_4}{P_{11}} = \frac{P_{sd2}}{P_{sd1}}\frac{P_{sd1}}{P_4}\frac{P_4}{P_{11}} \qquad \textit{Eqn 1.11}$$

$$T_{sd3} = T_{11}\left(\frac{P_3}{P_{11}}\right)^{\frac{\gamma_4 - 1}{\gamma_4}} = T_{11}\left(\frac{P_{sd2}}{P_{sd1}}\frac{P_{sd1}}{P_4}\frac{P_4}{P_{11}}\right)^{\frac{\gamma_4 - 1}{\gamma_4}} \textit{Eqn 1.12}$$

It is also true that velocity of the gas in front of the interface can be described by the following series of normal shock relations, where γ_{sd2} and γ_{sd1} are equal and represent the ratio of specific heats of the secondary driver gas. This is because, as Figure.1 shows, a shock precedes the contact surface, processing the gas which is initially stagnant in the secondary driver tube.

$$u_{sd2} = \frac{a_{sd1}}{y_{sd1}}\left(\frac{P_{sd2}}{P_{sd1}} - 1\right)\sqrt{\frac{\frac{2\gamma_{sd1}}{\gamma_{sd1}+1}}{\frac{P_{sd2}}{P_{sd1}}+\frac{\gamma_{sd1}-1}{\gamma_{sd1}+1}}} \qquad \textit{Eqn 1.13}$$

Since both the driver gas and secondary driver gas on either side of the interface have the same velocity ($u_{sd3} = u_{sd2}$), Equation 1.12 can be substituted into Equation 1.10 and set equal to Equation 1.13.

$$\frac{a_{sd1}}{y_{sd1}}\left(\frac{P_{sd2}}{P_{sd1}} - 1\right)\sqrt{\frac{\frac{2}{\gamma_{sd1}+1}}{\frac{P_{sd2}}{P_{sd1}}+\frac{\gamma_{sd1}-1}{\gamma_{sd1}+1}}} = \frac{\sqrt{\gamma_4 R_4 T_{11}}}{\gamma_4 - 1}\left(\left(\gamma_4 + 1\right) - 2\left(\frac{P_{sd2}}{P_{sd1}}\frac{P_{sd1}}{P_4}\frac{P_4}{P_{11}}\right)^{\frac{\gamma_4-1}{2\gamma_4}}\right) \qquad \textit{Eqn 1.14}$$

This equation can then be solved by numerical techniques to find the pressure ratio $\frac{P_{sd2}}{P_{sd1}}$.

By back substituting this pressure ratio into Equation 1.13 and the following Equation 1.15 the temperature (T_{sd2}) and velocity (u_{sd2}) of the secondary driver gas, directly before it encounters the secondary diaphragm, can be found.

$$T_{sd2} = T_{sd1}\frac{P_{sd2}}{P_{sd1}}\left(\frac{\frac{\gamma_{sd1}+1}{\gamma_{sd1}-1}+\frac{P_{sd2}}{P_{sd1}}}{1+\frac{\gamma_{sd1}+1}{\gamma_{sd1}-1}+\frac{P_{sd2}}{P_{sd1}}}\right) \qquad \textit{Eqn 1.15}$$

From these properties, the velocity of the test gas (u_3) can be found by employing the same unsteady expansion theory as in Equation 1.8 assuming an unsteady occurs at this diaphragm.

$$u_3 + \frac{2a_3}{\gamma_3 - 1} = u_{sd2} + \frac{2a_{sd2}}{\gamma_{sd2} - 1} \qquad \textit{Eqn 1.16}$$

Given $\gamma_3 = \gamma_{sd2} = \gamma_{sd1}$, $R_3 = R_{sd2}$, $a_3 = \sqrt{\gamma_3 R_3 T_3}$, and $a_{sd2} = \sqrt{\gamma_{sd2} R_{sd2} T_{sd2}}$, Equation 1.16 becomes:

$$u_3 = u_{sd2} + \frac{2\sqrt{\gamma_{sd2} R_{sd2}}}{\gamma_{sd2} - 1}\left(\sqrt{T_{sd2}} - \sqrt{T_3}\right) \qquad \textit{Eqn 1.17}$$

Isentropic expansion laws also dictate that:

$$T_3 = T_{sd2}\left(\frac{P_3}{P_{sd2}}\right)^{\frac{\gamma_{sd2}-1}{\gamma_{sd2}}} \qquad \textit{Eqn 1.18}$$

The expanded secondary driver gas then comes into contact with the test gas at a second interface. As was the case with the first interface, the pressure across this contact surface was constant($P_3 = P_2$). With this in mind, Equation 1.18 could be expanded as follows.

$$T_3 = T_{sd2}\left(\frac{P_{sd1}}{P_{sd2}}\frac{P_2}{P_1}\frac{P_1}{P_{sd1}}\right)^{\frac{\gamma_{sd2}-1}{\gamma_{sd2}}} \quad \textit{Eqn 1.19}$$

Also constant across the second interface are the velocities u_2 and u_3, therefore, as a normal shock separates region 1 and region 2, the following normal shock relation was valid.

$$u_3 = \frac{a_1}{\gamma_1}\left(\frac{P_2}{P_1} - 1\right)\sqrt{\frac{\frac{2\gamma_1}{\gamma_1+1}}{\frac{P_2}{P_1}+\frac{\gamma_1-1}{\gamma_1+1}}} \qquad \textit{Eqn 1.20}$$

Substituting Equations 1.19 and 1.20 into Equation 1.17:

$$\frac{a_1}{\gamma_1}\left(\frac{P_2}{P_1} - 1\right)\sqrt{\frac{\frac{2\gamma_1}{\gamma_{sd}+1}}{\frac{P_2}{P_1}+\frac{\gamma_1-1}{\gamma_1+1}}} = u_{sd2} + \frac{2\sqrt{\gamma_{sd2}R_{sd2}T_{sd2}}}{\gamma_{sd2}-1}\left(1 - \left(\frac{P_{sd1}}{P_{sd2}}\frac{P_2}{P_1}\frac{P_1}{P_{sd1}}\right)^{\frac{\gamma_{sd2}-1}{2\gamma_{sd2}}}\right) \qquad \textit{Eqn 1.21}$$

Given $a_1 = \sqrt{\gamma_1 R_1 T_1}$ (where T_1 is the known fill temperature of the shock tube), Equation 1.21 can be solved by various techniques to determine the pressure ratio $\frac{P_2}{P_1}$. $P_1$is the initial fill pressure of the shock tube and is known, therefore P_2, the pressure of the moving test gas in shock tube, can be easily found. The temperature (T_2) and speed (u_2)of the test gas could also be found using normal shock relations.

$$T_2 = T_1\frac{P_2}{P_1}\left(\frac{\frac{\gamma_1+1}{\gamma_1-1}+\frac{P_2}{P_1}}{1+\frac{\gamma_1+1}{\gamma_1-1}+\frac{P_2}{P_1}}\right) \qquad \textit{Eqn 1.22}$$

$$u_2 = \frac{a_1}{\gamma_1}\left(\frac{P_2}{P_1} - 1\right)\sqrt{\frac{\frac{2\gamma_1}{\gamma_1+1}}{\frac{P_2}{P_1}+\frac{\gamma_1-1}{\gamma_1+1}}} \qquad \textit{Eqn 1.23}$$

Finally, when the shock reaches the tertiary diaphragm, it causes it to rupture and begins the process the gas in the acceleration tube. Directly after this diaphragm is breached, a third unsteady expansion occurs, this time of the test gas. Again the unsteady expansion through the diaphragm can be described by an equation similar to that of 1.16, where γ_7 and γ_2 were the ratio of the specific heats of the test gas.

$$u_7 + \frac{2a_7}{\gamma_7 - 1} = u_2 + \frac{2a_2}{\gamma_2 - 1} \qquad \textit{Eqn 1.24}$$

Given the dependence of sound speed on temperature this relationship can be re-expressed in the same way as Equation 1.17.

$$u_7 = u_2 + \frac{2\sqrt{\gamma_2 R_2}}{\gamma_2 - 1}\left(\sqrt{T_2} - \sqrt{T_7}\right) \qquad \textit{Eqn 1.25}$$

Likewise equations 1.19 and 1.20 could be modified such that they were relevant to the behaviour of the flow in the acceleration tube. (Note γ_5 is the ratio of specific heats of the test gas)

$$T_7 = T_2\left(\frac{P_1}{P_2}\frac{P_6}{P_5}\frac{P_5}{P_1}\right)^{\frac{\gamma_2 - 1}{\gamma_2}} \qquad \textit{Eqn 1.26}$$

$$u_7 = \frac{a_5}{\gamma_5}\left(\frac{P_6}{P_5} - 1\right)\sqrt{\frac{\frac{2\gamma_5}{\gamma_5 + 1}}{\frac{P_6}{P_5} + \frac{\gamma_5 - 1}{\gamma_5 + 1}}} \qquad \textit{Eqn 1.27}$$

Combining Equations 1.25, 1.26 and 1.27 yields:

$$\frac{a_5}{\gamma_5}\left(\frac{P_6}{P_5} - 1\right)\sqrt{\frac{\frac{2\gamma_5}{\gamma_5 + 1}}{\frac{P_6}{P_5} + \frac{\gamma_5 - 1}{\gamma_5 + 1}}} = u_2 + \frac{2\sqrt{\gamma_2 R_2 T_2}}{\gamma_2 - 1}\left(1 - \left(\frac{P_1}{P_2}\frac{P_6}{P_5}\frac{P_5}{P_1}\right)^{\frac{\gamma_2 - 1}{2\gamma_2}}\right) \qquad \textit{Eqn 1.28}$$

This can then be solved to find the $\frac{P_6}{P_5}$ in the same way that that Equation 1.21 was solved. Since P_5 is the fill pressure of the acceleration tube, the value of P_6 could be easily determined. The pressures are constant across the third contact surface ($P_6 = P_7$), therefore this represented the pressure of the steady test flow and was the one of the three properties that could be used to fully define this flow. The other two, the temperature (T_7) and velocity (u_7), could be found

by back substituting P_6/P_5 into Equations 1.26 and 1.27. Hence fully characterizing the test flow produced by the shock expansion facility.

Reflected shock at the Secondary Diaphragm

In order to produce high pressure test flows in shock expansion tubes it is necessary to fill the shock tube to a high pressure. However if this pressure is high enough, when the secondary diaphragm is breached, the secondary driver gas cannot be expanded into the shock tube. Instead it must be processed by a reflected shock to raise the pressure of the driver gas equal to that of the test gas [1]. Therefore, a different analysis of the flow around the secondary diaphragm is required. This subsection details this analysis which is again adapted from *"Performance considerations for expansion tube operation with a shock heated secondary driver"* by David E Gildfind et al [6].

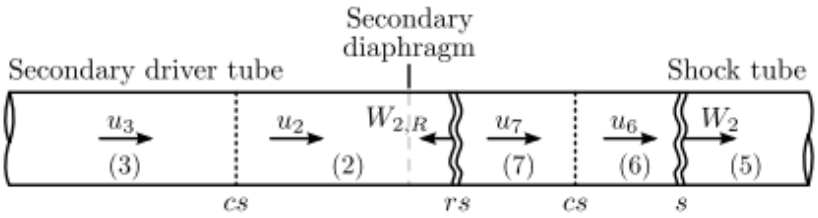

Figure.2: A diagram showing the behaviour of the flow in a shock expansion tube when a reflected shock is created as a result of the shock processed secondary driver gas being at a lower pressure than the stagnant test gas. The labels, "cs", "rs", and "s" represent "contact surface", "reflected shock wave", and "shock wave" respectively. (This diagram is directly adapted from "Development of High Total Pressure Scramjet Flow Conditions using the X2 Expansion Tube" *by David E Gildfind [1].)*

The first step of this analysis was to let W equal the velocity of the gas in front of the reflected shock wave shown in Figure.2 and $(W - u_p)$ be the induced velocity of the gas behind the shock, both measured in the shock frame of reference. Therefore, based on normal shock relations, the following two equations are valid where $W_{2,r}$ is the velocity of the shock in the absolute frame of reference.

$$W = u_{sd2} + W_{2,r} \rightarrow W_{2,r} = W - u_{sd2} \qquad \textit{Eqn 1.29}$$

$$W - u_p = u_3 + W_{2,r} \rightarrow W_{2,r} = W - u_p - u_3 \qquad \textit{Eqn 1.30}$$

These two relations can then be equated to yield:

$$u_p = u_{sd} - u_3 \qquad \textit{Eqn 1.31}$$

Therefore, making use of normal shock relations the induced velocity behind the shock in the absolute reference frame is:

$$u_p = \frac{a_2}{\gamma_{sd2}}\left(\frac{P_3}{P_{sd2}} - 1\right)\sqrt{\frac{\frac{2\gamma_{sd2}}{\gamma_{sd2}+1}}{\frac{P_3}{P_{sd2}}+\frac{\gamma_{sd2}-1}{\gamma_{sd2}+1}}} \quad \textit{Eqn 1.32}$$

However, given that pressures are constant across the contact surface in the shock tube this equation can be re-expressed as follows.

$$u_p = \frac{a_2}{\gamma_{sd2}}\left(\frac{P_{sd1}}{P_{sd2}}\frac{P_1}{P_{sd1}}\frac{P_2}{P_1} - 1\right)\sqrt{\frac{\frac{2\gamma_{sd2}}{\gamma_{sd2}+1}}{\frac{P_{sd1}}{P_{sd2}}\frac{P_1}{P_{sd1}}\frac{P_2}{P_1}+\frac{\gamma_{sd2}-1}{\gamma_{sd2}+1}}} \qquad \textit{Eqn 1.33}$$

This relation can then be substituted into Equation 1.31 along with Equation 1.20, given that $u_3 = u_2$.

$$u_{sd2} + \frac{a_1}{\gamma_1}\left(\frac{P_2}{P_1} - 1\right)\sqrt{\frac{\frac{2\gamma_1}{\gamma_1+1}}{\frac{P_2}{P_1}+\frac{\gamma_1-1}{\gamma_1+1}}} = \frac{a_2}{\gamma_{sd2}}\left(\frac{P_{sd1}}{P_{sd2}}\frac{P_1}{P_{sd1}}\frac{P_2}{P_1} - 1\right)\sqrt{\frac{\frac{2\gamma_{sd2}}{\gamma_{sd2}+1}}{\frac{P_{sd1}}{P_{sd2}}\frac{P_1}{P_{sd1}}\frac{P_2}{P_1}+\frac{\gamma_{sd2}-1}{\gamma_{sd2}+1}}} \qquad \textit{Eqn 1.34}$$

This equation can then be solved using any method desired to find the pressure ratio $\frac{P_2}{P_1}$ just as Equation 1.21 was solved to find the same ratio for the unsteady expansion case. In the case that a reflected shock forms this equation 1.34 can be substituted into the analysis procedure of the previous Section in place of Equation 1.21 [6].

This is only required if the pressure of the compressed and heated test gas (P_2) is greater than the shock processed secondary driver gas (P_{sd2}). Is typically determined via process of trial and error where either an unsteady expansion or a reflected shock is assumed. If P_2 is greater than P_{sd2} then the reflected shock assumption is the correct one, and vice versa.

Appendix – B

Probe Technical Drawings

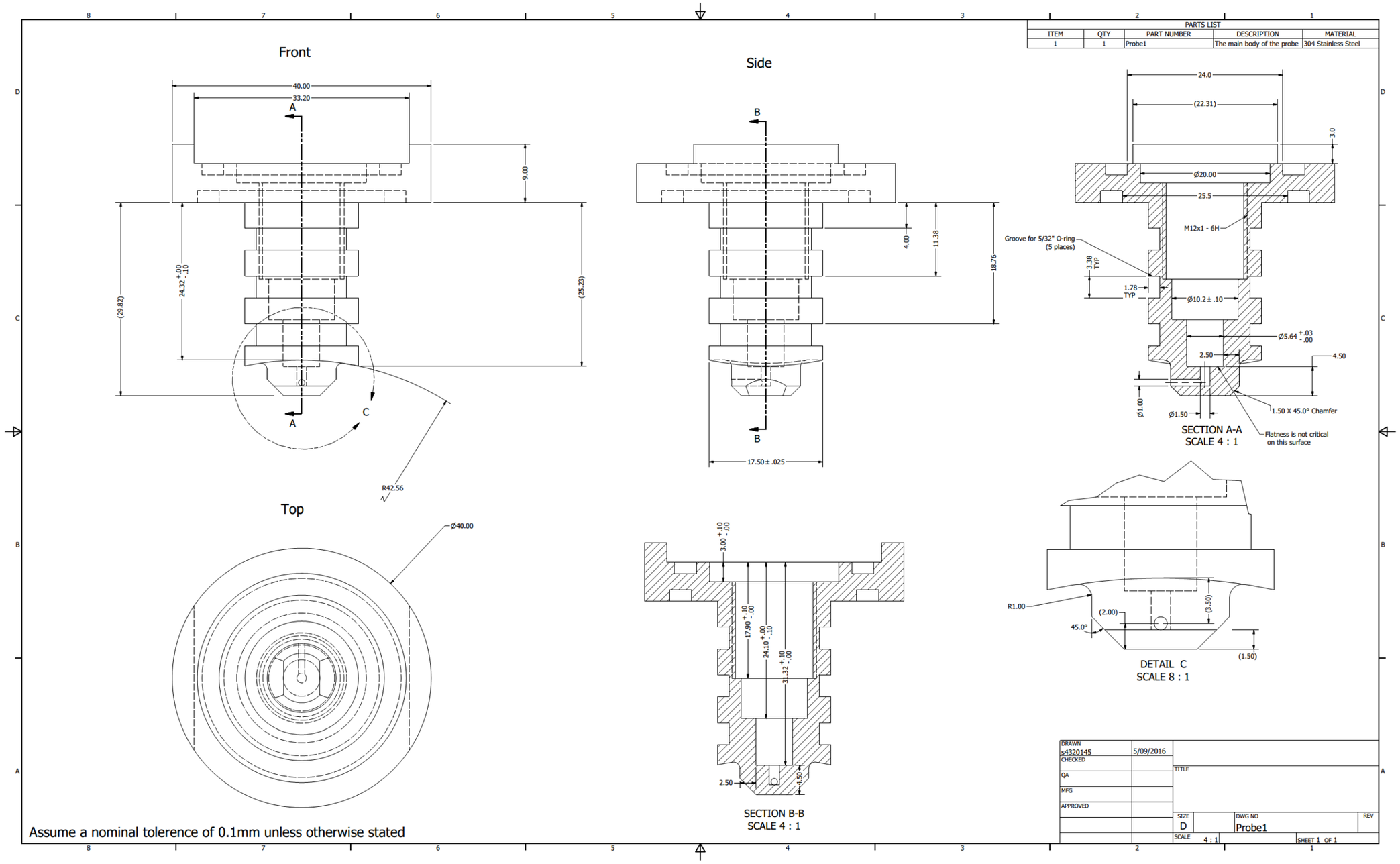

Appendix – C

The Full Pitot Probe Responses

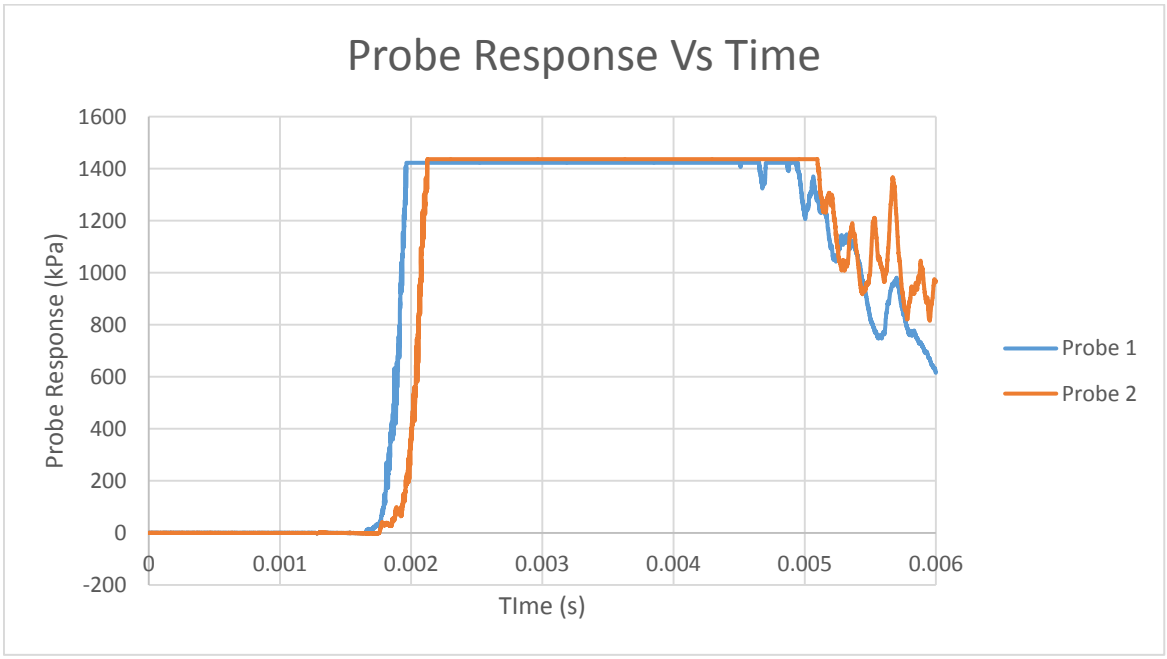

Figure 1: The pitot probe responses for the first test run in the X2.

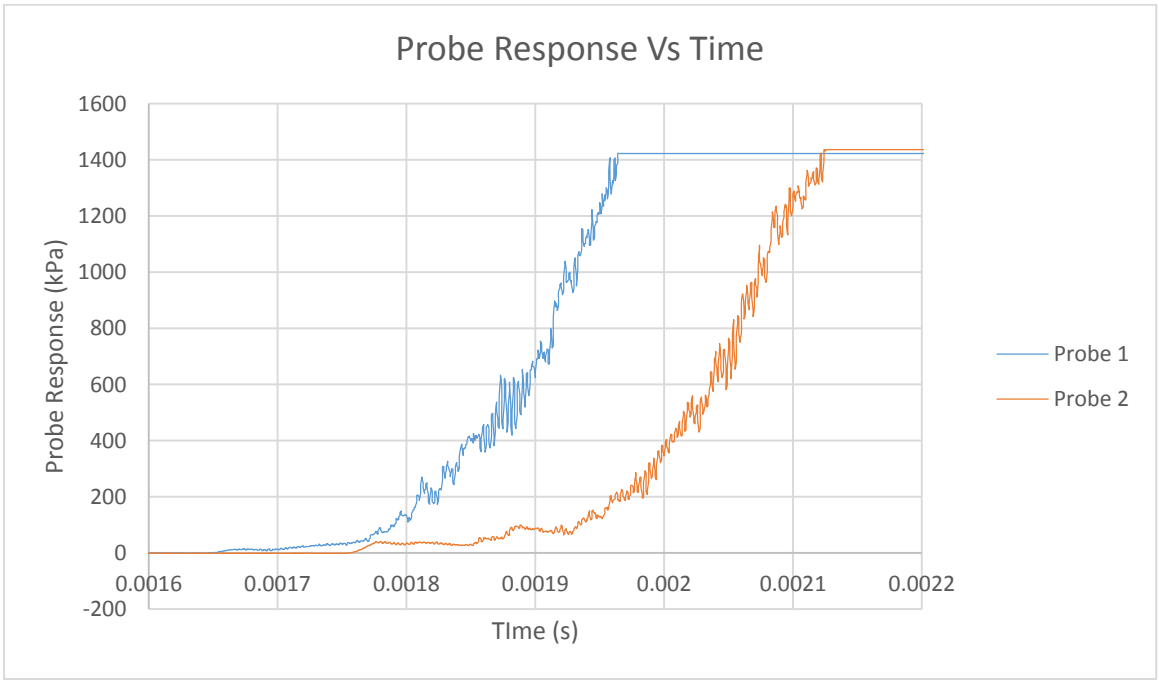

Figure.2: The pitot probe responses over the time period of interest for the first test run in the X2.

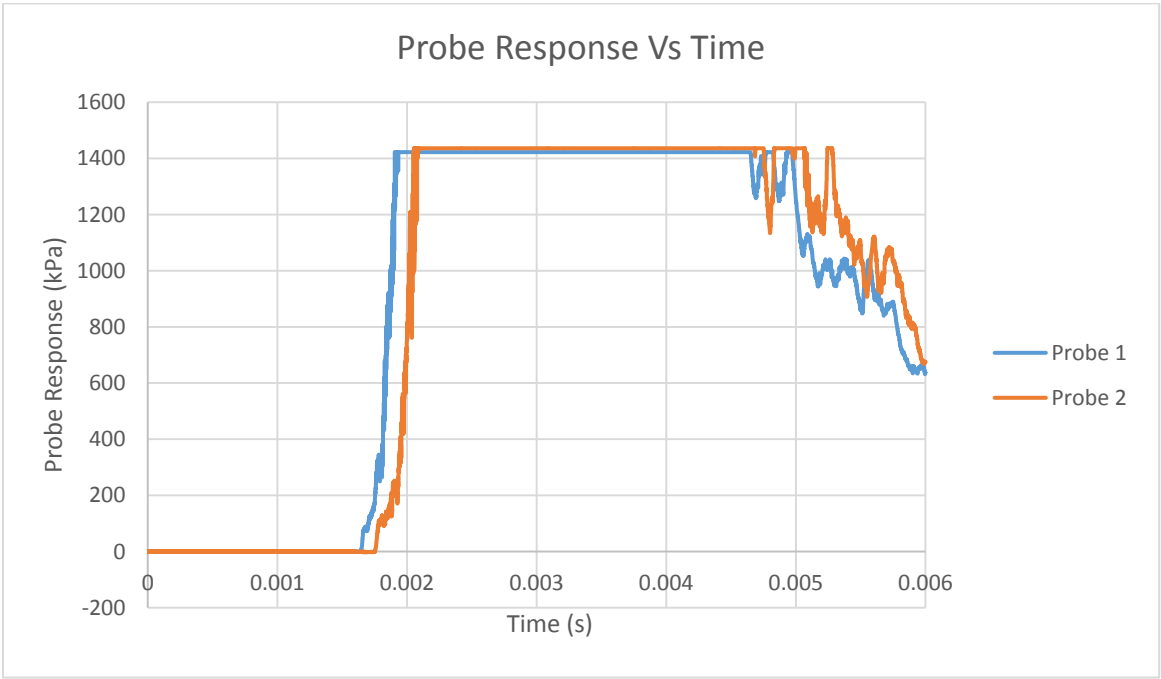

Figure.3: The pitot probe responses for the second test run in the X2.

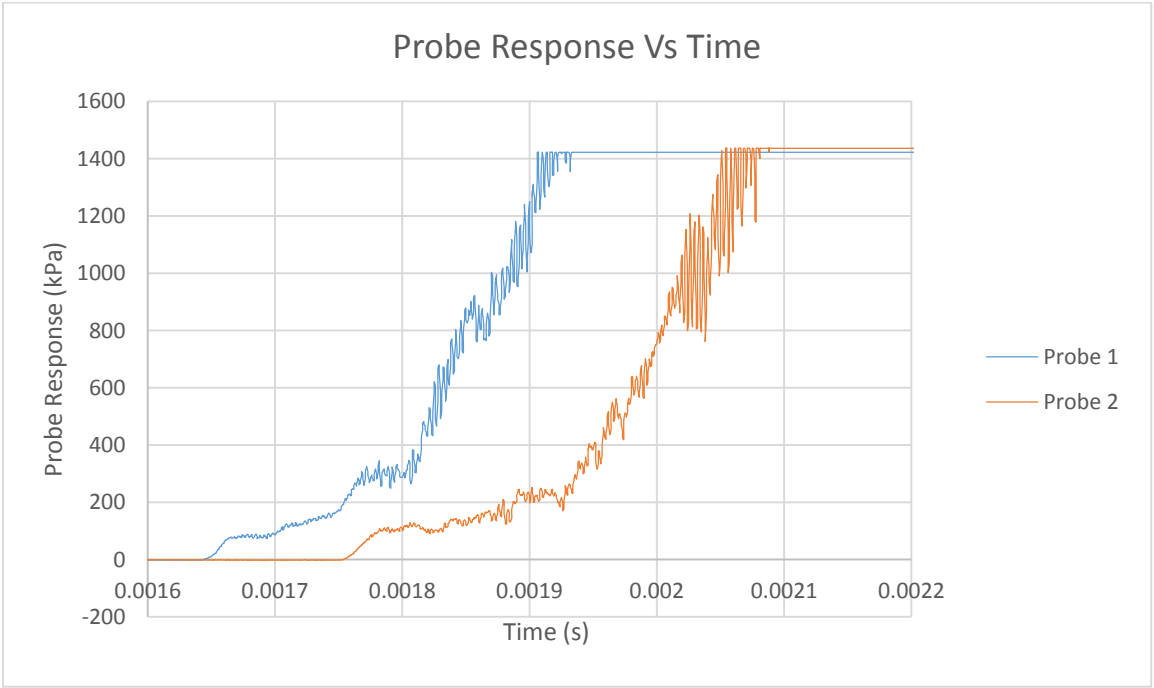

Figure.4: The pitot probe response over the time period of interest for the second test run in the X2.

The Static Pressure Sensor Responses

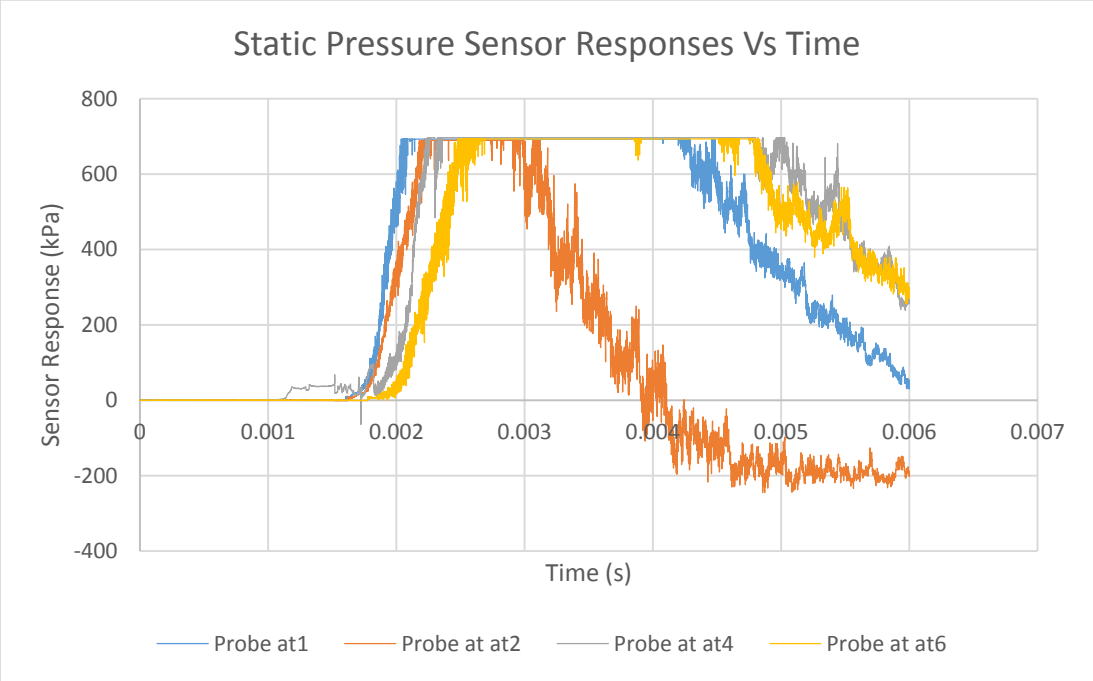

Figure 1: The static pressure sensor responses for the first test run in the X2. From these results it appears erroneous data has been recorded by the sensor at at4. (Refer to Figure 5.1.1 for the exact locations of the static sensors in the tubes.)

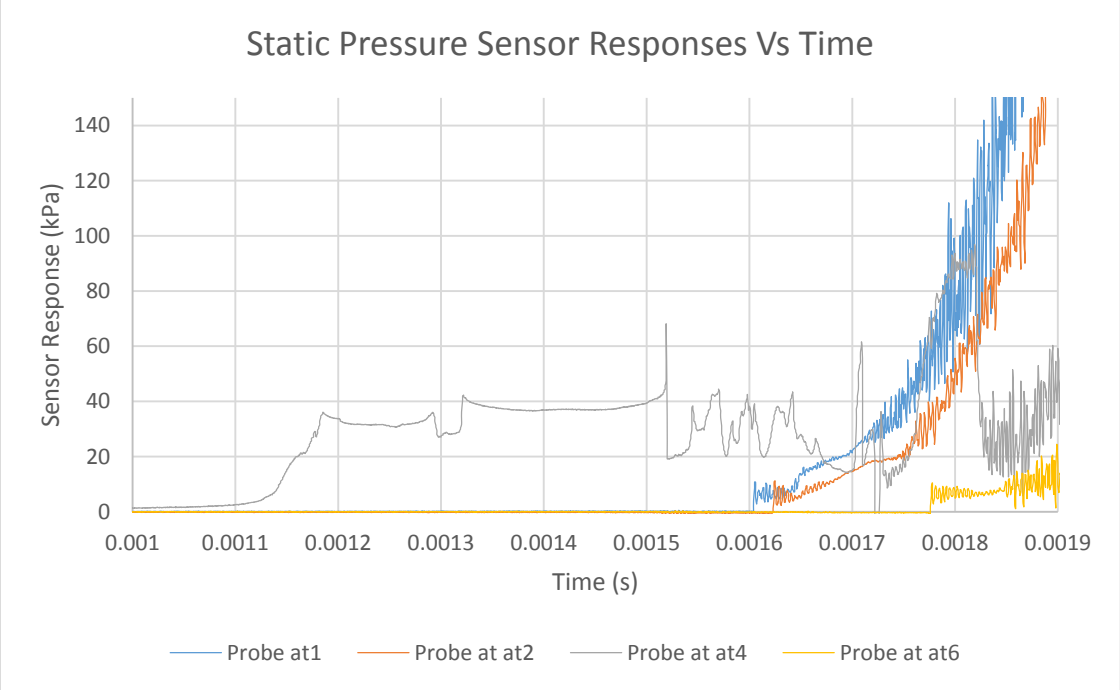

Figure.2: The static pressure sensor responses over the time period of interest for the first test run in the X2. From these results it appears erroneous data has been recorded by the sensor at at4. (Refer to Figure 5.1.1 for the exact locations of the static sensors in the tubes.)

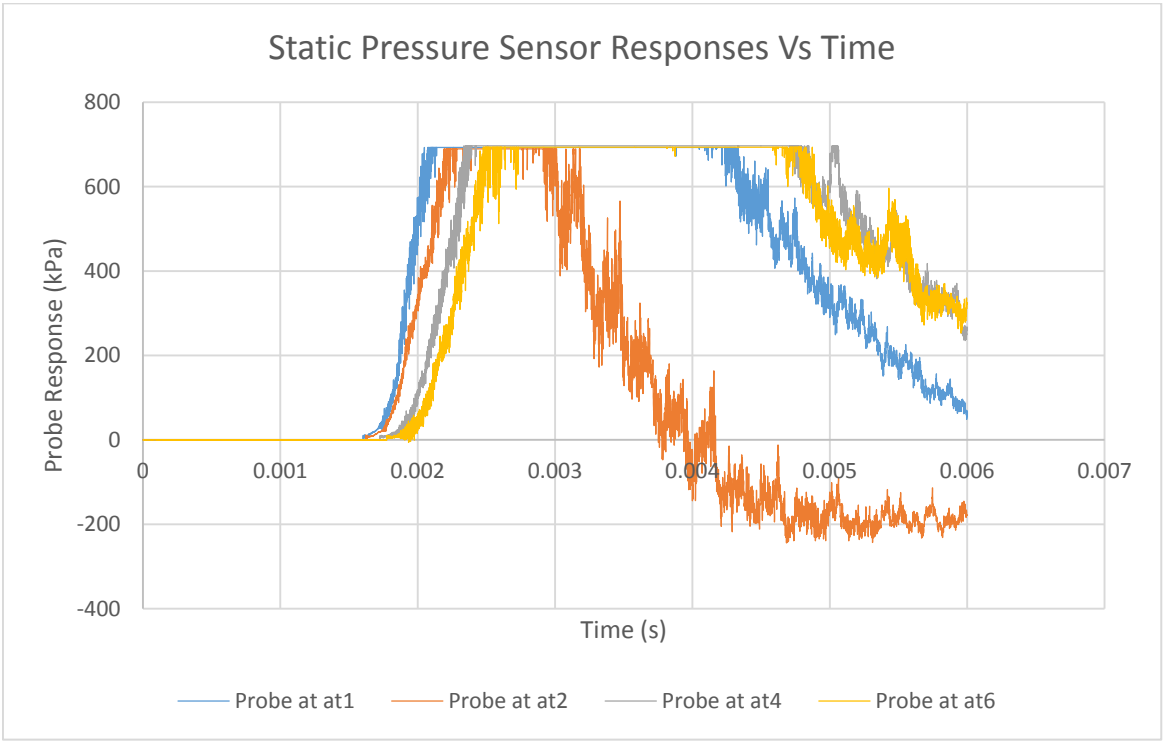

Figure.3: The static pressure sensor responses for the second test run in the X2. (Refer to Figure 5.1.1 for the exact locations of the static sensors in the tubes.)

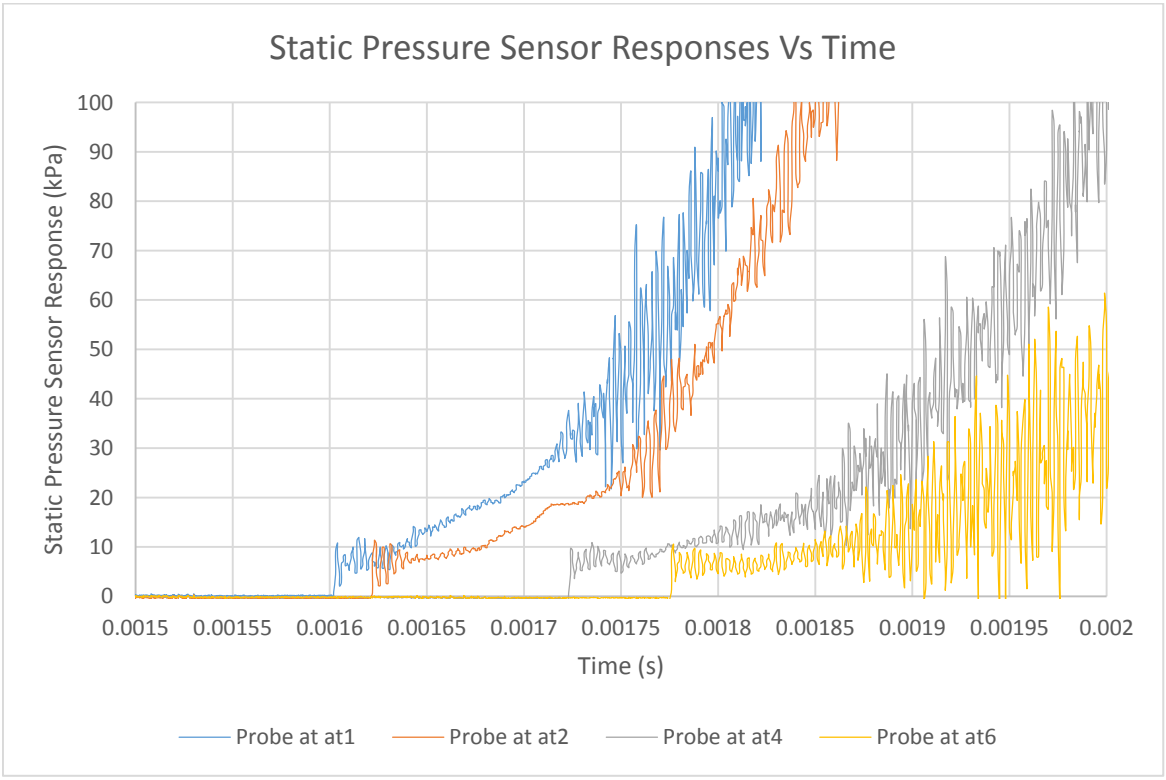

Figure.4: The static pressure sensor responses over the time period of interest for the second test run in the X2. (Refer to Figure 5.1.1 for the exact locations of the static sensors in the tubes.)

Appendix – D

Risk Assessment Associated with Change in X2 Operating Conditions for Testing

Task Risk Assessment-Word Document

This Task/Process Risk Assessment is not Complete

Printed By: David Gildfind

Task/Process Details

Task/Process ID: 69508 **Name:** X2 driven tube pitot probe

Effective Risk Level: Low **Action:** Risk is normally acceptable

Author: David Gildfind **Last Updated By:** David Gildfind On 20/10/2016 4:22:44PM

Audited By: **Audit Date:**

Workplace Location of the Task/Process

Campus: St Lucia Campus

Faculty/Division: EAIT - Engineering, Architecture and Information Technology Faculty

School/Centre: MechM - School of Mechanical and Mining Engineering

Workplace: Hawken Basement, xlabs, 50-C104

Supervisor: Richard morgan **Status: Not Approved**

Risks Associated with this Task/Process or Situation

Risk Situation: Probe projectile

Process\Job Desc: A new pressure probe is being trialled in X2. It is similar to the existing static pressure probes (see http://espace.library.uq.edu.au/view/UQ:372806), except it protrudes slightly into the freestream. The purpose is to stagnate the flow locally at the probe head. This will allow a pitot pressure measurement along the tube length, near the wall.

Energy Source: Fluid Pressure

Current Controls: 1. Ensure metallic mounting is used for probe.
2. Ensure approximate vertical alignment.
3. Keep direct path clear during experiment.

The probe is aligned vertically, and the path is kept clear, to prevent impact with anyone should it be fired outwards by high internal pressure or a failing cross-brace. So impact is unlikely in the case of release. However, a very robust steel brace is being used for tube mounting. This is secured with two M5 cap screws. Assuming a minimum tensile strength of 400 MPa (conservative) and a stress area of 14.2mm^2 (compared to 19.6mm^2 for 5mm diameter), these can resist 2*400*14.2=11,360N. Maximum exposed area of probe is 17.5mm, so area = 3.14*17.5*17.5/4=240mm^2 (which is much more than protruding section). Using P.A=F, P=F/A=11360/240=47 MPa. This is well in excess of possible stagnation pressures at this part of the tube, indicating a safety factor of the order of 10x for tensile failure of the two M5s.

Hazard Event: Bolts fail and probe is fired out into the lab.

Incident Category: Being hit by moving object

Assessment Date: 20/10/2016

Risk Analysis

Consequence: Serious **Rationale:** Probe is metallic and dense, and could foreseeably cause severe injury if fired at a vulnerable part of a person's body.

Exposure: Unusual **Rationale:** These are one off tests which will involve two shots of the facility with the proposed modified probes.

Probability: Conceivable **Rationale:** It is considered extremely unlikely that a failure could occur given the mechanical fastening, and extremely unlikely that it would result in injury.

Risk Level: Low **Action:** **Risk is normally acceptable**

No Additional Controls

References

1. Gildfind, D.E., *Development of high total pressure scramjet flow conditions using the X2 expansion tube*. 2012, The University of Queensland, School of Mechanical and Mining Engineering.
2. Lu, F. and D. Marren, *Advanced hypersonic test facilities*. Vol. 198. 2002, Reston, Va: American Institute of Aeronautics and Astronautics.
3. Ashby, G.C., *Miniaturized compact water-cooled pitot-pressure probe for flow-field surveys in hypersonic wind tunnels*. 1988.
4. David E. Gildfind, P.A.J., Richard G. Morgan, *Expansion Tubes in Australia.* Springer 2016.
5. Duff, R.E., *Shock-Tube Performance at Low Initial Pressure.* Physics of Fluids, 1959. **2**(2): p. 207-216.
6. David E. Gildfind, C.M., James, Pierpaolo Toniato, Richard G. Mordan *Performance considerations for expansion tube operation with a shock-heated secondary driver.* The Journal of Fluid Mechanics 2015. **777**: p. 364-407.
7. Moore, J.A., *A study of response time of pitot pressure probes designed for rapid response and protection of transducer - NASA-TM-80091*. 1979, Sponsoring Organization: NASA Langley Research Center.
8. Spence, D.A. and B.A. Woods, *A review of theoretical treatments of shock-tube attenuation.* Journal of Fluid Mechanics, 1964. **19**(2): p. 161-174.
9. Gildfind, D.E., et al., *Production of High-Mach-Number Scramjet Flow Conditions in an Expansion Tube.* AIAA Journal, 2013. **52**(1): p. 162-177.
10. McGilvray, M., et al., *Helmholtz Resonance of Pitot Pressure Measurements in Impulsive Hypersonic Test Facilities.* AIAA Journal, 2009. **47**(10): p. 2430-2439.
11. Lafferty, J.F. and D.E. Marren, *Hypervelocity Wind Tunnel No. 9 Mach 7 Thermal Structural Facility Verification and Calibration*, V.A. Naval Surface Warfare Center Dahlgren Div, Editor. 1996.
12. Davis, L.M. and D.B. Carver, *Initial Calibration of the HEAT-H2 Arc-Heated Wind Tunnel*, T.N. Arnold Engineering Development Center Arnold Afs, Editor. 1992.
13. Demetriades, A. and A.J. Laderman, *Advanced Penetration Problems Program*, D.I.V. Philco-Ford Corp Newport Beach Ca Aeronutronic, Editor. 1973.

14. Mirels, H., *Shock tube test time limitation due to turbulentwall boundary layer.* AIAA Journal, 1964. **2**(1): p. 84-93.
15. Mirels, H., *Boundary layer behind shock or thin expansion wave moving into stationary fluid.* UNT Digital Library, 1956.
16. Petersen, E.L. and R.K. Hanson, *Improved Turbulent Boundary-Layer Model for Shock Tubes.* AIAA Journal, 2003. **41**(7): p. 1314-1322.
17. Wegener, M., M. Sutcliffe, and R. Morgan, *Optical study of a light diaphragm rupture process in an expansion tube.* Shock Waves, 2000. **10**(3): p. 167-178.
18. Danehy, P.M., et al., *Flow-Tagging Velocimetry for Hypersonic Flows Using Fluorescence of Nitric Oxide.* AIAA Journal, 2003. **41**(2): p. 263-271.
19. Danehy, P.M., et al., *Fluorescence Velocimetry of the Hypersonic, Separated Flow over a Cone.* AIAA Journal, 2001. **39**(7): p. 1320-1328.
20. Hiller, B., et al., *Velocity visualization in gas flows using laser-induced phosphorescence of biacetyl.* Review of Scientific Instruments, 1984. **55**(12): p. 1964-1967.
21. Miles, R.B., et al., *Fundamental turbulence measurements by relief flow tagging.* AIAA Journal, 1993. **31**(3): p. 447-452.
22. Boutier, A., *New trends in instrumentation for hypersonic research*. Vol. no. 224. 1993, Dordrecht: Kluwer Academic Publishers.
23. Gustavsson, J.P.R. and C. Segal, *Filtered Rayleigh scattering velocimetry—accuracy investigation in a M=2.2 axisymmetric jet.* Experiments in Fluids, 2005. **38**(1): p. 11-20.
24. Bathel, B.F., et al., *Velocity Profile Measurements in Hypersonic Flows Using Sequentially Imaged Fluorescence-Based Molecular Tagging.* AIAA Journal, 2011. **49**(9): p. 1883-1896.
25. Lackner, M., *TUNABLE DIODE LASER ABSORPTION SPECTROSCOPY (TDLAS) IN THE PROCESS INDUSTRIES – A REVIEW*, in *Reviews in Chemical Engineering*. 2007. p. 65.
26. Philippe, L.C. and R.K. Hanson, *Laser-absorption mass flux sensor for high-speed airflows.* Optics Letters, 1991. **16**(24): p. 2002-2004.
27. Werle, P., *Tunable diode laser absorption spectroscopy: recent findings and novel approaches.* Infrared Physics & Technology, 1996. **37**(1): p. 59-66.

28. Porro, A.R., *Pressure Probe Designs for Dynamic Pressure Measurements in a Supersonic Flow Field - NASA/TM-2001-211096*. 2001, Sponsoring Organization: NASA Glenn Research Center.
29. Simmons, J.M., *Experimental methods in Thermal and Fluid ScienceMeasurement techniques in high-enthalpy hypersonic facilities.* Experimental Thermal and Fluid Science, 1995. **10**(4): p. 454-469.
30. Matthews, R.K. and W.D. Williams, *Hypersonic Flow-Field Measurements - Intrusive and Nonintrusive*, T.N. Arnold Engineering Development Center Arnold Afs, Editor. 1994.
31. Bergh, H. and H. Tijdeman, *Theoretical and experimental results for the dynamic response of pressure measuring systems*. 1965.
32. Nyland, T.W. and D.R. Englund, *Dynamics of short pressure probes*. 1971.
33. Ladoon, D.W., S.P. Schneider, and J.D. Schmisseur, *Physics of Resonance in a Supersonic Forward-Facing Cavity.* Journal of Spacecraft and Rockets, 1998. **35**(5): p. 626-632.
34. Engblom, W.A., et al., *Experimental and numerical study of hypersonic forward-facing cavity flow.* Journal of Spacecraft and Rockets, 1996. **33**(3): p. 353-359.
35. PCB_Group_Inc. *Pressure Transducer Model 112A22 Specifications*. 2016; Available from: http://www.pcb.com/products.aspx?m=112A22.